NASA CR-54061

THE FEASIBILITY OF BUILDING A 150-KILOGAUSS, LARGE-VOLUME SUPERCONDUCTIVE MAGNET WITH VAPOR-DEPOSITED Nb_3Sn RIBBON

by

W. S. Freedman (Project Supervisor), E. R. Schrader (Project Engineer),
F. Kolendra, F. R. Nyman, H. C. Schindler, and K. Strater

prepared for

NATIONAL AERONAUTICS AND SPACE ADMINISTRATION

CONTRACT NAS 3-2520

RADIO CORPORATION OF AMERICA
SPECIAL ELECTRONICS COMPONENTS DIVISION
SUPERCONDUCTOR MATERIALS AND DEVICES LABORATORY
PRINCETON, NEW JERSEY

NASA CR-54061

FINAL REPORT

THE FEASIBILITY OF BUILDING A 150-KILOGAUSS, LARGE-VOLUME SUPERCONDUCTIVE MAGNET WITH VAPOR-DEPOSITED Nb_3Sn RIBBON

by

N. S. Freedman (Project Supervisor), E. R. Schrader (Project Engineer),
F. Kolondra, F. R. Nyman, H. C. Schindler, and K. Strater

prepared for

NATIONAL AERONAUTICS AND SPACE ADMINISTRATION

July 24, 1964

CONTRACT NAS 3-2520

TECHNICAL MANAGEMENT
NASA LEWIS RESEARCH CENTER
CLEVELAND, OHIO
SPACECRAFT TECHNOLOGY DIVISION
ELECTROSTATIC PROPULSION SECTION

PROJECT MANAGER: A. E. ANGLIN
TECHNICAL ADVISOR: J. C. LAURENCE

RADIO CORPORATION OF AMERICA
SPECIAL ELECTRONIC COMPONENTS DIVISION
SUPERCONDUCTOR MATERIALS AND DEVICES LABORATORY
PRINCETON, NEW JERSEY

THE FEASIBILITY OF BUILDING A 150-KILOGAUSS, LARGE-VOLUME SUPERCONDUCTIVE MAGNET WITH VAPOR-DEPOSITED Nb_3Sn RIBBON

by

N. S. Freedman (Project Supervisor), E. R. Schrader (Project Engineer), F. Kolondra, F. R. Nyman, H. C. Schindler, and K. Strater

ABSTRACT

Extensive testing of RCA vapor-deposited Nb_3Sn ribbon in the form of short samples and coils has shown that an inherent low magnetic field instability of this high-current-density superconductor is a major cause of solenoid degradation. The factors which affect these instabilities at all stages from the initial deposition of the Nb_3Sn on the substrate to the final winding and testing of a coil are indicated. The practical result of this work is shown in the form of a 92-kilogauss, 1/2-inch bore vapor-deposited Nb_3Sn ribbon magnet. Practical considerations involving encapsulation of coils, superconducting-to-normal contacts, and ribbon plating parameters are treated. It is concluded that the design and construction of large-bore, high-field superconductive magnets is feasible using the RCA vapor-deposited Nb_3Sn ribbon.

Author

TABLE OF CONTENTS

LIST OF ILLUSTRATIONS

LIST OF ILLUSTRATIONS (Continued)

LIST OF ILLUSTRATIONS (Continued)

THE FEASIBILITY OF BUILDING A 150-KILOGAUSS, LARGE-VOLUME SUPERCONDUCTIVE MAGNET WITH VAPOR-DEPOSITED Nb_3Sn RIBBON

by

N. S. Freedman (Project Supervisor), E. R. Schrader (Project Engineer),
F. Kolondra, F. R. Nyman, H. C. Schindler, and K. Strater
Radio Corporation of America

I. SUMMARY

Under Contract No. NAS 3-2520, RCA has been engaged in a feasibility evaluation for NASA, Lewis Research Center, since March 15, 1963. The objective of this nine-month study was to demonstrate the feasibility of constructing a large-volume (12-inch bore), 150-kilogauss superconductive magnet using RCA vapor-deposited Nb_3Sn ribbon.

Progress under this contract has established the following:

1. That the feasibility of constructing small-volume, high-field (100-kilogauss) magnets with vapor-deposited Nb_3Sn ribbon has been demonstrated.
2. That it is now appropriate to scale-up and study construction parameters of larger intermediate-volume, high-field magnets.
3. That the RCA vapor-deposited Nb_3Sn ribbon is superconductive as coated, requires no further heat treatments, and retains its high-current, high-field superconductive properties after winding and handling. This, together with the high strength properties of the Hastelloy substrate, provides a practical winding material for large-volume (12-inch bore), very-high-field (150-kilogauss) superconductive magnets in the foreseeable future.

The original empirical insight into the basic factors responsible for magnet "degradation" from expected short-sample critical currents came as a result of extensive tests using the NASA, Lewis Research Center (LeRC), high-field magnet to supply high magnetic field backgrounds. In parallel, hundreds of tests were conducted at RCA to probe the sensitive low-field region.*

---

* Superconductive testing was performed in low magnetic fields at RCA and in high (and to a lesser extent--low) fields in the high-field magnet located at LeRC in Cleveland, Ohio. The availability of the LeRC high-field testing facilities as well as the ready assistance, cooperation, and suggestions of the LeRC personnel helped make possible the development of what is perhaps the most extensive and reliable low- and high-field performance data of large-current superconductors available today.

As a result of work under this contract as well as other RCA-funded work, the following main accomplishments were achieved:

1. Meaningful test techniques were developed for evaluating the critical current and magnetic field properties of superconductive Nb_3Sn ribbon. These techniques have provided information on superconductor behavior previously not understood and have, therefore, significantly advanced the state of this knowledge.

2. With the development of these sophisticated test techniques, the superconductive electrical properties of Nb_3Sn ribbon were found to vary from extremely stable critical current and field performance to unstable critical current and field performance, the latter particularly at the lower magnetic fields. It was shown that stable current and field performance generally accompanied lower current densities. Conversely, unstable performance was generally associated with higher current densities.

3. Progress was made on superconductive coil behavior which, when added to the knowledge gained from testing of Nb_3Sn ribbon, serves to explain some of the unknowns contributing to the phenomenon of "degradation" generally experienced with superconductive solenoids. This provided even greater confidence that development of very-high-field superconductive magnets is feasible. Small-bore coils already tested in the high-field NASA magnet demonstrate critical $H_c - I_c$ curves that definitely duplicate short sample data. Such correlations suggest several approaches to high-field-magnet design.

4. It is now known that the so-called "degradation" effect is more correctly a result of low-field instabilities rather than degradation of high-field superconductor material performance.

5. A three-section, all-vapor-deposited Nb_3Sn ribbon magnet was constructed and tested which experimentally verified the validity of the conclusions detailed in this feasibility study. The 92-kilogauss field achieved within the 1/2-in. inner diameter winding was attained with several coil sections achieving predicted critical currents.

II. INTRODUCTION

A. BACKGROUND

Early in 1961, while working under a basic research program on superconductivity sponsored by the Air Force Systems Command,* RCA Laboratories developed a high-temperature gas-phase reaction process for depositing niobium-tin (Nb_3Sn) continuously on platinum wire and ribbon (Hanak, 1963).

Recognizing the unusual potential afforded by this unique chemical process for depositing superconductive Nb_3Sn, RCA through its Direct Energy Conversion Department of the Special Electronic Components Division, undertook a program to 1) further develop the deposition process and 2) develop applications of Nb_3Sn-coated ribbon to magnet devices. This program, initiated in mid-1961, was wholly financed by RCA.

Prior to the start of this contract (NAS 3-2520), RCA had made notable technical progress in this field. The process equipment had been improved through several successive stages so that long lengths (>300 meters) of high-performance superconductive ribbon were being made in pilot production facilities located at Harrison, New Jersey. Ribbon cross section had been increased to 0.090 inch in width by 0.002 inch thick. Even more significant, however, the pure platinum substrate had been replaced by a low-cost, high-strength Hastelloy substrate.

Development of a special electroplating process had solved the difficult electrical contact problem and also facilitated the continuous electroplating of copper coating on the Nb_3Sn-coated ribbon.

Concomitant with magnet device development, Nb_3Sn-coated ribbon was tested in many coil and magnet configurations. The magnets were designed on a modular basis so that data were obtained on both material and magnet geometries. Certain coil performance degradation effects compared with short-sample test results as ribbon lengths were wound into magnets. The electroplated copper coating made a substantial performance improvement of the Nb_3Sn ribbon in actual magnet configurations, and a successful superconductive 14.5-kilogauss magnet was completed. Until superseded by higher field magnets, this magnet

---

* Contract No. AF33(616)-6405, Physics Laboratory, A.S.D., Wright-Patterson Air Force Base. (Report ASD-TDR-62-269), 1962.

(bore = 1-3/8 in., O.D. = 3-3/8 in., working length = 1-7/8 in.) remained in constant use at the RCA Laboratories during the entire first six months of this contract, providing an extremely reliable and reproducible low-magnetic-field magnet for materials testing. The magnet exhibited no training effects and was turned on or switched off as rapidly and as often as required.

B. CONTRACT NAS 3-2520

A major objective of this contract and the main purpose in high-field testing of coils was to determine the feasibility of designing and constructing a large-volume (12-inch bore), 150-kilogauss solenoid magnet using the RCA Nb_3Sn-coated ribbon. An additional aim of this contract was to more thoroughly high-field-test the RCA superconductive ribbon and to utilize high-field data for further process optimization. In addition, available methods and techniques for magnet design and technology were to be tested. These objectives have been realized and the methods by which they have been attained are described in the following pages. Section III describes the results of Nb_3Sn materials tests, and Section IV, the work on superconductive coils and magnets. Many of the results described in this report were obtained from work not supported by this contract. However, they are included because they complement the aims of this contract.

III. PROCESS

A. HISTORICAL DEVELOPMENT OF THE NIOBIUM STANNIDE DEPOSITION PROCESS

1. Development of Dual Chlorination Process

Early in 1961, while working under a basic research program on superconductivity sponsored in part by the Air Force System Command,* RCA Laboratories developed a high-temperature gas phase reaction process for depositing single-phase, superconducting niobium stannide (Nb_3Sn) continuously on platinum wire or ribbon (Hanak, 1963).

Soon after the process was established, the RCA Special Electronic Components Division assumed responsibility for developing the wire-making technology. For this purpose, the Superconductor Materials and Devices Laboratory was established as an affiliated applied research laboratory at the RCA David Sarnoff Research Center, Princeton, New Jersey.

The Nb_3Sn is formed in a gaseous-phase hydrogen-reduction reaction from the metal chlorides. The reaction is as follows:

$$Nb + 2Cl_2 \xrightarrow{\triangle} NbCl_4 \qquad (1)$$

$$Sn + Cl_2 \xrightarrow{\triangle} SnCl_2 \qquad (2)$$

$$3NbCl_4 + SnCl_2 + 7H_2 \rightleftharpoons Nb_3Sn + 14HCl \qquad (3)$$

After some modifications to the original laboratory process a pilot line as shown in Fig. 1 was assembled. A photograph of the deposition apparatus located at RCA, Harrison, is shown in Fig. 2. In the vertical portion of the apparatus of Fig. 1, sintered niobium and tin bars are reacted with chlorine to form tin and niobium chloride at approximately 1100°C. The horizontal deposition chamber is maintained at a somewhat lower temperature, and the ribbon is resistance-heated above the deposition chamber temperature. Hydrogen chloride gas is added to the process in the vertical section to control the Nb_3Sn deposit on the quartz tube in the horizontal deposition chamber. This is accomplished by shifting the equilibrium value of Eq. (3) to the left such that little or no deposit occurs on the quartz wall. Nb_3Sn deposits on the ribbon since the ribbon is maintained hotter than the quartz wall, and the equilibrium value for the section at the ribbon is greater than that for the

---

* Contract No. AF 33(616)-6405, Physics Lab, A.S.D., Wright-Patterson Air Force Base. (Report ASD-TDR-62-269), 1962.

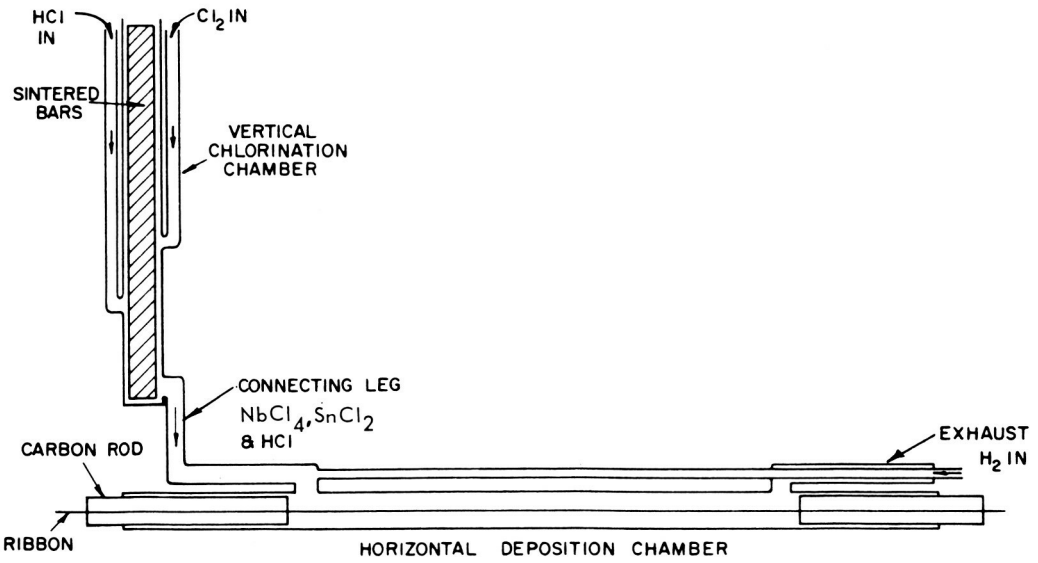

Fig. 1. Schematic Diagram of Nb_3Sn Vapor-Deposition Apparatus.

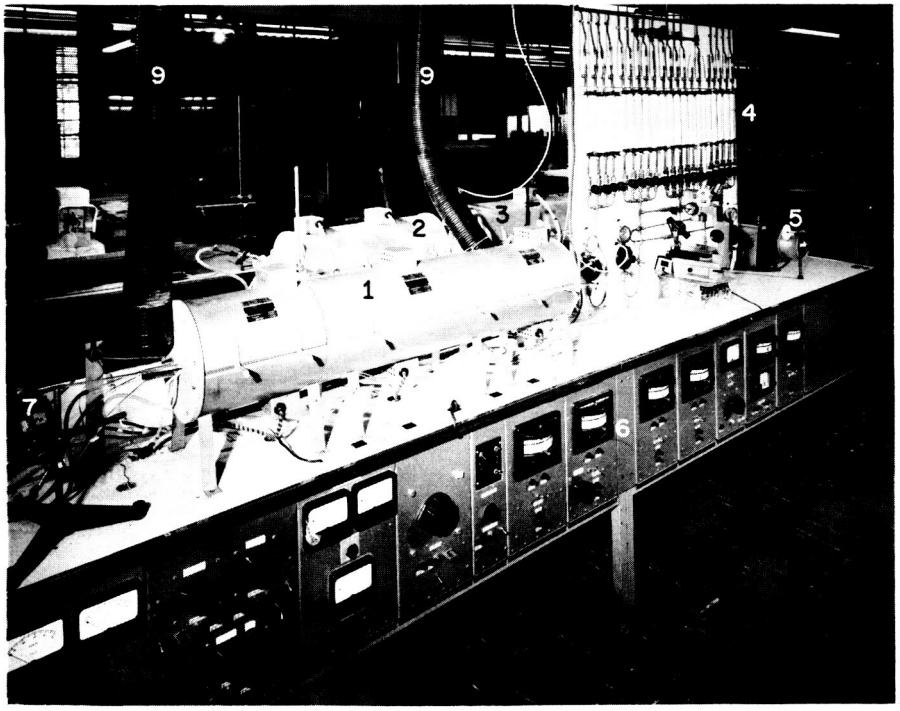

1-DEPOSITION FURNACE
2-TIN CHLORINATION FURNACE
3-NIOBIUM CHLORINATION FURNACE
4-GAS FLOW METERING BOARD
5-WINDING HEAD
6-FURNACE CONTROLLERS
7-EXHAUST STIRRER MOTOR
8-INSPECTION MICROSCOPE
9-EXHAUST GAS VENTS

Fig. 2. Photograph of Nb_3Sn Vapor-Deposition Apparatus.

deposition chamber. The metal chlorides, diluted with helium and the hydrogen chloride gas, are gravity-fed into the deposition chamber. The hydrogen mixes with the metal chlorides at the entrance of the deposition chamber. Overall utilization rate of the metal chloride to deposited Nb_3Sn is approximately 20% efficient. With this early pilot line, ribbon lengths up to 200 meters were processed.

In the early pilot equipment, deposits of Nb_3Sn formed at the chloride inlet to the deposition chamber at the point where the hydrogen gas is added. Later experimentation included multiple hydrogen inlets and separate chlorination of niobium and tin as well as direct introduction of niobium and tin chloride powder mixtures into the reaction chamber.

2. Development of Ribbon Substrate and Geometry

In the original laboratory vapor-deposition apparatus niobium-stannide was deposited on a platinum substrate approximately 0.018 in. wide by 0.002 in. thick. Physical properties of this material have been published (Hanak 1963), and current densities in the superconductive layer as high as 7×10^5 A/cm^2 at 90 kilogauss were attained.

For eventual large-size, high-field magnets requiring miles of ribbon, the use of platinum as a ribbon substrate was considered impractical, not only due to cost but also due to its physical properties of low strength and high ductility.

After much experimentation, Hastelloy, a nickel-base alloy combining high tensile properties with suitable thermal expansion characteristics was developed as a relatively inexpensive but superior substrate. The ribbon width was also increased to 0.088 in. This increase in width leads to higher deposition equipment and process efficiencies as well as improved coil-packing factors.

As the Nb_3Sn coating on the Hastelloy substrate was improved to carry higher current densities, the problem of normal-to-superconducting electrical connections became more critical due to I^2R losses and resultant heating. The early process using a conventional copper electroplating on the Nb_3Sn surface was replaced by a specially developed nickel-flash plating process. The advantage is readily seen in Fig. 3 where the voltage drops across the two types of contacts are shown. Conventional copperplating and/or lead-tin soldering of the nickel-flash deposit is easily controlled once initial bonding to the Nb_3Sn is accomplished.

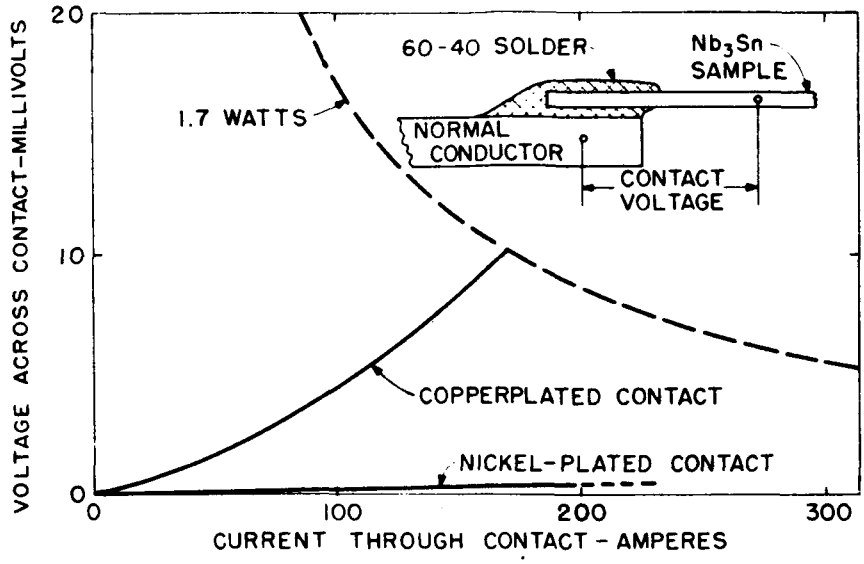

Fig. 3. Voltage Drop Developed across Straight (Short) Sample Contacts. Nb_3Sn Plated with Copper and Nickel.

With nickelplating technique as a base, it was then possible to continuously plate an adherent layer of copper on long lengths of ribbon. The copper layer [approximately equal to the thickness of Nb_3Sn (0.0002 in. to 0.0003 in.)] provides both an excellent electrical conductor as well as a relatively flexible protective sheath over the Nb_3Sn which permits handling and spooling with only moderate care. The copper coating permits winding over as little as a 3/8-in. mandrel diameter.

Processing parameters for producing RCA Nb_3Sn vapor-deposited superconductive ribbon were established early on the basis of data obtained from a 0 to 7,500-gauss Varian magnet. Tests in the 4-in. bore copper magnet, made available by NASA (Lewis Research Center, Cleveland) in December 1962, had corroborated high-field performance of the RCA vapor-deposited Nb_3Sn ribbon.

B. DISCUSSION OF OPERATING PARAMETERS AND PROCESS

1. Operating Parameters Influencing Process

The composition and high-field magnetic properties of the ribbon are variously influenced by the following process parameters:

a. Ratio of tin chloride to niobium chloride.

b. Effect of hydrogen chloride concentration.

c. Effect of substrate temperature.

d. Effect of substrate speed.

e. Effect of initial nucleation.

The parameters are discussed below. A summary of the deposition conditions for the Nb_3Sn ribbon mentioned in the subsequent text can be found in the Appendix.

a. Ratio of Tin Chloride to Niobium Chloride

Table 1 illustrates the change in composition on the ribbon obtained by varying the ratio of tin chloride to niobium chloride.

Table 1

Effect of $SnCl_2/NbCl_4$ Ratio on Ribbon Composition

Run No.	$SnCl_2/NbCl_4$ Ratio	Flow of Cl_2 in ml/min to Chlorination Chambers		Superconductive Layer Composition Atom. % Nb
		Nb Chamber	Sn Chamber	
PNDC 88	1/1	93.5	46.6	77.9
87	2/1	65.0	65.0	76.9
86	3/1	53.0	78.0	76.1
83	4/1	44.0	86.0	75.0
82	5/1	36.0	94.0	73.9
81	6/1	33.0	97.0	68.4

The chemical composition was determined by X-ray fluorescence. In this series of experiments the horizontal furnace was maintained at 750°C, and total chlorine flow was 140 ml/min.

At a lower chloride concentration (total flow of chlorine:100 ml/min), the same experiment was repeated, with comparable results as shown in Table 2.

Table 2

Effect of $SnCl_2/NbCl_4$ Ratio on Ribbon Composition

Run No.	$SnCl_2/NbCl_4$ Ratio	Flow of Cl_2 in ml/min to Chlorination Chambers		Superconductive Layer Composition Atom.% Nb
		Nb Chamber	Sn Chamber	
PNDC B	6.3/1	24	76	71.1
C	4/1	34	66	75.1
D	2/1	50	50	76.2
E	1/1	66	33	77.7
F	1/2	80	20	77.8
G	1/3	85	14	78.3
H	1/4.4	90	10	78.6
I	1/6.4	93	7	79.1

To obtain stoichiometric Nb_3Sn (75 atomic percent niobium), it is necessary to maintain a 3/1 to 4/1 $SnCl_2/NbCl_4$ gas ratio. These experiments were likewise conducted with the deposition furnace temperature at 750°C. Due to the shift of equilibrium constant with temperature, at lower furnace temperatures a lower ratio of $SnCl_2/NbCl_4$ is required to obtain stochiometric material while at higher temperatures the reverse is true.

b. Effect of Hydrogen Chloride Concentration

In the formation of Nb_3Sn, hydrogen chloride gas is released as a product.

$$3\ NbCl_4 + SnCl_2 + 7\ H_2 \rightarrow Nb_3Sn + 14\ HCl \qquad (4)$$

and the equilibrium constant is:

$$Kp = \frac{(HCl)^{14}}{(SnCl_2)\ (NbCl_4)^3\ (H_2)^7} \qquad (5)$$

From the equilibrium constant it is seen that hydrogen chloride gas influences the above-mentioned reactions. As discussed before, deposition of Nb_3Sn on the furnace wall occurs at 750°C. Since the temperature of the ribbon is maintained higher than the furnace-wall temperature, it is possible to add controlled amounts of hydrogen chloride gas to prevent the niobium-tin from forming at the furnace wall, but yet not interfere with deposition on the ribbon. Changes in chemical composition of the ribbon as a function of hydrogen chloride gas added to the system are shown in Tables 3 and 4. Table 3 shows

the results obtained with a 3/1 ratio and Table 4 shows the results obtained with a 4.5/1 ratio. Niobium content increases in both cases with increase in hydrogen chloride. Apparently, hydrogen chloride prevents deposition of Nb_3Sn on the furnace wall, leaving a higher concentration of niobium in the gas stream. Thus, higher niobium concentration in the gas stream results in higher niobium content in the deposit as shown in Table 2. In addition, hydrogen chloride shifts the niobium and tin reduction reaction [reaction (4)] such that less reduction occurs with the specie that is more difficult to reduce ($SnCl_2$).

Table 3

Effect of HCl on Ribbon Composition

With a Constant $SnCl_2/NbCl_4$ Ratio of 3/1

Run No.	Total Flow of Cl_2 to Chlorination Chambers ml/min	Flow of HCl to Nb Chlorination Chambers ml/min	Superconductive Layer Composition Atom.%·Nb
PNDC 74	130	0	75.9
70	130	14	75.7
71	130	36	76.0
72	130	63	76.4
73	130	78	76.7

Table 4

Effect of HCl on Ribbon Composition

With a Constant $SnCl_2/NbCl_4$ Ratio of 4.5/1

Run No.	Total Flow of Cl_2 to Chlorination Chambers ml/min	Flow of HCl to Nb Chlorination Chamber ml/min	Superconductive Layer Composition Atom.% Nb
PNDC 101	130	0	74.5
102	130	14	74.7
103	130	36	75.5
104	130	63	75.9

c. Effect of Substrate Temperature

Inasmuch as the equilibrium constant (Kp) of Nb_3Sn formation changes with temperature, it is expected that a shift in composition should occur as ribbon

temperature is varied. The temperature of the ribbon is monotonically related to the wattage on the ribbon at a constant furnace temperature. Thermocouple, pyrometric, and resistive ribbon temperature measurement techniques have not been successful due to many experimental difficulties (e.g., corrosiveness of chlorides, deposition of Nb_3Sn on quartz walls). Accordingly, ribbon temperature is specified only in a relative sense by the measured applied wattage. This was verified experimentally and is shown below in Table 5.

Table 5

Effect of Ribbon Temperature on Composition

Run. No.	Wattage on Ribbon	Superconductive Layer Composition Atom.% Nb
PNDC 78	20	75.1
77	30	75.9
75	75	76.1

d. Effects of Substrate Speed

As ribbon speed is varied, residence time of the ribbon in the deposition furnace is changed. Changes in deposit composition as ribbon speed is varied are shown in Tables 6 and 7 for $SnCl_2/NbCl_4$ ratios of 3/1 and 4/1. As ribbon speed is increased and process inputs remain constant, the ribbon composition shifts to a lower niobium content.

Table 6

Effect of Ribbon Speed on Composition
With $SnCl_2/NbCl_4$ Ratio of 3/1
and Constant Ribbon Temperature

Run No.	Ribbon Speed (meters/hour)	Superconductive Layer Composition Atom.% Nb
PNDC 96R	10	76.2
97R	15	75.7
98R	17.5	75.7
99R	20	75.4
100	22.5	75.3

Table 7

Effect of Ribbon Speed on Composition

With $SnCl_2/NbCl_4$ Ratio of 4/1

and Constant Ribbon Temperature

Run No.	Ribbon Speed (meters/hour)	Composition Atom. % Nb
PNDC 114	10	77.0
115	15	76.9
116	17.5	76.4
117	20	76.1
118	22.5	75.7

e. Effect of Initial Nucleation

In the reaction chamber, deposition of Nb_3Sn occurs over a 20-in. zone. As deposition progresses, composition changes of the reactant gas stream include a reduction in $NbCl_4$ and $SnCl_2$ concentration and an increase in the HCl concentration. The niobium-stannide can be deposited either with the ribbon and gases moving concurrently or countercurrently.

Materials deposited countercurrent to the gas stream are designated by the prefixes HP, PNDC, HDC. Since initial nucleation of Nb_3Sn strongly influences composition, crystal size and orientation, experiments were conducted in which the Nb_3Sn was deposited on the ribbon concurrent to the gas stream flow.

In these experiments, initial nucleation occurs in the chloride-rich gas stream as opposed to the countercurrent feed where initial nucleation occurs in the chloride-lean and hydrogen chloride-rich region. PNDCR 3 was deposited in this manner. This material was, electromagnetically, almost completely stable over the magnetic field tested. The Nb_3Sn composition also was more uniform throughout its thickness from initial nucleation to final deposit.

2. Uniformity of Nb_3Sn over 1000-Meter Lengths

Under low magnetic field testing, short-sample performance characteristics of ribbon indicated that no major differences in superconductive current-carrying capacity existed over 1000-meter lengths. However, several portions of long lengths were wound into 2-inch-long by 1-1/4-inch-I.D. coils and tested

at LeRC in high magnetic fields. Some differences in current-carrying capacity were then observed. For the present, all ribbon is produced in 500- to 600-meter lengths, thus ensuring uniformity over the entire length of deposition.

C. CHARACTERISTICS OF Nb_3Sn VAPOR-DEPOSITED RIBBON

1. *Initial Characterization*

The predominant effort of Phase I was an exhaustive test program to electromagnetically evaluate Nb_3Sn ribbon uniformity as a function of ribbon length. To this end, a 150-meter length (HDC6) was processed using standard dual chlorination equipment. The ribbon was not copperplated in order to obtain the basic Nb_3Sn high-magnetic-field superconductive properties. This length was divided into six 20-meter sections and straight samples from each section prepared for tests in the LeRC 4-inch magnet.

Since it was generally known that the critical currents of superconductors are sensitive to test conditions, such as the rate of application of current, contact resistance, mechanical movement, the HDC6 reference length test results were analyzed for validity of test procedures. It was found that mechanical movement of the dipstick due to the forces on the superconductor in the field does introduce a variable into testing and affects the critical current in the sample.

To avoid the possibility of prematurely making samples under test go normal, it was necessary to rigidly center the test "dipstick" in the test dewar. Tests on rate dependence and effects of different waiting times between subsequent tests are shown in Fig. 4. Several conclusions for HDC6 are drawn from these tests:

a. At any one field, successive critical current tests at a constant rate of current rise can yield a scatter in I_c by a factor of 2. There is no obvious hysteresis or dependence upon history. Several attempts to yield consistent values of I_c (Not shown in Fig. 3) by raising the sample above T_c between tests show the same random behavior.

b. Rate of current application at any one field has a definite effect over and above the scatter mentioned in a.

c. The interval of time between successive critical current tests is not significant for short samples to as short a time period as 5 seconds after the sample goes normal.

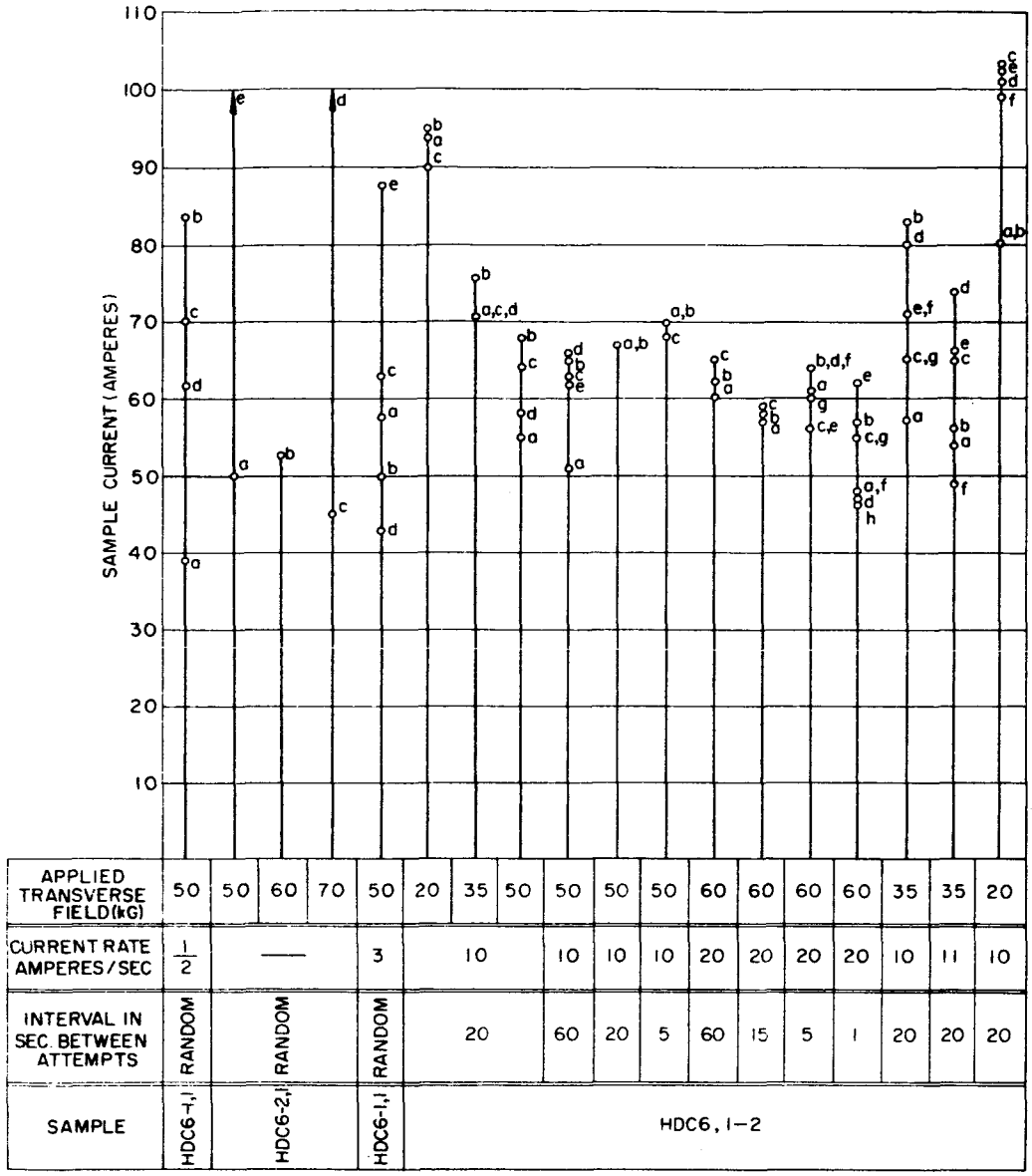

Fig. 4. Effects of Current Rate and Waiting Interval (Time at Zero Current) between Subsequent Tests on Short Samples of Nb_3Sn Unplated Ribbon.

2. Concept of the Relative Stability of Nb_3Sn

Another factor which was generally recognized as a testing "anomaly" is the lack of reproducibility in critical data when interchanging the sequence of field and current application in short samples. Table 8 gives the results of a test in which the differences in critical characteristics are shown when the testing is done in reversed sequence. First, the current is set at the value indicated in the first column (I_{set}) with zero background field. The

field is then increased until the sample goes normal. This field is listed in the second column (H_c). Therefore, I_{set} and H_c are the critical current and field for the condition of changing field. When the sample goes normal, the background field is maintained at the same value, H_c. Current to the sample is interrupted so as not to heat the substrate and the sample is allowed to attain thermal equilibrium with the helium bath. Sample current is then increased at this constant field, H_c, until it again goes normal, this critical current being I_c (third column). It is obvious from Table 8 that a wide difference exists between I_{set} and I_c, and that the manner in which experiments are conducted determines the results for Nb_3Sn exhibiting unstable characteristics. Many other tests confirmed this pattern.

Table 8

Effect of the Sequence of Application of Current and Field Upon the Critical Current Level of Unstable Nb_3Sn

Sample No.	I_{set}, Amperes	H_c, Kilogauss	I_c, Amperes
HDC6, 2-1	60	0	125
	35	0.5	88
Test 7	39	1.4	101
	42	2.8	107
	30	5.0	58
HDC6, 3-1	26	4	145
	26	5	94
Test 8	26	13	134
	26	14	73
	26	26	66
	26	37	68

Further extensive tests on the HDC series are summarized in Fig. 5 where the upper limit of the critical currents of bare (not copperplated) short samples are indicated. Depending upon the severity of the tests (i.e., field and current rates and sequence of application), the points at which samples became normal fell within most of the region of the curve below this upper limit. It is apparent that this superconductor is characterized by its scattered H_c-I_c characteristics, and is generally representative of what we have since labeled

as "unstable" material. One run of the HDC series and several experimental runs of the PNDC series showed partial to almost complete "stability" when tested for I_c and I_{set}.

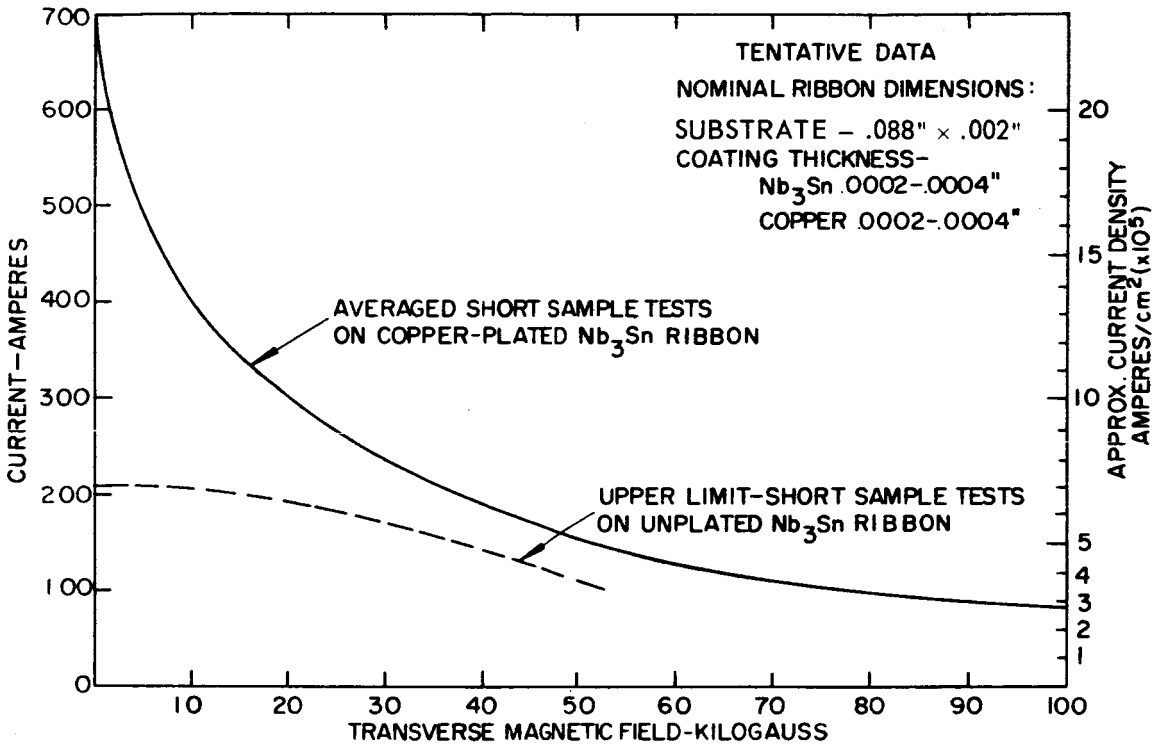

Fig. 5. RCA Superconductive Ribbon Critical Current vs. Magnetic Field.

Figure 6 gives several examples of borderline cases where some stability was evident above 50 kilogauss but a breakdown of the pattern appears to an increasing degree below 50 kilogauss. While conducting these tests it soon became evident that an extensive amount of probing by changing the current and magnetic field would be necessary to find definitive regions of the H_c-I_c curve. It was found that the critical currents and fields, when in any region of partial stability, are statistical in nature, and that the statistics for such a region are, to some extent, dependent upon test conditions such as rate of current and field application.

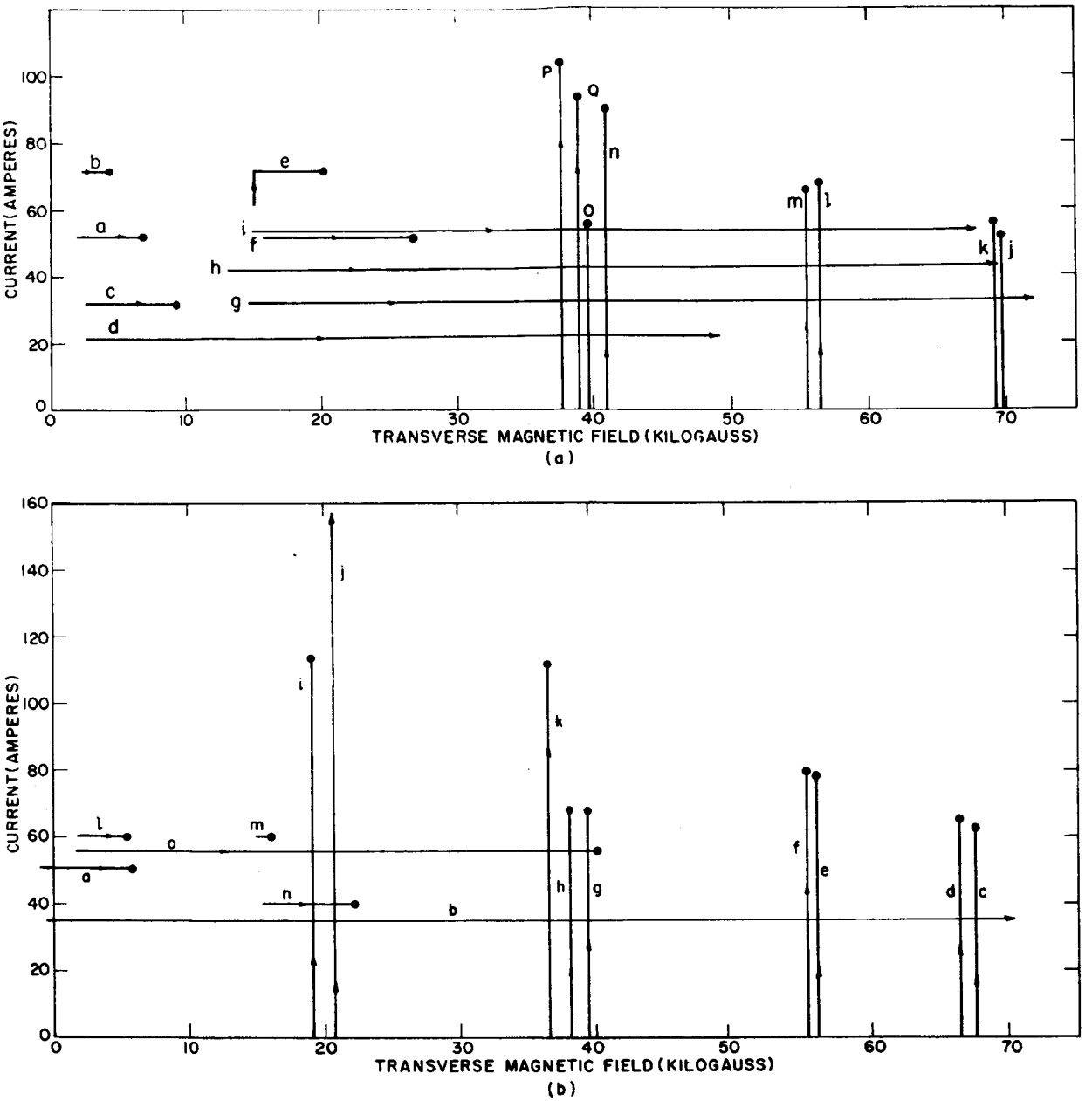

Fig. 6. Critical Current vs. Magnetic Field for Straight Samples Showing Partial Reproducibility. (a) PNDCR 12, Test 4; (b) PNDCR 14, Test 12.

In Fig. 6 (a), with current initially set and field increased, normality occurred at low fields. The applied field was then increased to 70 kilogauss and a series of I_c points determined down to 37 kilogauss. Although a general H_c-I_c curve could be drawn through these I_c points, such a curve is not well defined, with the accuracy of definition decreasing in the lower fields.

Figure 6 (b) shows a situation where I_c points above 50 kilogauss lie on a curve well defined to within 1 ampere. Below 40 kilogauss the I_c points are scattered and are similar to unstable material shown in Fig. 4. The I_{set} points are particularly noteworthy for demonstrating that the region cut out of the H_c-I_c curve by unstable effects is not a sharply defined dip. Point "o" is the result of an initially set current which is between those of points "a" and "ℓ". Yet, it was possible to extend the field out to 40 kilogauss for the current of point "o" as opposed to between 5 and 6 kilogauss for points representing currents both above and below this value.

Approaching cases of a greater degree of stability, Fig. 7 shows excellent "classical" H_c-I_c characteristics down to 28 kilogauss. Below 28 kilogauss there are noticeable deviations. Point "s" shows a case of superconducting-to-normal transition occurring in a decreasing field. This is an example of a relatively sharp transition existing between stable and unstable conditions.

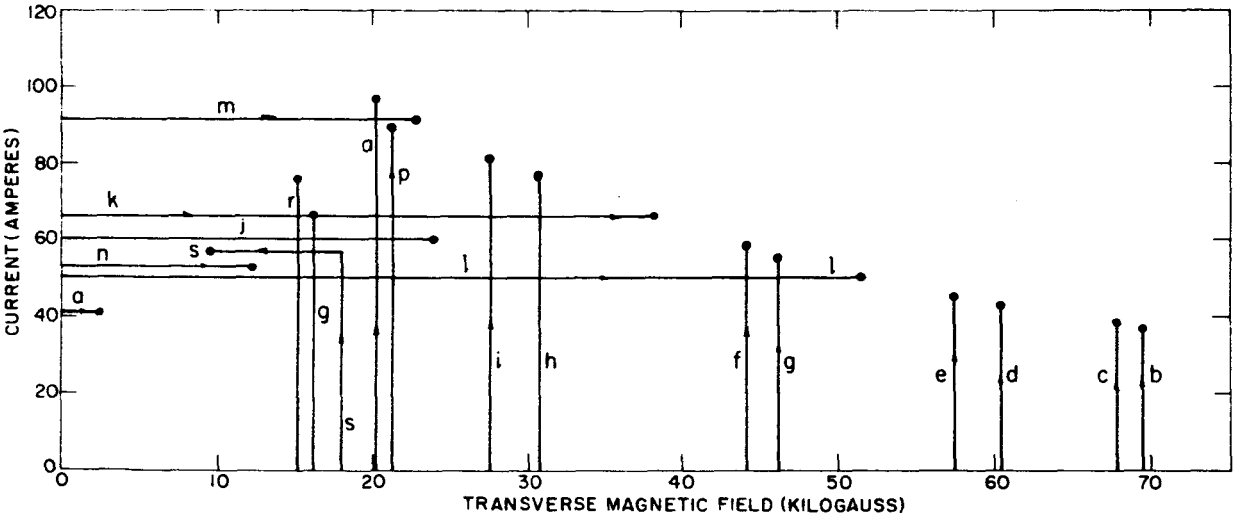

Fig. 7. Critical Current vs. Magnetic Field for Straight Samples Showing Partial Reproducibility (Sample HDC 15).

Figure 8 represents almost complete stability where, after some point during the test, some minor change occurred in the superconductive sample to yield a second H_c-I_c curve somewhat lower than the first, but which still retained stable characteristics.

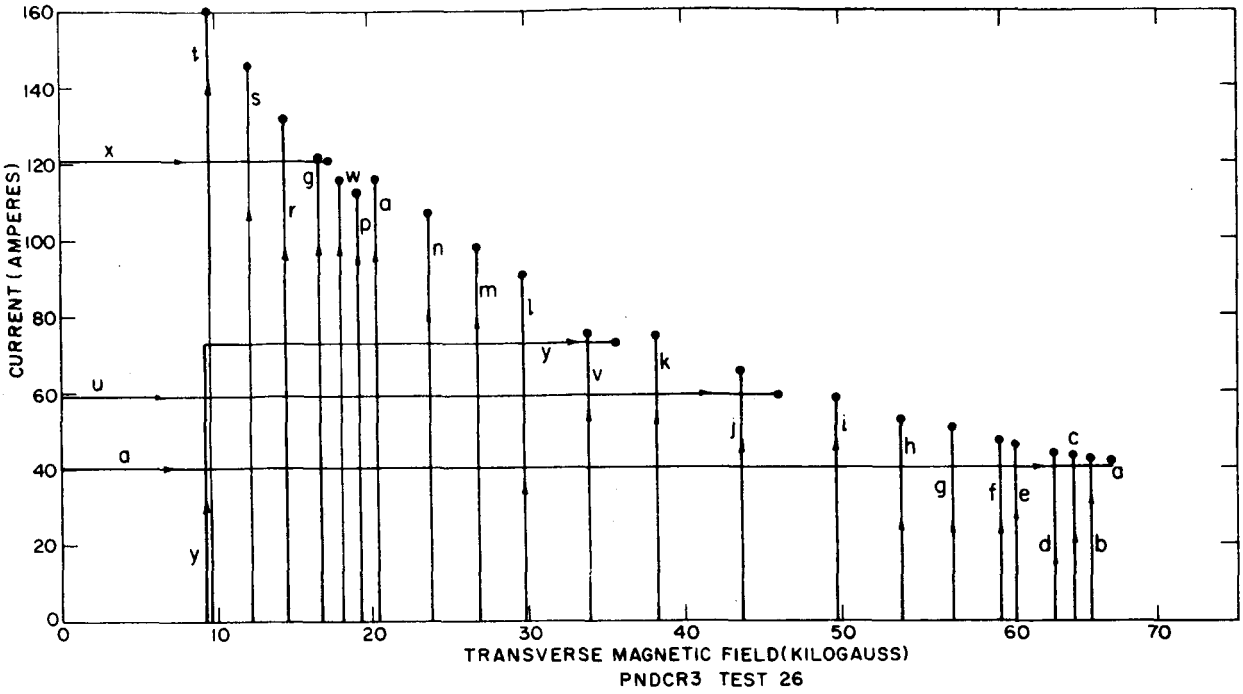

Fig. 8. Critical Current vs. Magnetic Field for Straight Samples Showing Partial Stability.

3. Factors Influencing Degree of Nb_3Sn Ribbon Stability

Vapor-deposited Nb_3Sn ribbon materials vary in stability from unstable to complete stability. Material with various degrees of stability can be deposited, depending on the operating conditions of the vapor-deposition chamber. Even though these materials are made under controlled and reproducible conditions, a full physical understanding of the causes and differences between stable and unstable material has not yet been obtained. Five carefully selected samples of niobium-stannide ribbon utilizing two substrate materials and falling into both the stable and unstable class of materials were investigated and are listed in Table 9.

The data developed on these materials covered (1) low-field (0 to 13 kG) electromagnetic characteristics, (2) critical temperature, (3) chemical composition, (4) metallographic examination, (5) crystal orientation, (6) impurities in Nb_3Sn deposit, and (7) X-ray diffraction.

Table 9

Factors Influencing Degree of Nb_3Sn Ribbon Stability

Sample No.	Substrate	Electrical Type	Mode of Manufacture
HDC-46 END	Platinum	Stable	Dual Chlorination
PF 10	Platinum	Stable	Powder Feed
HDC-46 BEG	Hastelloy Platinum-Plated	Not Stable	Dual Chlorination
PF 2B	Hastelloy Platinum-Plated	Stable	Powder Feed
PF 8C	Hastelloy	Stable	Powder Feed

The results of low-field (0 to 13 kG) electrical measurements are given in Figs. 9 to 13. All samples are stable with the exception of "HDC-46 BEG". The current levels of the first four samples range between 60 to 100 amperes at 12 kG. The current level of HDC-46 BEG is considerably higher, but difficult to define since it is unstable.

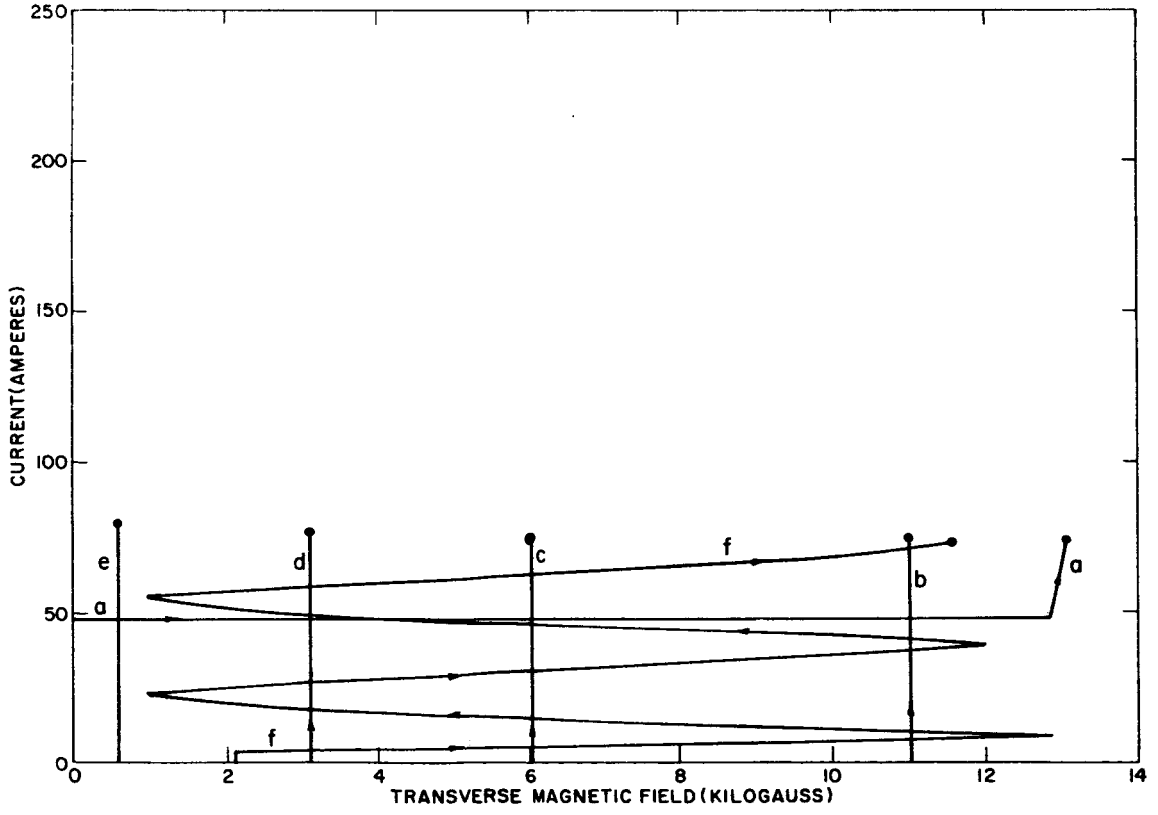

Fig. 9. Critical Current vs. Magnetic Field for Sample HDC-46 END.

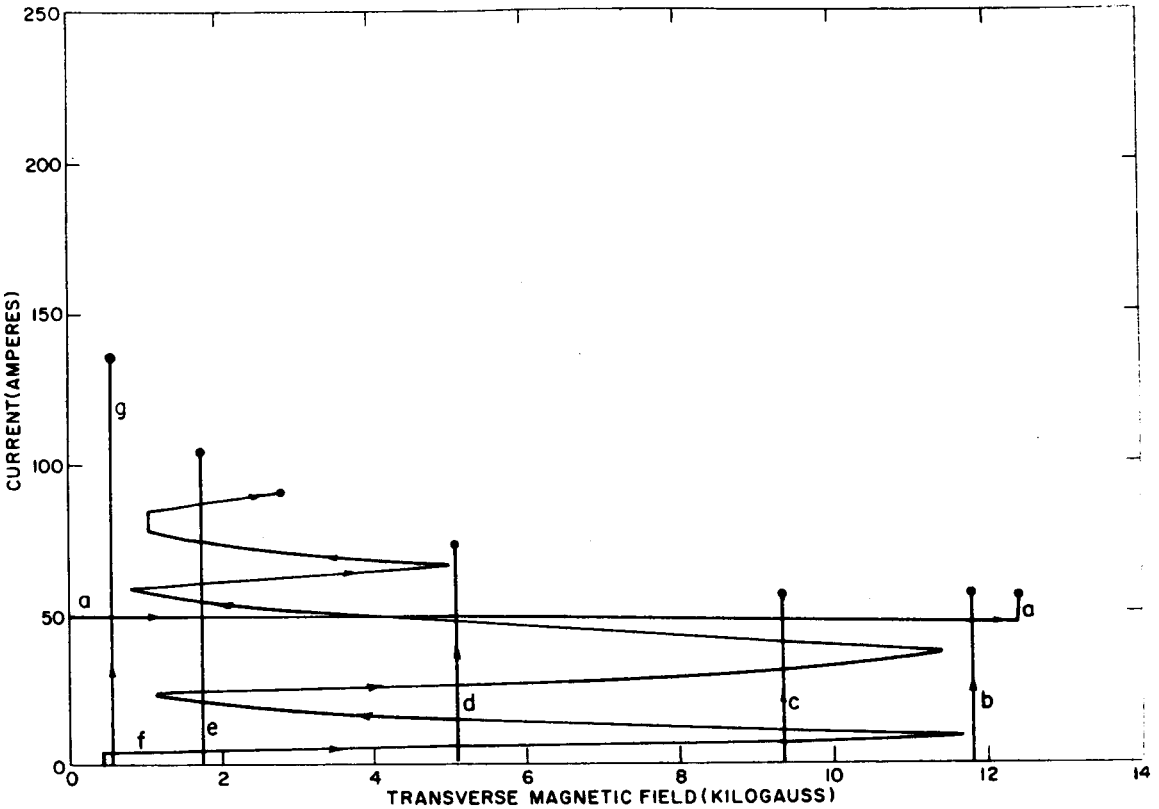

Fig. 10. Critical Current vs. Magnetic Field for Sample PF 10.

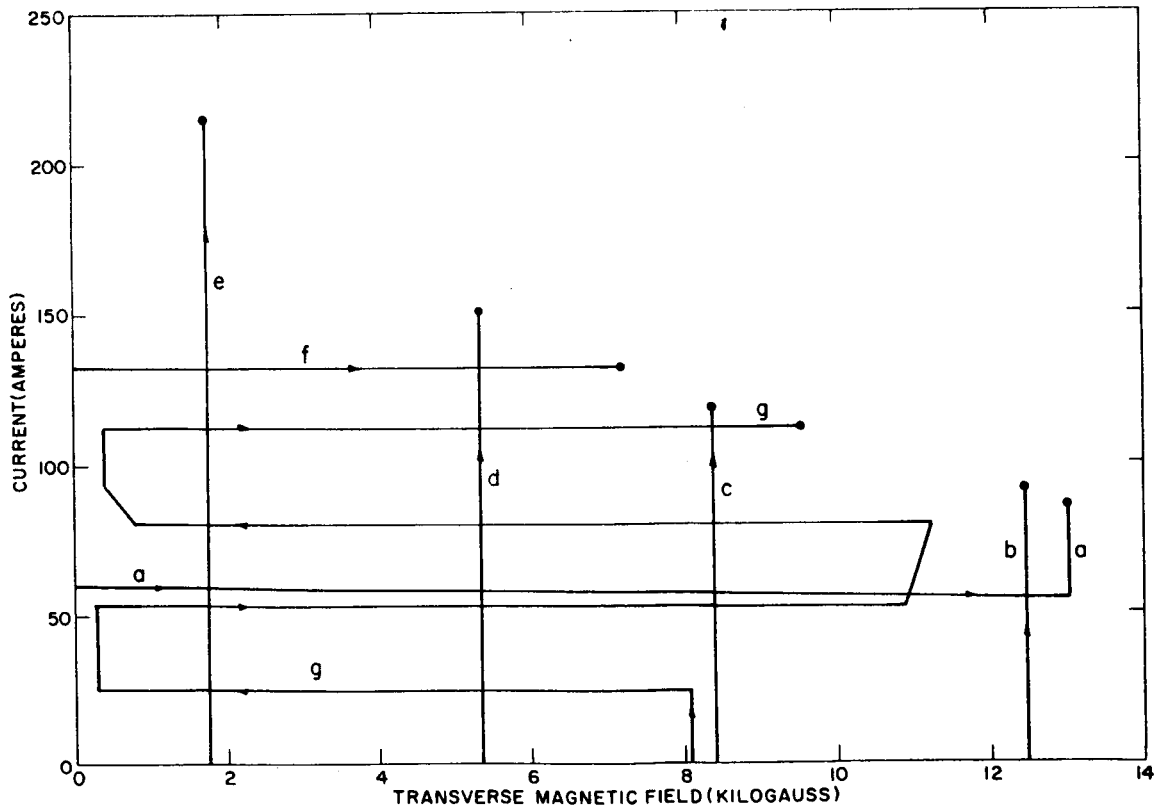

Fig. 11. Critical Current vs. Magnetic Field for Sample PF 2B.

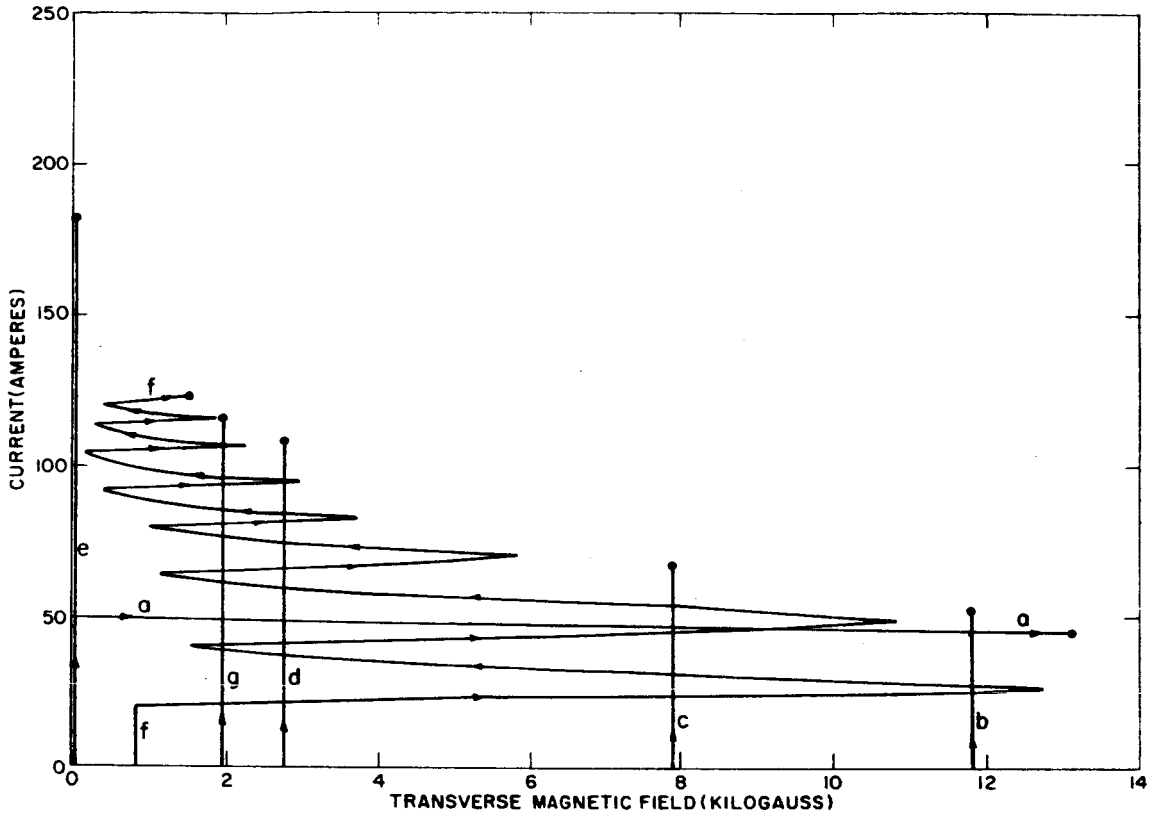

Fig. 12. Critical Current vs. Magnetic Field for Sample PF 8C.

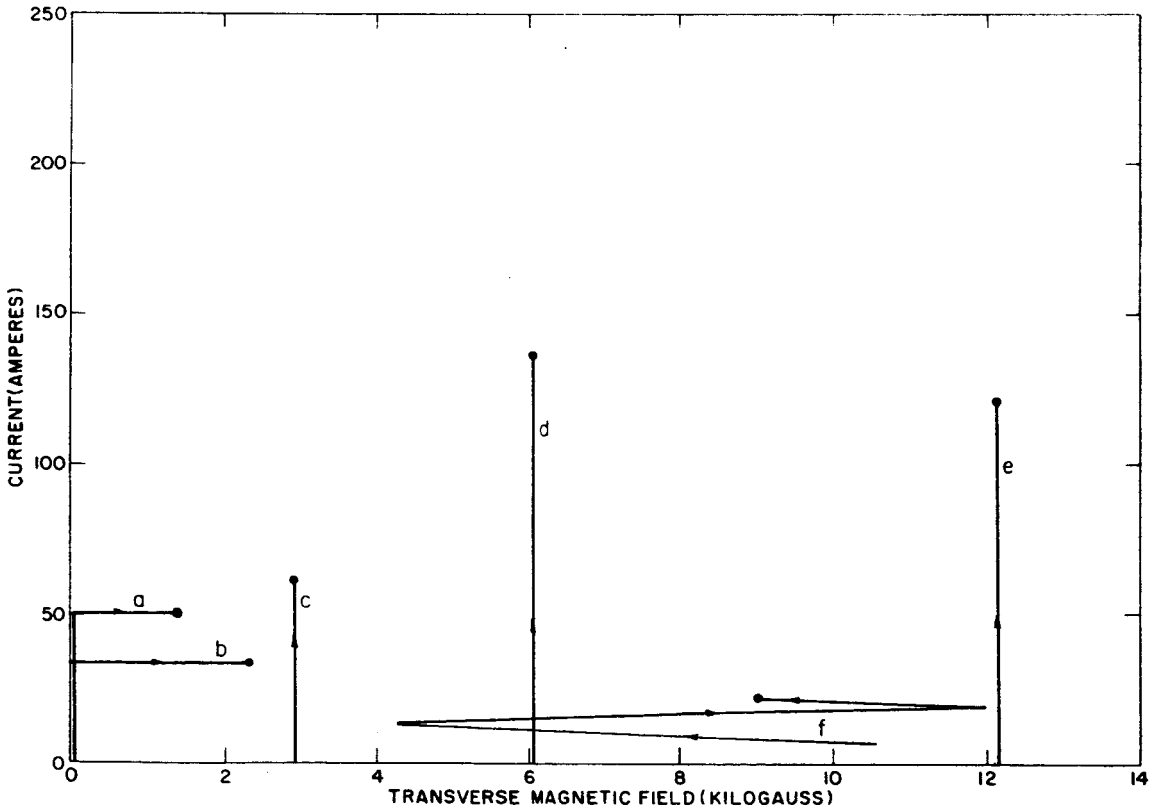

Fig. 13. Critical Current vs. Magnetic Field for Sample HDC-46 BEG.

The critical temperature curves of the five samples are shown in Fig. 14. In general, the critical temperature varies over a broad range of temperatures ranging from 4^{o} to $16^{o}K$, with the major transition from 9^{o} to $16^{o}K$. No major

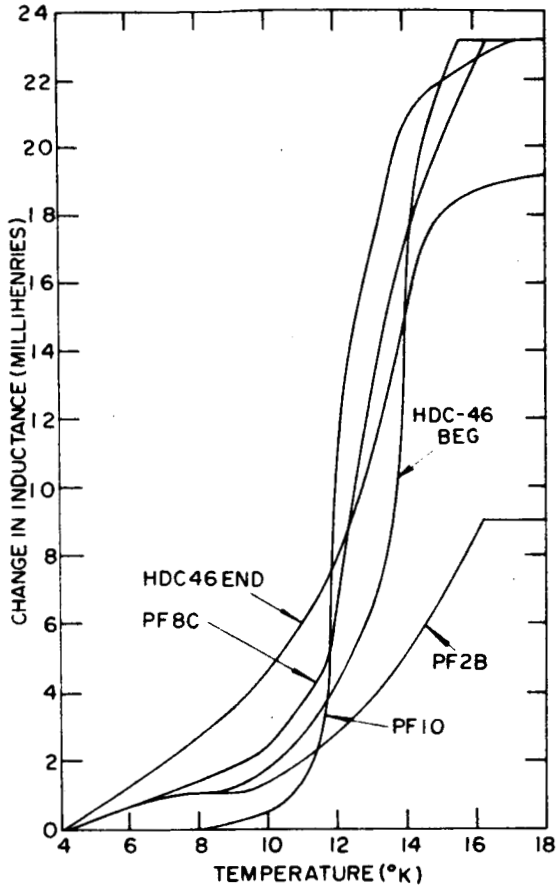

Fig. 14. Critical Temperature of Nb_3Sn Ribbon Samples Exhibiting Different Stability.

differences in critical temperature are observed except in sample PF 10 (platinum substrate) where the transition temperature range is narrower than the others and the transition starts at a higher temperature ($8^{o}K$). These broad transition temperature ranges are observed when one side of the Nb_3Sn is removed from the ribbon, thus exposing magnetically the entire deposit thickness. If the one side is not removed, the highest critical-temperature material deposited at the outer surface obscures the underlying material, and a misleading sharp transition at about $16^{o}K$ is observed.

Due to the changing gas reactant conditions along the length of the deposition chamber, the Nb_3Sn composition and crystal structure deposited on the

substrate changes from an initial deposit of 70 atomic percent niobium to a final deposit of 79 atomic percent niobium. The broad transition temperature for niobium-stannide ribbon is associated with this range of niobium-tin composition.

The composition of the five samples, obtained by X-ray fluorescence, is as follows:

Run No.	X-ray Fluorescence of Superconductive Layer Atomic % Nb
HDC-46 END	75.8
PF 10	72.7
HDC-46 BEG	74.9
PF 2B	76.0
PF 8C	76.0

Metallographic examination of the above samples has revealed gross differences in grain structure. These differences are due primarily to the difference in substrate (platinum vs. Hastelloy). However, stability does not appear to correlate with crystal size. Likewise, crystal orientation studies did not reveal major differences in these samples. All crystals grew with a preferred orientation in the [211] direction. The same concentration levels of impurities were present in all samples.

Powder diffraction patterns confirm that the lattice spacing of all five samples is 5.293 ± 0.005 Å, and show considerable broadening of X-ray lines. All five samples appear to be single phase; a second phase was not observed in the diffraction patterns. The broadening of X-ray lines further indicates variation in chemical composition of the Nb_3Sn deposit.

The phase diagram (Enstrom, 1963) for the niobium-tin system is shown in Fig. 14 A.

The information gathered on these selected samples indicates no apparent correlation between stability and (1) critical temperature, (2) composition, (3) metallographic structure, (4) impurities in Nb_3Sn deposit, (5) crystal orientation, and (6) lattice spacing. Consequently, the differences between stable and unstable ribbons are considered to be associated with some less obvious physical property. Further work in this direction was not done since it would require extensive research and was beyond the scope of this contract.

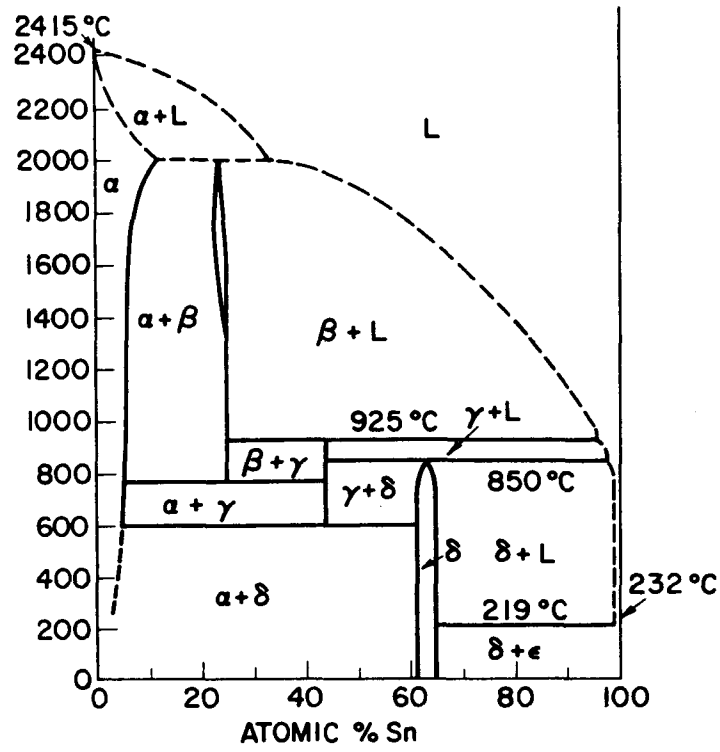

Fig. 14A. Tentative Phase Diagram of Nb-Sn System. β is Nb_3Sn, γ is Nb_3Sn_2, and δ is Nb_2Sn_3.

4. Effect of Annealing on Stability of Nb_3Sn Ribbon

Pilot line run HDC 41 was heat-treated for periods ranging from 1/2 to 1 hour at temperatures ranging from 300 to 700°C. The results are set forth in Table 10.

Table 10

HDC 41 Annealed in H_2 for 1/2 Hr at Indicated Temperatures

Condition	Initial	320°C	440°C	500°C	600°C	700°C
Copperplated	Material Unstable. I_c @ 12 kG > 350A	No change	I_c decreased. Material more stable.	Material completely stable. I_c decreased to 280 A @ 12 kG	Material partially stable. I_c=280A @ 12 kG	Material unstable. I_c = 280 A @ 12 kG
Not Copperplated	Material Unstable. I_c @ 12 kG > 350A	No change	———	Material partially stable.	I_c decreased from 500°C level. Material partially stable.	Material completely unstable. I_c increased.

In addition to these tests, unstable Nb_3Sn deposited on a platinum substrate, stable Nb_3Sn deposited on platinum-plated Hastelloy, and stable Nb_3Sn deposited on a platinum substrate were also heat-treated over the same range of temperatures as HDC 41. All results indicated that unstable material could be made stable and vice versa. The above results cannot be explained in terms of the phase diagram for niobium-tin inasmuch as the annealing periods were of short duration and at the relatively low annealing temperatures diffusion processes in the solid state are very slow. A quantitative understanding of the observed results requires additional detailed investigation and is beyond the scope of this contract.

5. Substrate

a. Effect of Substrate Material on Superconductive Performance

The original substrate for the RCA vapor-deposition process was platinum from which the high performance superconductive properties of vapor-deposited Nb_3Sn was first proven. In terms of cost, strength, and expansion properties, Hastelloy was later developed as a superior substrate material for practical usage. The deposition process parameters were optimized to yield high currents as tested at RCA in the available 7,500-gauss field. Previous to this contract, several high-field tests at NASA (LeRC) and at the Lawrence Radiation Laboratory confirmed the extrapolated high currents at high magnetic fields.

During the course of this contract, when the concept of "stability" was discovered for Nb_3Sn, it became desirable to re-evaluate the role of the substrate in terms of this new concept. The degree of stability of the superconductive layer was indeed different on platinum and Hastelloy substrates, even though the Nb_3Sn was deposited under identical process conditions. Previously, it was shown that degree of stability can be altered by process parameters. It is apparent that the substrate exhibits a strong effect on Nb_3Sn crystal growth by its effect on initial nucleation.

b. Effect of Ribbon Size on Performance

The need for precise control of coil geometry to study superconductive magnet degradation led to the single ribbon width module design which can be conveniently stacked to any desired coil length. It was not practical to retain similar geometry and construction with narrow width ribbons. To approximate these coil geometries with a narrow ribbon width, standard 0.088-in.

ribbon was prepared in approximately 40-meter lengths with a scribed narrow groove of Nb_3Sn etched out on both sides continuously down the center of the ribbon width, effectively converting the single-width superconductive ribbon into two superconductive ribbons approximately 0.040 in. wide and electrically connected in parallel. Figure 15(b) shows a cross section of the scribed portion.

Since the scribed ribbon is essentially copperplated in the same manner as the material described previously, the high currents attained make valid H_c-I_c curves difficult to attain. One scribed sample did not go normal at 130 amperes and 70 kilogauss. Additional results on scribed ribbon are presented in the section on coils.

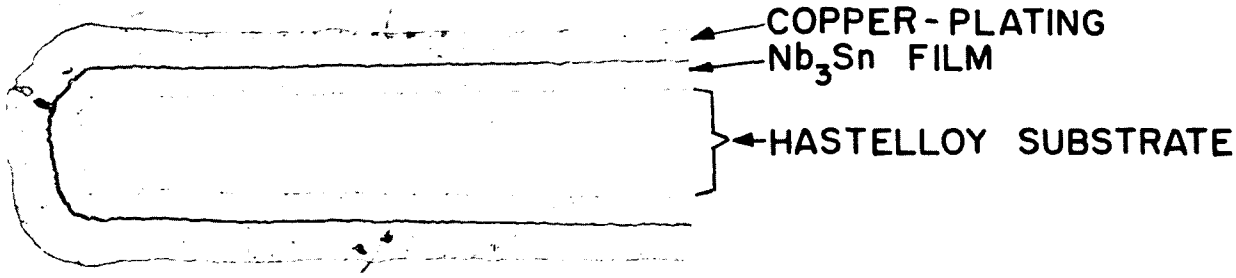

Fig. 15(a). Cross Section of End of Copperplated Nb_3Sn Ribbon on Hastelloy Substrate.

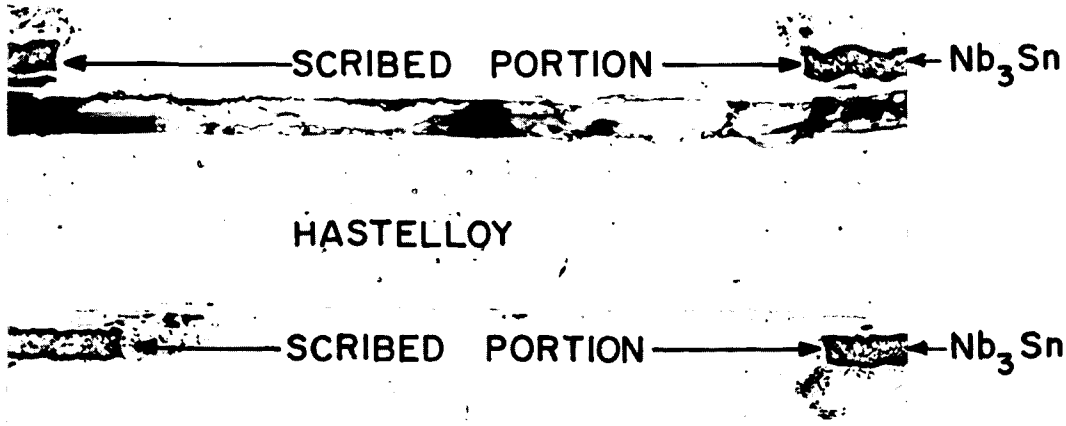

Fig. 15(b). Cross Section of Scribed Portion of Copperplated Nb_3Sn Ribbon.

6. Effect of Plating on Nb_3Sn Ribbon

The role of plating or cladding a superconductor with a normal conductor to improve coil characteristics is thought to be an alteration of the normal state resistance and normal front propagation velocity (Stekly 1963), and as a sink for unwanted induced eddy currents (Montgomery 1962). When short samples of copperplated Nb_3Sn ribbon are tested, the H_c-I_c pattern is drastically modified. Not only is the current at any field 2 to 3 times higher, but there is also a great increase in stability. Figure 16 is an example of a copperplated sample which showed no evidence of instability when swept by changing

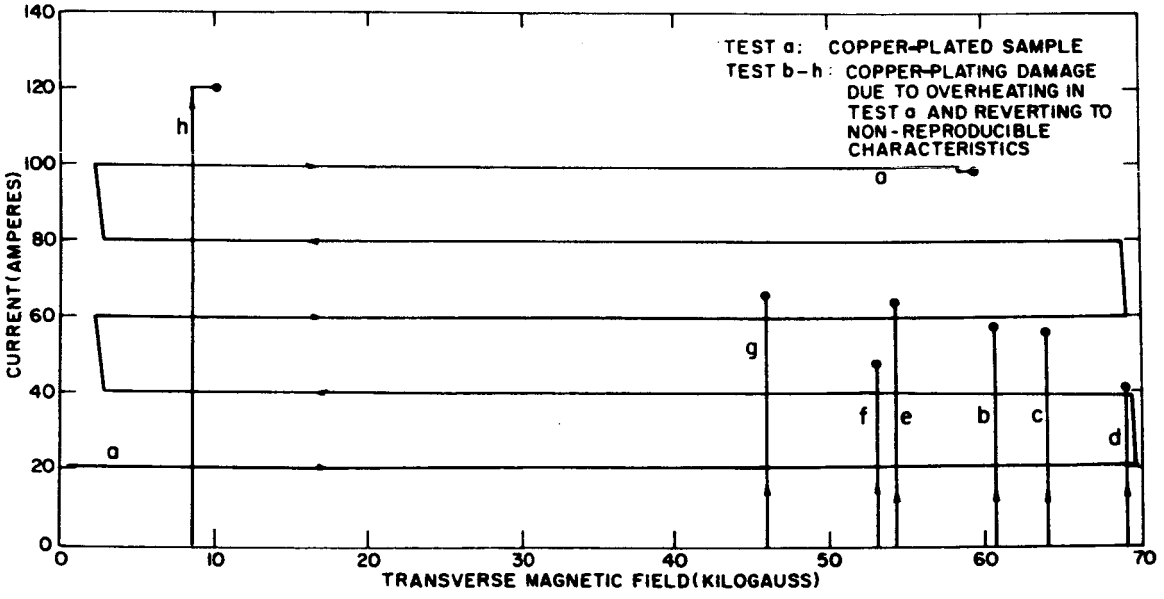

Fig. 16. Examples of Characteristics of Copper and Non-Copperplated Material for Sample HDC 8, Test 38.

magnetic fields and increasing currents. However, after this sample went normal at 100 amperes and 60 kilogauss, the plating was visibly melted off in a ring approximately 1/32 in. long completely around the periphery of the sample. Further testing of this same sample yielded the typical nonreproducible pattern shown by points "b" to "h". Another example is shown in Fig. 17. This material is from the same run as in Fig. 6 except that it is copperplated. Multiple H_c-I_c values at lower fields and high currents could not be attained due to sample damage upon going normal. However, the average data from many

tests at several laboratories give an approximate H_c-I_c curve for short sample, copperplated HDC-type Nb_3Sn ribbon. This is given in Fig. 5 along with the unplated short-sample results.

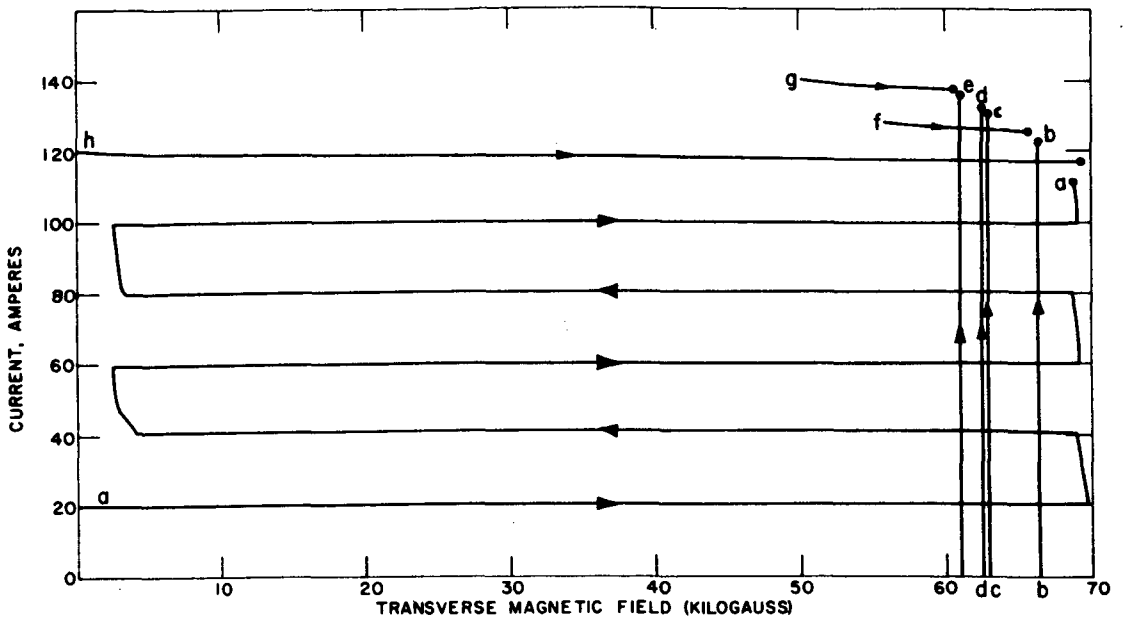

Fig. 17. Example of Characteristics of Copperplated Material.

To obtain a better understanding of the role of metal coating on a superconductor, a separate RCA-funded program was initiated to investigate this. Pertinent information is presented below.

Initial investigation of low magnetic field (0 to 13 kG) superconductive properties of copper- and silver-clad Nb_3Sn ribbon indicate that:

1. Silverplating is superior to copperplating at equivalent electro-deposition rates in stabilizing Nb_3Sn ribbon.
2. Slow deposition rates are superior to fast deposition rates.

Figures 18(a) and 18(b) show the improvement of silver- over copperplating, and Figs. 19(a) and 19(b) show the increased stability of a slow deposition rate versus a fast deposition rate of silver. Decreasing the electro-deposition rates decreases the electrical and thermal resistivity of the plated normal conductor and improves ribbon stability due to the lower resistance eddy-current paths as well as better thermal cooling.

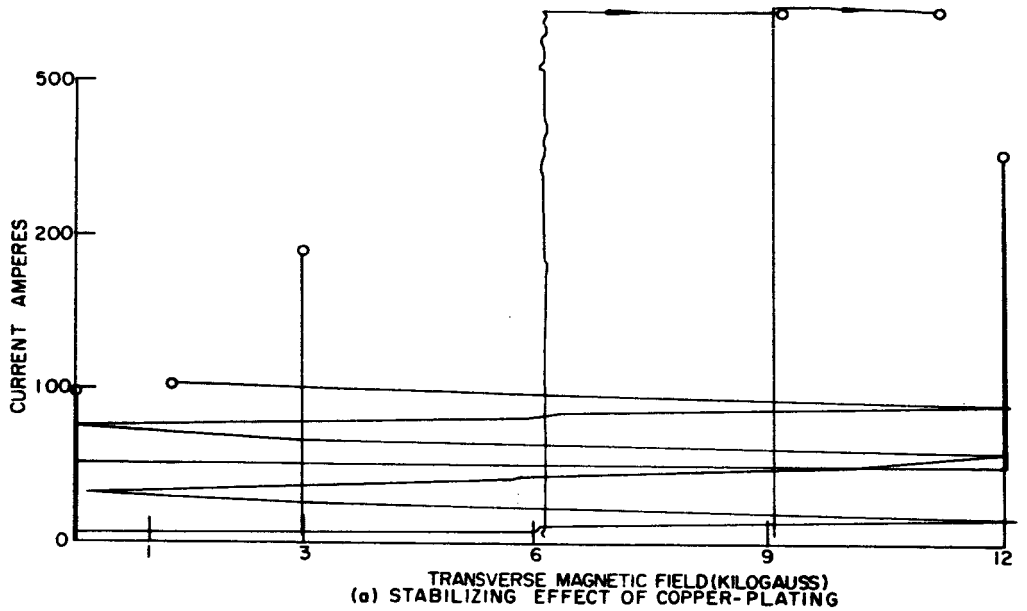

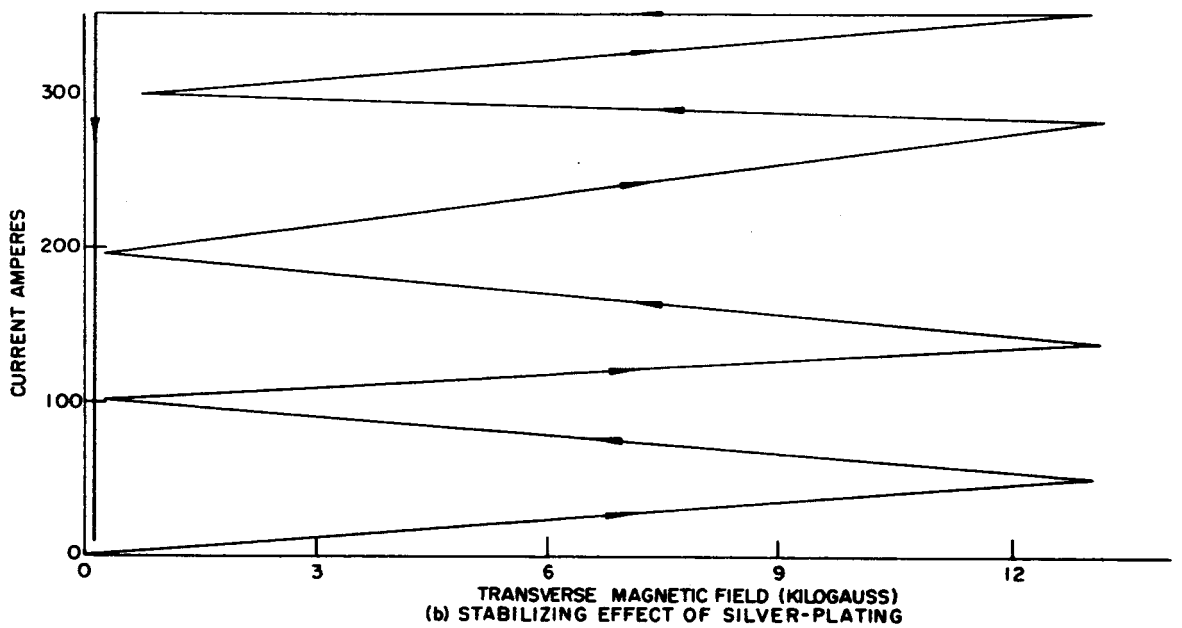

Fig. 18. Stabilizing Effect of Copper (a) and Silver (b) Deposited at Same Current Density, on HDC 56.

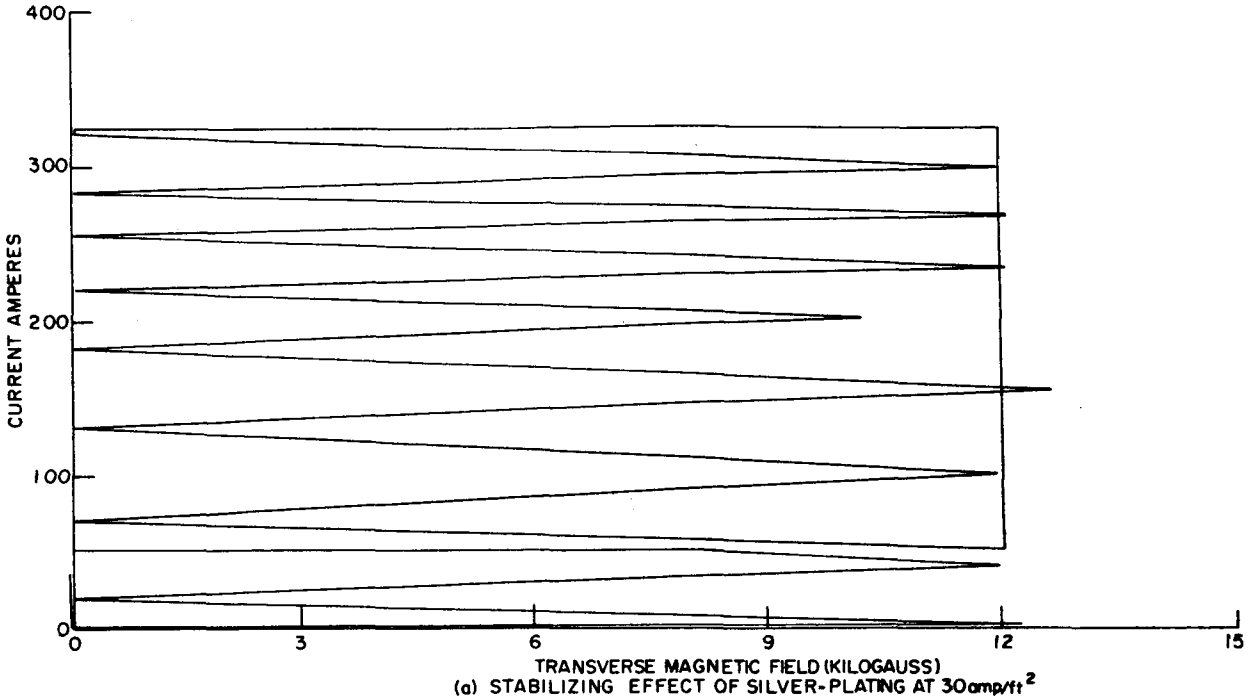

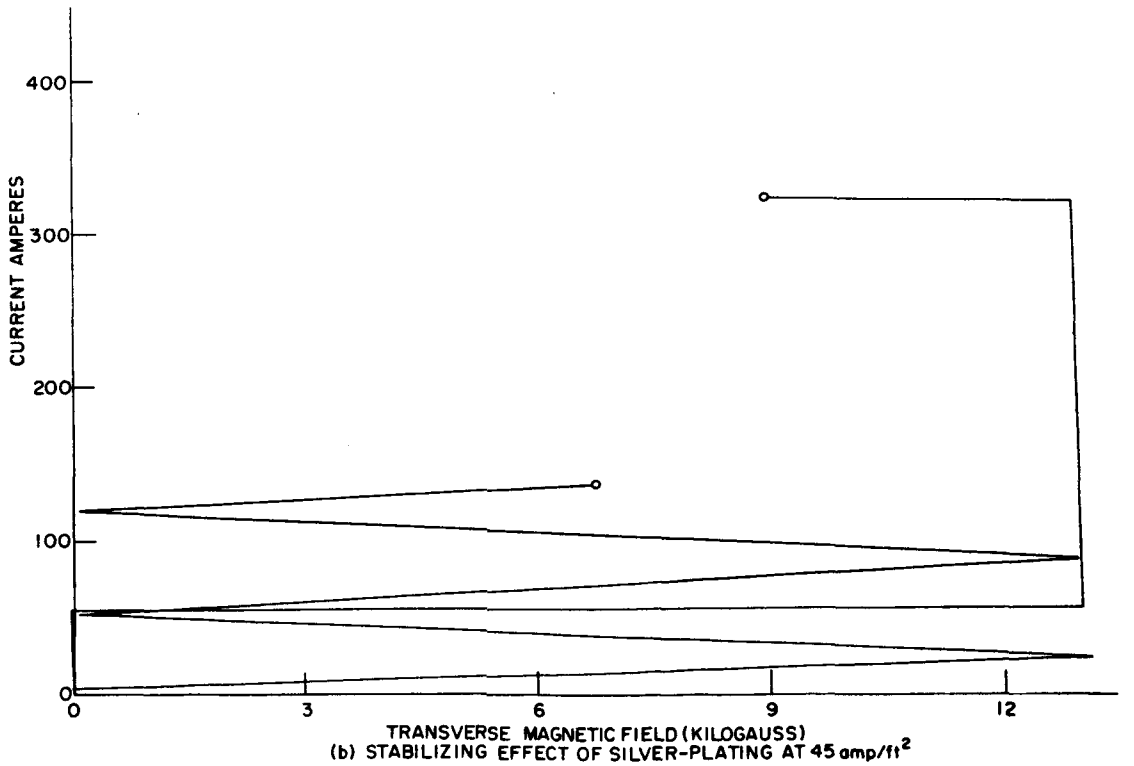

Fig. 19. Stabilizing Effect on HDC 58 Plated at Different Current Densities. (a) Silver-Plating at 30 amp/ft^2; (b) Silver-Plating at 45 amp/ft^2.

Attempts were made to decrease the electrical resistivity of the metal plating. The resistivity of a normal metal containing impurity atoms and lattice defects can be written in the form

$$\rho = \rho_i + \rho_l \tag{6}$$

where ρ_l is the resistivity caused by the thermal motion of the lattice and ρ_i is the resistivity caused by scattering waves by impurity atoms and lattice imperfections. At low temperature $\rho_l \rightarrow 0$; therefore

$$\rho = \rho_i \tag{2}$$

Furthermore, since at room temperature ρ_l is the dominant term, the ratio of

$$\frac{\rho_{room}}{\rho_{liquid\ helium}} = \frac{\rho_l}{\rho_i + \rho_l} \approx \frac{\rho_l}{\rho_i} \tag{7}$$

This ratio gives an indication of the impurities and imperfections of the clad metal.

Resistance and resistance ratio measurements of 1.5-cm-long silver- and copperplated Hastelloy ribbon samples are shown below. The results seem to correlate with small coil tests. Maximum coil stabilities (keeping winding technique and coil dimensions constant) have been obtained with the slowest plating rates.

Table 11

Effect of Plating Conditions on Resistivity

Test No.	Plating Rate amp/hour	Plating Materials	R_{He}, Resistance at 4.2°K, mΩ	Ratio $\frac{R_{room}}{R_{He}}$
4-1	134	Silver	0.387	23.0
4-3	67	Silver	0.257	32.0
4-4	33	Silver	0.135	50.0
4-5	10	Silver	0.0525	104.5
4-6	123	Copper	1.3	15.0

IV. COILS WOUND WITH RCA VAPOR-DEPOSITED Nb_3Sn RIBBON

A. EXPERIMENTAL MAGNET WORK PRIOR TO THE START OF THE CONTRACT

1. Single Modules

The bulk of the work on coils prior to the start of the contract consisted of experiments on 2-in. ID, 3-in. OD, 0.15-in.-wide modules [also called (2,3) modules] which were stacked in series to form larger coils. Work had also begun on 2-in. ID, 5-in. OD, 0.15-in.-wide modules [(2,5 modules]. The pertinent geometric and magnetic parameters of these modules and their combinations are given in Tables 12 and 13. Figure 20 is a photograph of a (2,3) module and a stack of six together, and Fig. 21 a photograph of a (2,5) module and associated hardware.

The nomenclature used in describing magnet parameters are those conventionally used and are described here for convenience.

a_1 = inner winding radius

a_2 = outer winding radius

b = half the axial length

$\alpha = \frac{a_2}{a_1}$

$\beta = \frac{b}{a_1}$

H_o = field at the radial and axial center of the coil

H_m = field at the axial center and inner coil winding-(maximum field)

$H_{o/I}$ = central field developed per ampere of coil current

$H_{m/I}$ = maximum field developed at the inner coil windings per ampere of of coil current

I_c = critical current

The earliest (2,3) modules were wound with HP series Nb_3Sn ribbon, non-copperplated and with 0.0005-in. Mylar ribbon for insulation. The method of winding is to solder one end of the Nb_3Sn ribbon to an inner copper ring which is then clamped between guide flanges on a winding machine as shown in Fig. 22. The ribbon is wound with 200 to 300 grams of tension and the Mylar is continuously interleaved. The winding is continued to a fixed outer diameter

Table 12

(2,3) Magnet Parameters

($a_1 = 2.38$cm) ($a_2 = 3.65$cm) ($\alpha = 1.53$)

No.of Modules	b (cm)	β ($=\frac{b}{a_1}$)	H_m/H_o	Non-Copperplated				Copperplated			
				No.of Turns	Length (m)	H_o/I	H_m/I	No.of Turns	Length (m)	H_o/I	H_m/I
1	0.114	0.048	3.21	155	30	32	103	135	26	28	90
2	0.312	0.131	2.45	310	60	62	152	270	52	54	132
4	0.707	0.298	1.85	620	120	123	227	540	104	107	198
6	1.106	0.464	1.58	930	180	173	273	810	156	151	248
8	1.502	0.630	1.38	1240	240	224	308	1080	208	196	270
10	1.90	0.796	1.27	1550	300	260	330	1350	260	226	287
12	2.30	0.962	1.18	1860	360	304	359	1620	312	265	313

Table 13

(2,5) Magnet Parameters

($a_1 = 2.38$cm) ($a_2 = 6.18$cm) ($\alpha = 2.60$)

No.of Modules	b (cm)	β ($=\frac{b}{a_1}$)	H_m/H_o	Non-Copperplated				Copperplated			
				No.of Turns	Length (m)	H_o/I	H_m/I	No.of Turns	Length (m)	H_o/I	H_m/I
1	0.114	0.048	2.0	536	144	98	196	420	113	76	152
2	0.312	0.131	1.76	1072	288	172	301	840	226	134	236
4	0.707	0.298	1.50	2144	576	333	500	1680	452	260	390
6	1.106	0.464	1.38	3216	864	470	650	2520	678	367	506
8	1.502	0.630	1.28	4288	1152	626	800	3360	904	490	628
10	1.90	0.796	1.20	5360	1440	750	900	4200	1130	590	708
12	2.30	0.962	1.16	6432	1728	840	975	5040	1356	659	764

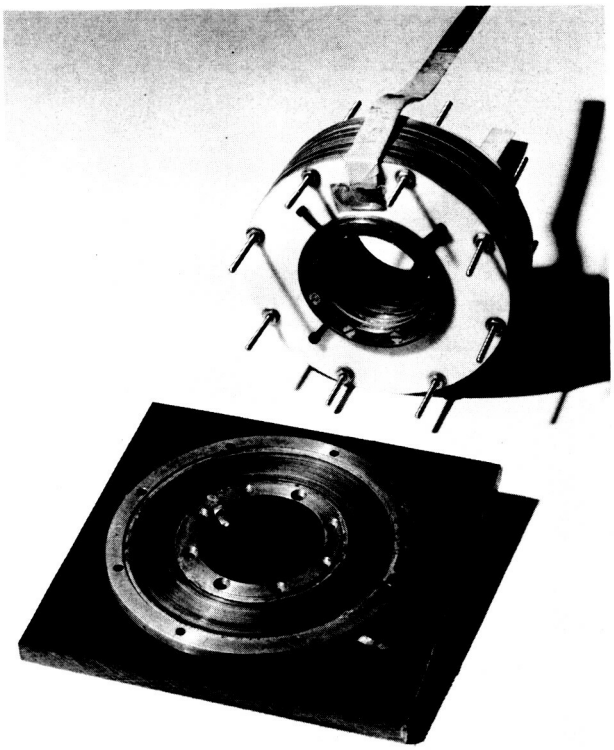

Fig. 20. Photograph of a (2, 3) Module and a Stack of Six in Series.

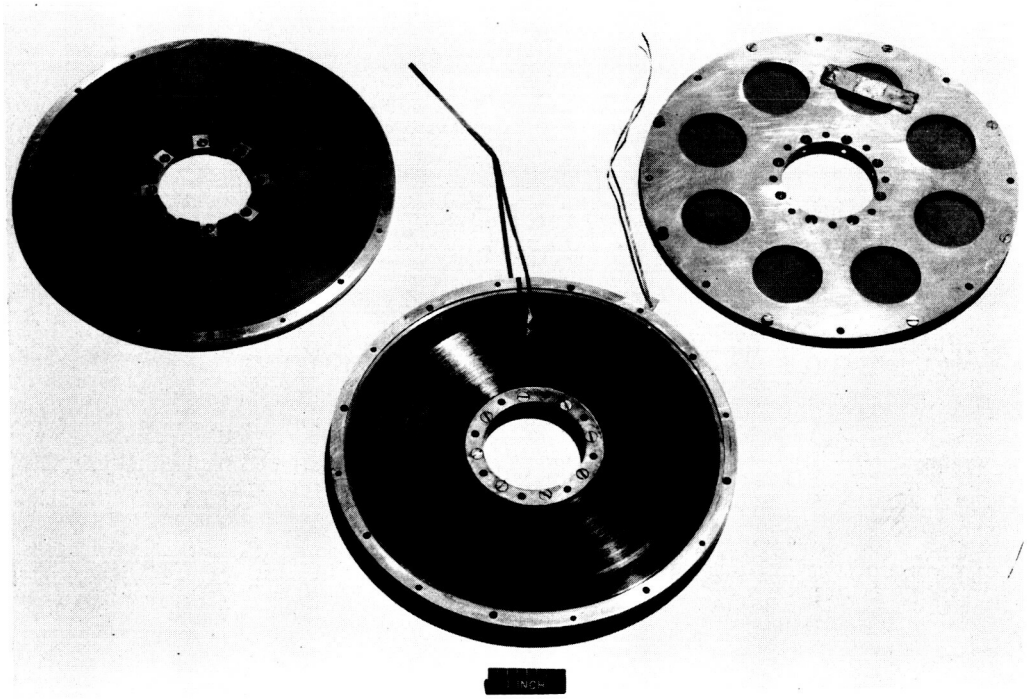

Fig. 21. A Single (2, 5) Module and Associated Contact Plates and Insulator.

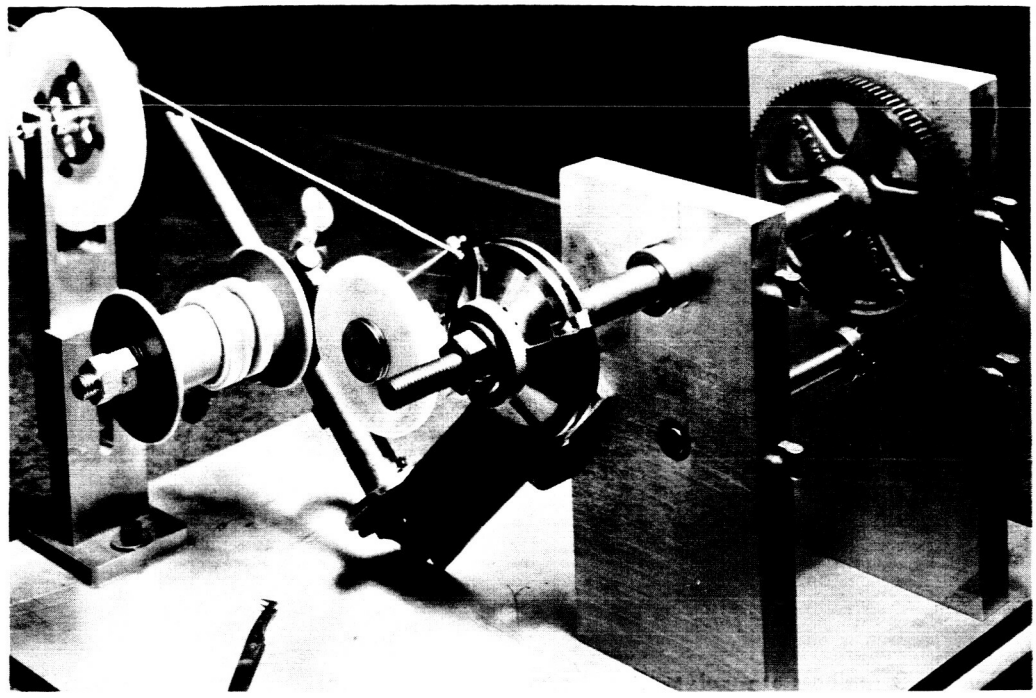

Fig. 22. Method of Winding Nb_3Sn Ribbon and Interleaved Mylar into Modular Configuration.

and the ribbon is then soldered to an outside copper ring. Special fixtures are used to hold and locate the rings and ribbon. 1/32-inch-thick Bakelite discs on both sides of the windings permit handling and stacking of the modules.

The critical current of short samples of the HP series of Nb_3Sn ribbon was steadily improved as time progressed. However, the 2-in. ID, 3-in. OD modules wound from this material actually decreased in self-field critical current as the short-sample critical current increased. Figure 23 is a plot showing this effect. The critical current of different 2-in. ID, 3-in. OD modules are shown as a function of the critical current of the short samples of the same material used in each coil winding. The earlier, lower critical current material is indicated by the points beginning on the left (each point represents a coil and short sample) with the points on the right showing the short-sample critical current improvement with improved processing. If there were no coil degradation, the points representing each coil should lie on the 45° dashed line so that coil and short-sample critical currents are the same. It is obvious from the plot, however, that coil current is effectively independent of short-sample critical current, and perhaps may even be considered

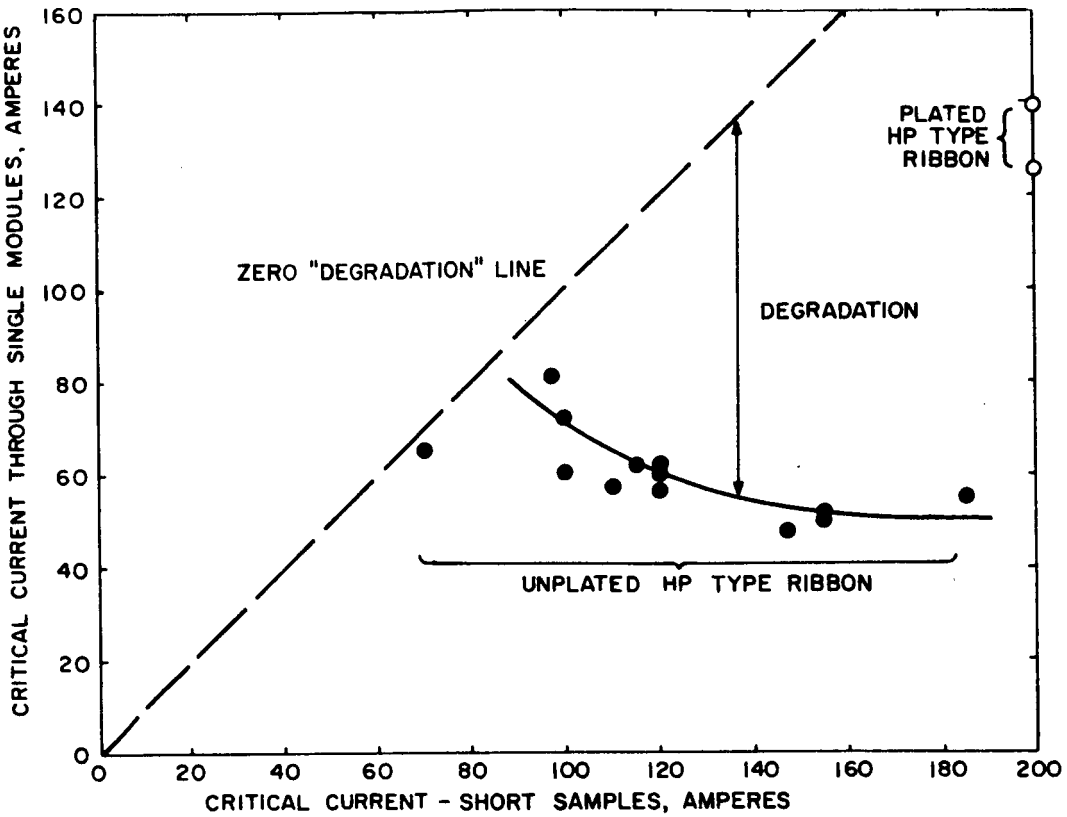

Fig. 23. Critical Current of 2-in. ID, 3-in. OD Modules vs. Short-Sample Data at 7500 gauss.

to be decreasing with improved quality material. An actual trend is difficult to establish since the plotted points are averages of critical currents obtained at rates of increase of coil current from 1/4 to 10 amperes per second.

In the range of 60 amperes of (2,3) module critical current, "degradation" begins to occur, and the windings of Nb_3Sn ribbon having higher critical currents, as determined by short-sample tests, show no improvement on coil current. It is now certain that this degradation of the (2,3) module critical currents is due to the unstable characteristics of the HP material.

When this material was stabilized to some degree by copperplating, the coil current increased significantly as is shown by the points on the right side of Fig. 23. It is noteworthy that degradation (being below the 45^{o} dashed line) still exists, but to a lesser degree.

When (2,3) modules were wound from the improved HDC series of copperplated Nb_3Sn ribbon, critical current increased to a range of 135 to 195 amperes. An approximate 10-ampere spread in I_c with current rate remained as with previous

coils. Repeated quenching of (2,3) modules wound with HDC material and with 0.0005-in. Mylar showed no signs of any effect resembling the "training" reported in niobium-zirconium coils.

(2,5) modules were wound in a similar fashion. When the HP series (unplated ribbon using 0.0005-in. Mylar) was used, I_c values of approximately 50 amperes were achieved. With the HDC series, copperplated and with 0.0005-in. Mylar, currents ranged from 120 to 160 amperes. At the start of this contract, the HDC series of materials, obviously superior in both short-sample and single-module tests, was established as "standard" material for the vapor-deposition process.

2. Stacked Modules

Extensive stacking data were available on (2,3) modules early in 1963. Data were taken for combinations of 2, 4, 6, 8 and 10 modules for those wound from copperplated HDC material. For the coils wound from the HP series, data were obtained for stacks of 2, 6, 8 and 10 modules. Measurements of the total resistance across complete stacks, where the value reflects the superconductor-to-copper joints, the copper ring resistance, and the pressure contact between rings yield an average resistance of 50 micro-ohms per module. By observations of the resistance as a function of time and current it was established that excessive heating at the superconductor-to-normal contacts was not a significant factor in limiting the critical current of these modules.

Figure 24 gives the highest critical current achieved for stacks of (2,3) modules wound with unplated HP material and plated HDC material. Since the quality of the HP ribbon varied for each module, there is no one H_c-I_c short-sample curve which can be included for reference. For referencing the performance of the copperplated (2,3) coils to short-sample data, Fig. 5 should be used. The degree of "degradation" from the short-sample data is most readily seen in that the H_c-I_c curve of Figure 5 is entirely above the upper limiting coordinates of Figure 24. The fields plotted in Fig. 24 are those developed at the windings. The reduction to the field developed at the center of each coil is obtained from Table 12 where values of H_o/I are given as well as H_m/I.

Although (2,5) modules were also stacked and tested early in 1963, additional data on this coil geometry were obtained after the start of the contract.

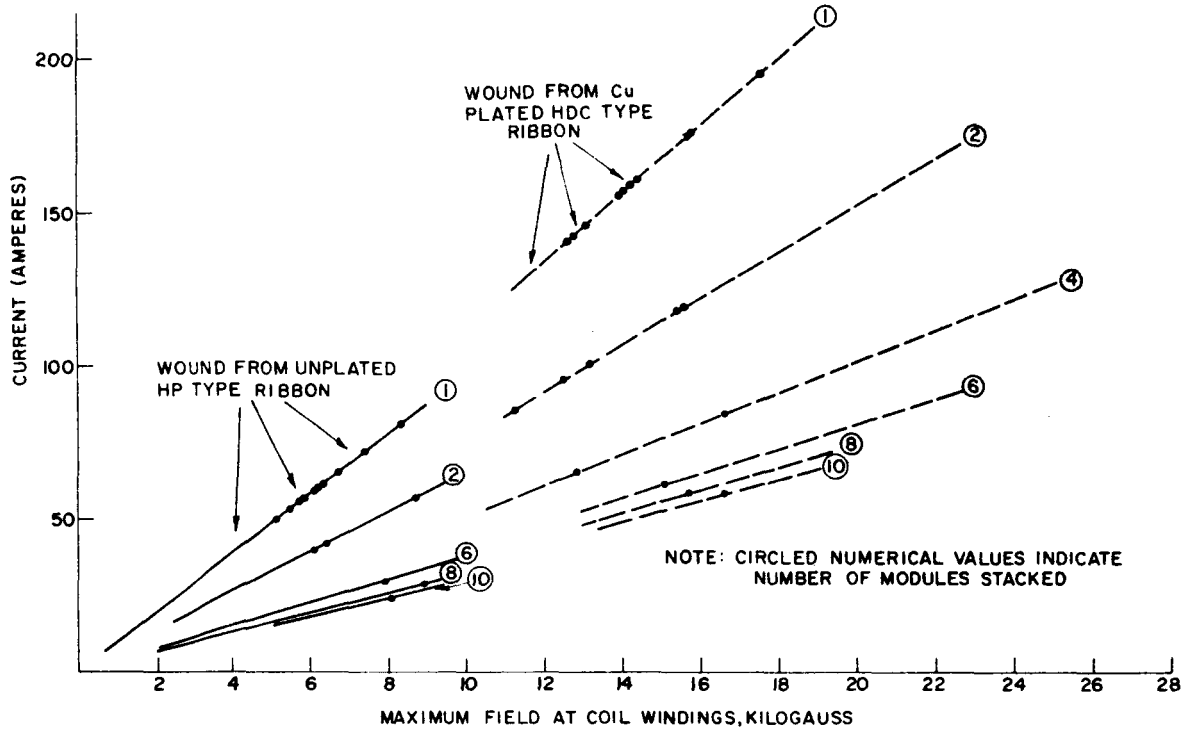

Fig. 24. Critical Current and Field of Stacked (2,3) Modules.

For convenience, all (2,5) coil data are reported in the section on work done during the contract. This also includes encapsulation of these modules.

3. 14.5-Kilogauss Test Magnet

The 1-3/8-in. bore of the inner copper rings of stacks of (2,3) coils provided a convenient dimension for the insertion of short samples for testing in transverse fields. A series-connected stack of 12 modules developed 14.5 kilogauss at 53 amperes. This performance was attainable consistently and with the field traversing its full range in seconds, thus permitting easy determination of critical fields under swept-field conditions. A second coil of similar geometry but layer-wound was constructed, yielding comparable results. These magnets have been extensively used and have proven the practicability of using the Nb_3Sn vapor-deposited ribbon for superconductive magnets. A photograph of the stacked test magnet is shown in Fig. 25.

4. Layer-Wound Solenoids

Spools made of Hastelloy were fabricated in 1962 to permit layer-winding of complete process runs of 250-meter lengths for testing superconductive continuity. The 3-in. length and 2-3/4-in. inner diameter solenoid dimensions

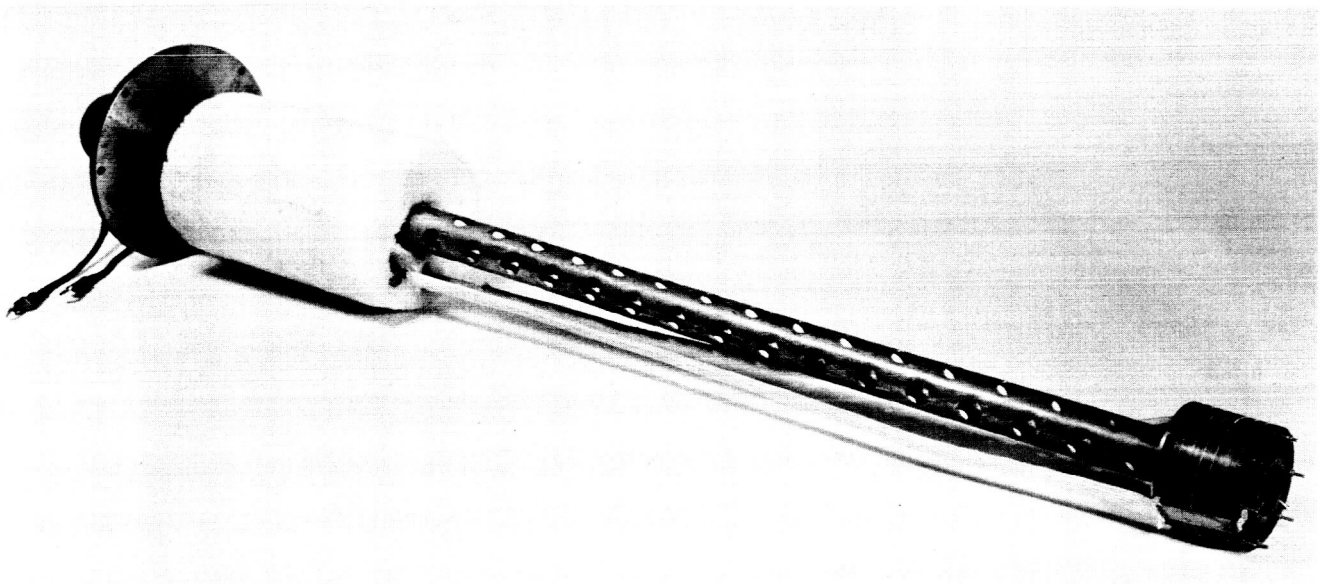

Fig. 25(a). 14.5-kgauss RCA Superconductive Test Magnet Mounted on "Dipstick" Shown with Current Leads. The "Dipstick" is 41-in. Long. The ¾-in.-diam. Holes Minimize Heat Conduction.

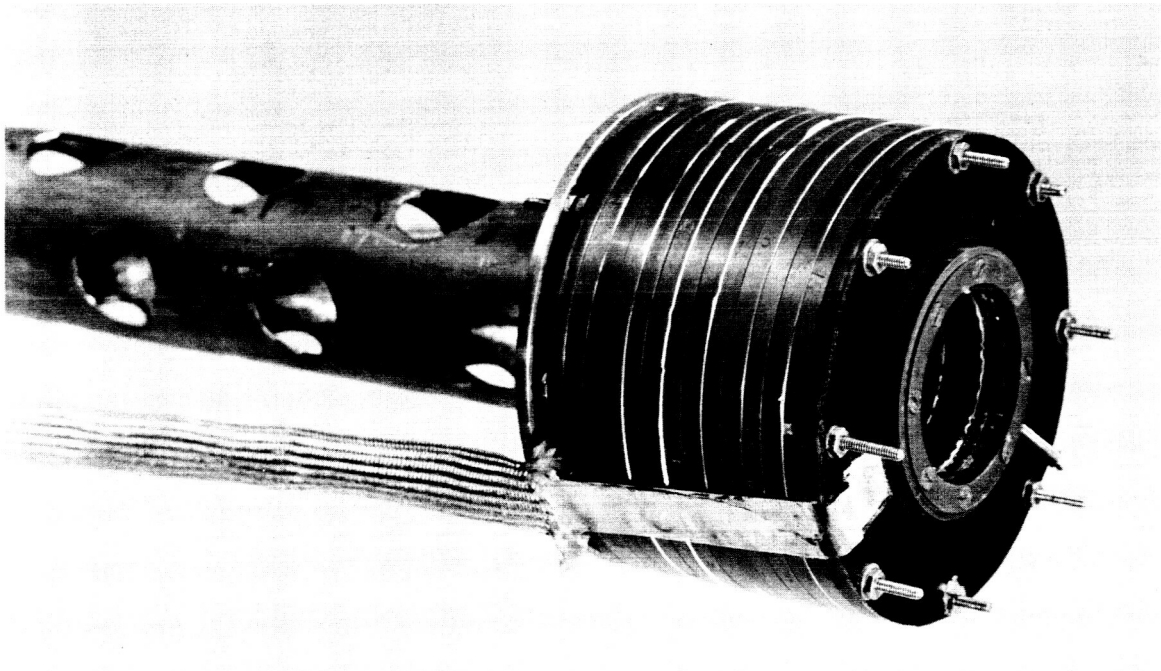

Fig. 25(b). Close-Up View of 12-Section, Series-Connected Modular Construction of 14.5-kgauss Superconductive Magnet. Samples under Test are Inserted through "Dipstick" to 1-3/8-in.-diam. Working Bore of Magnet.

coupled with a designed low packing factor upon winding was intended to yield magnetic fields around the windings which would be low enough so as not to be a factor in coil degradation. However, lengths of HP material of 100 meters or more all gave critical coil currents close to 20 amperes. With layers of copper sheet interleaved as shorted turns between, and insulated from, the layers of Nb_3Sn ribbon, the same HP material yielded increased critical currents of approximately 40 amperes. Copperplated HDC material wound with Mylar sheets between layers gave I_c's of approximately 60 amperes. These currents were, for equivalent length of superconductive ribbon (i.e., 110 meters), half those achieved in single modules.

To test the possibility that the statistical probability of hitting "bad spots" accounts for reduced performance with larger magnets (i.e., longer lengths of material), the same length was wound on the Hastelloy spool and as a (2,5) module. This was done with several different lengths. In each case, critical currents were different and were typical of the geometry. Critical currents were in no way influenced by winding history, and obviously not upon "bad spots".

In a similar test, a 180-meter length of unplated type HP material was wound on the Hastelloy spool with Mylar interleaved between each layer and with adjacent turns isolated. After determining the critical current of the complete 180-meter winding, two (2,3) pies, each containing 28 meters were wound from a portion of the ribbon on the Hastelloy spool. The critical currents of each pie as well as that for the spool with the remaining length of ribbon were then determined. These steps were repeated three times until only 50 turns remained on the Hastelloy spool. Except for electrical contacts, all of the original ribbon length was either on the Hastelloy spool or contained in pies at each step so that, if present, any "bad spots" would eventually be evident by an increased critical current on the Hastelloy spool accompanied by a decreased critical current on one of the pies.

The results of the Hastelloy spool tests are given in Table 14 below. All six (2,3) pies tested to within 10% of the expected critical current of 60 amperes, indicating no defective low-current portions. The Hastelloy spool critical currents increased only as ribbon was removed. It is evident from these tests that the geometric configuration of the ribbon in a coil was a

Table 14

Hastelloy Spool Test Results

No. of Turns Remaining	Approximate Length of Ribbon Remaining (meters)	Critical Current (amperes) of the ribbon on Hastelloy spool	Total No. of (2,3) pies wound from Hastelloy Spool
794	180	23	0
559	125	20	2
311	70	27	4
50	15	50	6

determining factor in the critical-current level attained. Subsequently, geometry will be shown to be a factor insofar as it affects the H/I of the coil in addition to inherent low-field instabilities of the Nb_3Sn ribbon.

B. MAGNET WORK DURING THE CONTRACT PERIOD

1. Stacking of 2-in. ID, 5-in. OD Coils

a. Critical Currents

The (2,5) type coils were series-stacked up to 8 modules. In Fig. 26 as in Fig. 24, the field plotted is the maximum at the inside windings. The short-sample data of Fig. 5 can be used for comparison. There is an approximate difference of over 200 amperes between coil and short-sample performance along the length of the curve.

At the time this degradation from expected short-sample performance was noted, the full implication of hard superconductor instability and its effect upon critical coil currents were not yet fully appreciated. The possibility of ribbon movement due to field, and current-dependent forces as the cause for premature reduction to the normal phase, resulted in further work on plastic encapsulation which is treated in a following section. Later knowledge attained on superconductor stability, described in other sections of this report, points out that the most likely cause of the observed degradation of the (2,5) pies as

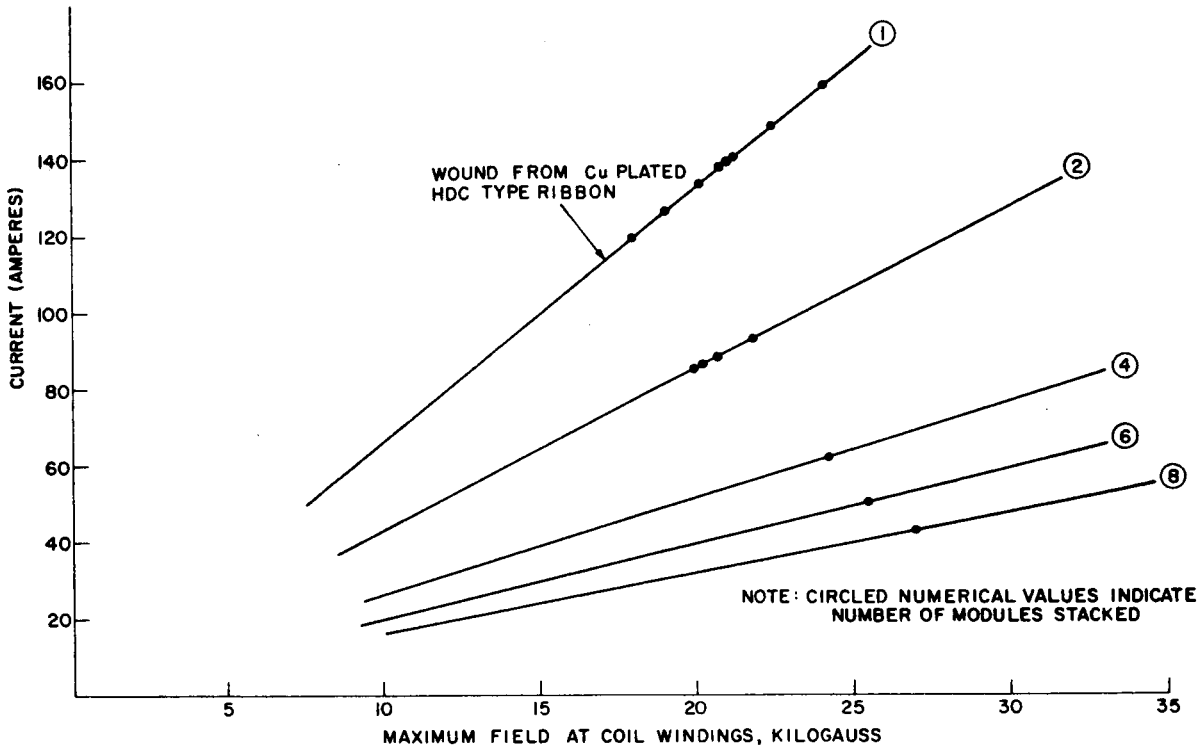

Fig. 26. Critical Current and Field Stacked of (2,5) Modules.

they were stacked to form longer coils were the unstable low-field characteristics of the Nb_3Sn ribbon. Ribbon movement may also have contributed to this effect. The necessity of connecting the outer turn of the pie to an encircling copper contact ring minimizes the tension that can be built into the coil by the winding operation. This occurs because the clearance necessary to slip the copper ring over the outer winding eventually results in a relaxation of the spiral winding.

b. Coil Encapsulation

Various encapsulants, such as Emerson and Cummings' "Stycast" (chosen chiefly for values of thermal coefficient of expansion which most closely matched that of Nb_3Sn) were tried on short samples and on (2,3) pies. The usual filler in plastic encapsulants which sufficiently lowers thermal expansion resulted in high viscosities so that vacuum impregnation of the Nb_3Sn ribbon and Mylar windings was not satisfactory. In the tests that were run, encapsulation reduced critical currents up to as much as 50 percent. At present, it is not known whether this reduction in I_c is due to reduced thermal conductivity or to mechanical stresses on the Nb_3Sn surface.

A more successful approach was to cast coils in urethane. This plastic remains somewhat elastomeric down to almost liquid-nitrogen temperature, thus reducing some of the difficulties which can be expected by differential contraction over large temperature ranges. Table 15 summarizes coil performance from these experiments. Figure 27 is a photograph of a (2,5) module which has

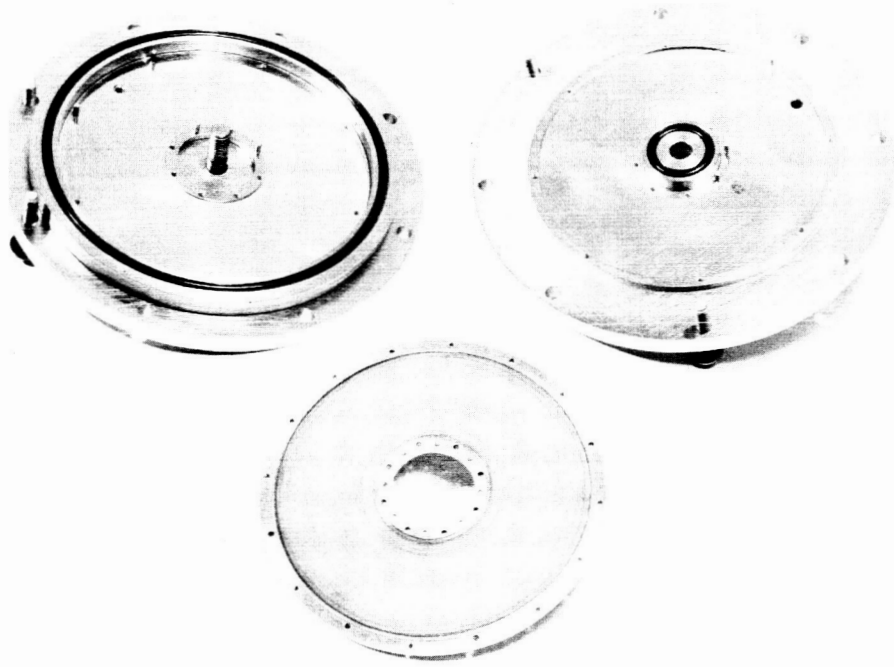

Fig. 27. Mold for Encapsulation of (2, 5) Module.

been encapsulated in urethane and the mold used for polymerization. Figure 28 shows a cross section of the encapsulated windings. Early experimental evidence indicates that encapsulation will be feasible, perhaps accompanied with a small drop in maximum coil current.

On this contract, a total of eight (2,5) pies were encapsulated. The critical currents of three are listed in Table 15 below in addition to results of encapsulation work on other geometries. After the third (2,5) pie was tested the work on coil instabilities made it evident that the critical currents being attained did not reflect the true critical currents of the Nb_3Sn materials. It would be necessary to immerse the pies in a background field as described in a later section of this report. At the time, no background field was available for coils this size.

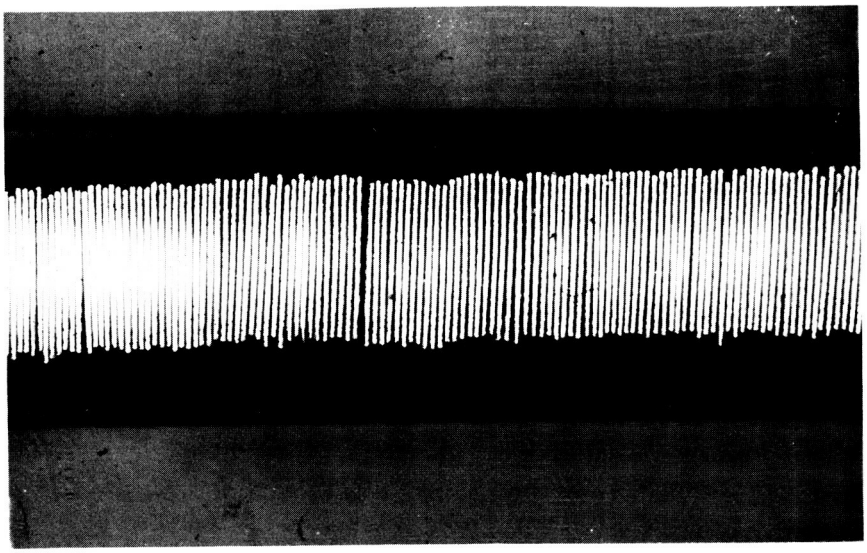

Fig. 28. Cross Section of Encapsulated Portion of (2,5) Module.

Table 15

Effect of Encapsulation on Critical Currents

Coil Type	Coil No.	Current Before Encapsulation (A)	Current After Encapsulation (A)	% Decrease	Encapsulant
2" ID 3" OD Single Pie	2 3	68 40	60 37	12 7.5	Urethane
2" ID 5" OD Single Pie	11A 12A 10	75 119 133	39 119 118	48 0 11	
9/16"ID 1-1/4"OD Stack of 4 Pies	I_{18+} I_{14+} I_{11+} I_{12+}	110	100	9	Mineral Oil

2. Coils of 9/16-in. ID and 1¼-in. OD

Individual "pies" of 9/16-in. ID, 1-1/4-in. OD, and one ribbon width wide are easily constructed with copperplated Nb_3Sn ribbon by soldering several of the inner turns together and several outer turns together. With this technique, the need for copper rings is eliminated. By soldering short lengths of superconductive ribbon between adjacent coils these small modules are connected in series to form stacks of various lengths. Table 16 gives the parameters of these coils. Critical currents of single modules ranged from 160

Table 16

Parameters of 9/16-in. ID, 1-1/4-in. OD "Pies"

($a_1 = 0.71$cm) ($a_2 = 1.59$cm) ($\alpha = 2.23$)

No. of Modules	b (cm)	β ($=\frac{b}{a_1}$)	H_m/H_o	Non-Copperplated				Copperplated			
				No. of Turns	Length (m)	H_o/I	H_m/I	No. of Turns	Length (m)	H_o/I	H_m/I
1	0.114	0.161	1.84	130	10*	92	169	90	7*	65	119
2	0.252	0.355	1.52	260	20	156	237	180	14	109	166
4	0.526	0.741	1.24	520	40	290	360	360	28	202	250
6	0.800	1.127	1.13	780	60	390	440	480	42	275	310
8	1.077	1.517	1.08	1040	80	450	485	720	56	320	346
10	1.348	1.900	1.05	1300	100	510	535	900	70	360	378
12	1.623	2.285	1.03	1560	120	538	554	1080	84	383	394

* In winding coils, 6.5 meters of ribbon are needed for 90 turns. An additional 1/2 meter is used for inner and outer turns which are shorted to hold the current contacts.

to 200 amperes, and I_c for a stack of 10 coils was approximately 100 amperes. Figure 29 gives the H_c-I_c sequence as these coils are assembled. A stack of 12 such coils in the center of a 10-module (2,3) magnet gave a total field of 43 kilogauss. Because of their dimensions, coil degradation as dependent upon size effects is not as pronounced as in the (2,3) and (2,5) coil stacks.

The dimensions of these small coils were convenient for insertion into the Lewis Research Center 2-3/8-in. ID magnet dewar for studying the effects of a variable background magnetic field in critical current. The resulting

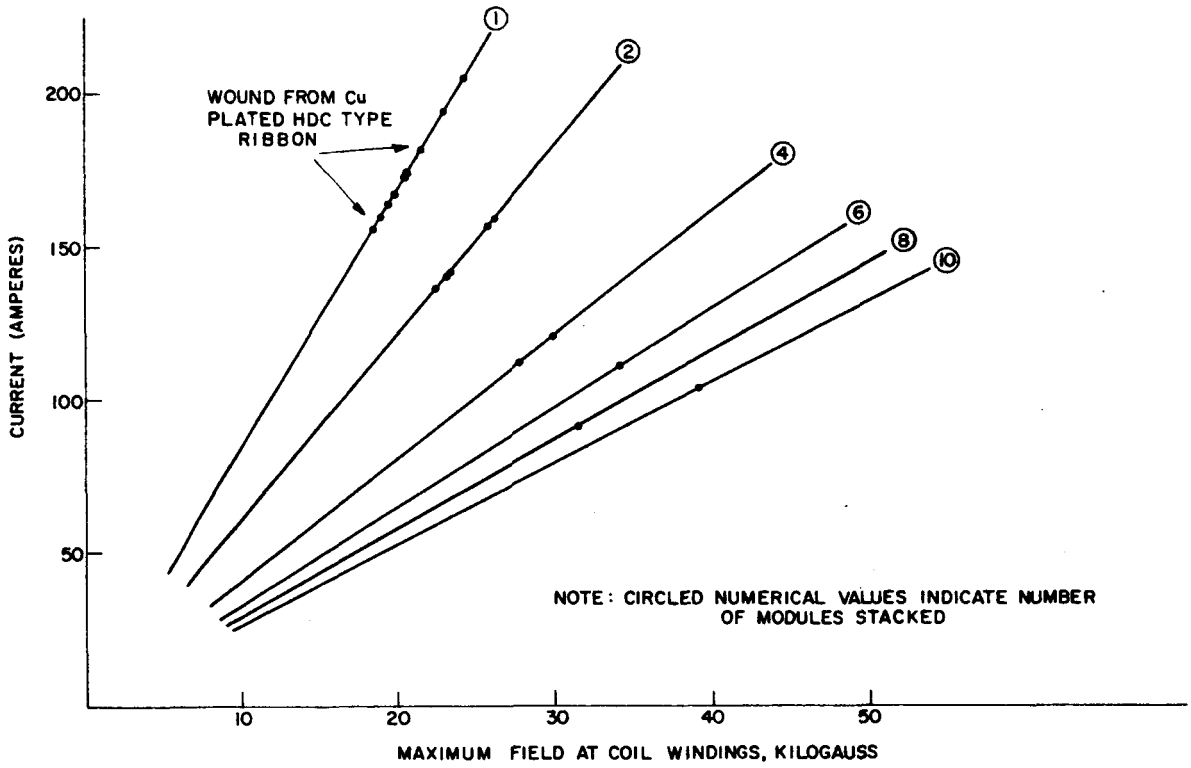

Fig. 29. Critical Current and Field of Stacked (9,20) Modules.

data provided the first indication of an Nb_3Sn coil attaining the same values as indicated in the earlier short-sample data. The 7- to 10-meter lengths of the small coils are enough to reduce some of the randomness of the critical characteristics of short samples. Tests on these coils supply a bridge between the difficult-to-interpret short-sample data and the critical currents of larger coils.

Critical field-current data for short samples are characterized by varying degrees of deviation from a smooth monotonically decreasing curve. Coincident with such deviation is an increasing degree of scatter on the critical points of repeated tests on the same sample, making it almost impossible, in some cases, to define a specific curve. This latter type of result has been used to categorize the sample tested as "unstable" as compared with a "stable" sample which results in a critical-current, critical-field curve which is well defined. This remains true with the background field and sample current applied in any order and with rates covering a wide range.

With the bare and copperplated short samples described in the section on the deposition process (Section III), various degrees of stability are evident,

with the copperplating significantly adding to stability. Unstable behavior of Nb_3Sn short samples is always more evident in the 0-10 kilogauss region, especially when the transport current is fixed at some value and the magnetic field is varied. This shows up as a "dip" cut out of the low field region of the H_c-I_c curve. The use of the terminology "stable" and "unstable", or "reproducible" and "nonreproducible", is a reference to an observation of the test pattern for a sample and not necessarily to a basic property of the Nb_3Sn. As will be shown below, however, patterns shown in the short samples are reflected in coil behavior.

Figure 30 shows the critical currents for a coil of HDC material in the sum of its self-field and the applied field. The output was measured by an

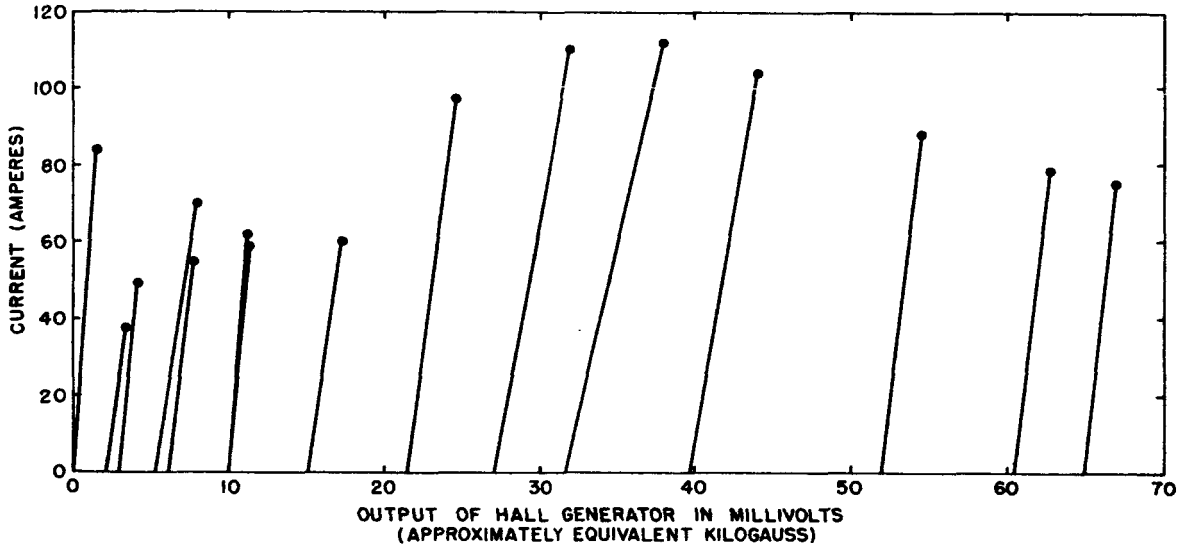

Fig. 30. Critical Current vs. Magnetic Field for (9,20)/16 Module Wound with Copperplated HDC 26 Ribbon and Tested in the NASA 4-in. Magnet.

axial Hall probe in the center of the small pie which, in turn, is held with its axis coinciding with the axis of the LeRC 4-in. copper magnet. The regularity of the points of normality above 35 kilogauss coupled with the large area "cut out" of the classical H_c-I_c curve and the instability below that field follow directly from short-sample data such as is indicated in Fig. 7.

Nb_3Sn ribbon which was made to have a greater degree of stability was tested in the form of short samples as well as a 9/16-in. ID, 1-1/4-in. OD coil. The results are shown in Fig. 31. Once again a definite dip in the curve occurs which appears to represent a measure of the effects of low field

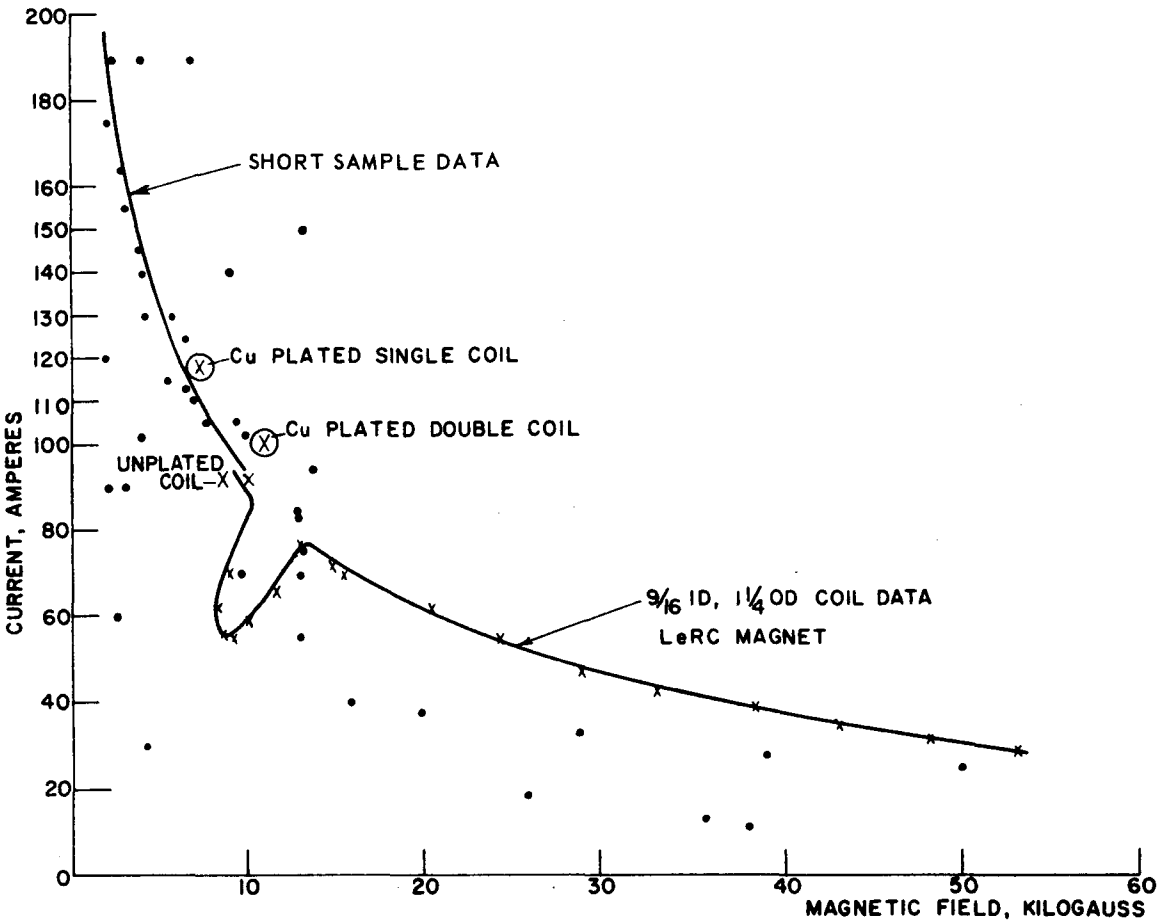

Fig. 31. Short Sample and Coil Data; Run PNDC 136 Exhibiting Partial Stability.

instability. The best line through the greatest density of short-sample points matches the data for the coil quite well. Although not shown, the points at which the coil went normal for the more sensitive condition of first setting the current and then changing the field corresponds to the indicated curve to within a few percent. The more stable material, therefore, results in a coil which is less dependent upon sequence of field and current application. It is interesting to note that copperplated material from the same run gives critical currents similar to unplated short samples. The lower critical currents of this more stable ribbon in coil configuration compared with the higher currents for a less stable ribbon in a similar coil configuration follow the same results found in short-sample testing.

Figures 32 and 33 give the classical axial and radial components of the self-generated field of a 9/16-in. ID, 1-1/4-in. OD pie wound with nonplated ribbon as determined by computer using a program supplied by R. Boom. (Boom,

Livingston, 1962). The components are plotted as percent of central field vs. axial distance from the central plane with various radii as parameters. For such a thin coil there is a large calculated field gradient across the width of the ribbon at some points. Due to the expected Meissner effect at low fields and an inhomogeneous distribution of current across the Nb_3Sn cross section [(Cullen, Cody, 1963), (Meyers, 1960), and (Marcus, 1960)] field distribution differs from the value calculated. However, it might be expected that, if a field gradient does exist across a single ribbon width, a varying degree of inherent instability would result with the possibility of preferred "channels" for current conduction.

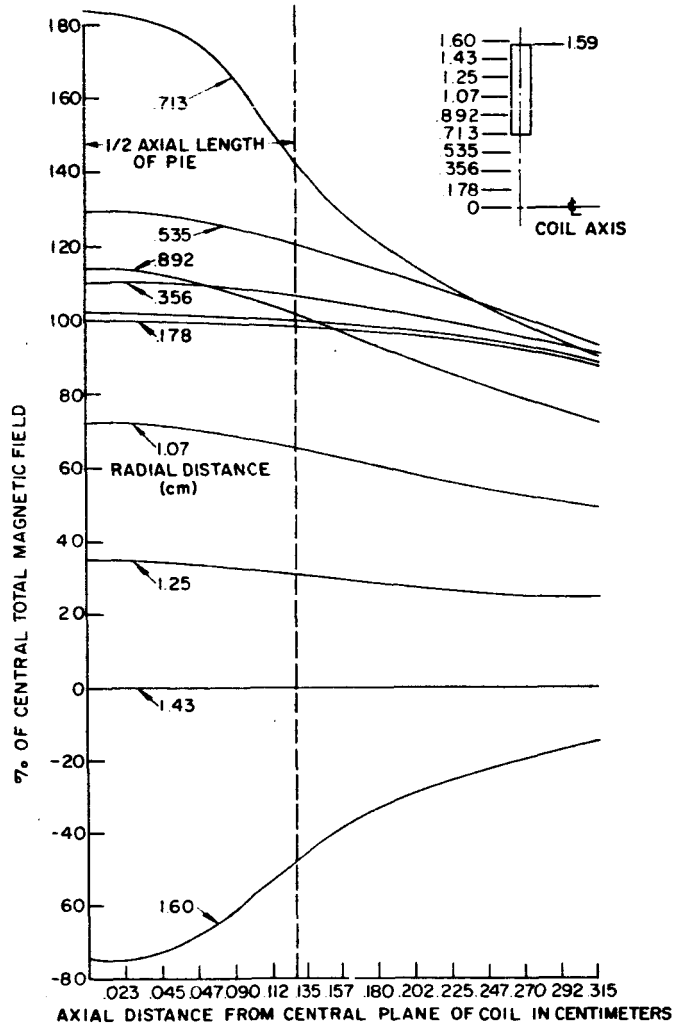

Fig. 32. Axial Magnetic Field Components of 9/16-in. ID, 1¼-in. OD Pie at Various Radial Distances.

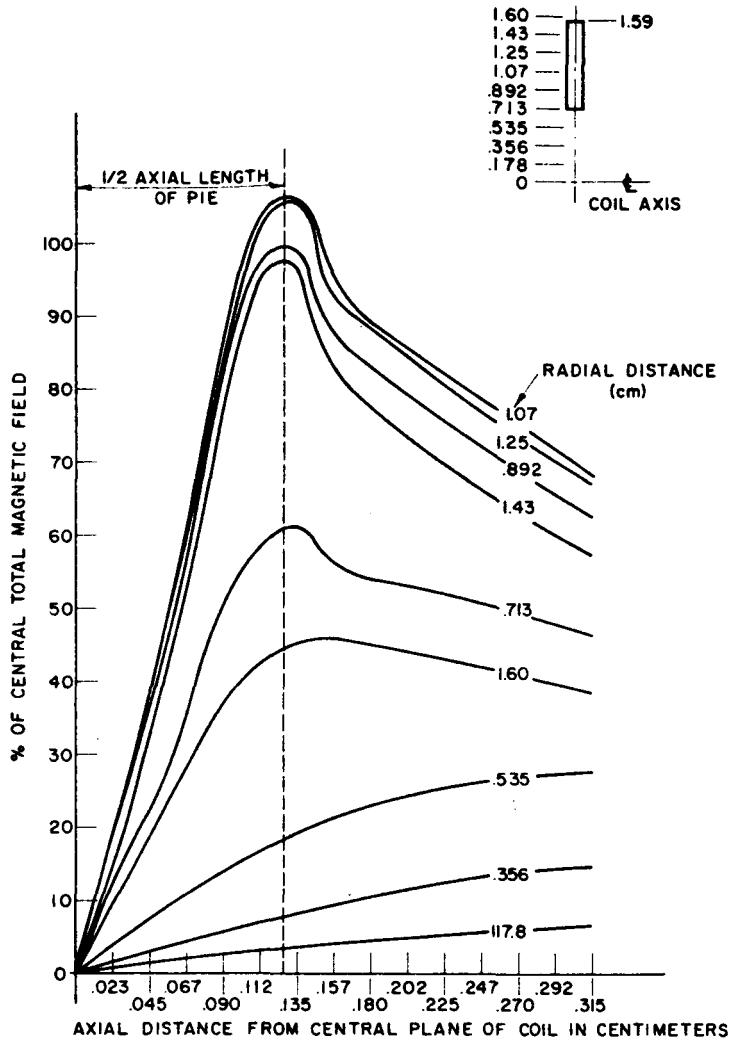

Fig. 33. Radial Magnetic Field Components of 9/16-in. ID, 1¼-in. OD Pie at Various Radial Distances.

In an axial background field, only the axial component will be altered (assuming ideal magnet behavior). In Fig. 30, the low axial background field of 32 kilogauss is sufficient to bring the small coil into the region of what is considered stable behavior. With 110 amperes in the pie, the central field is approximately 39 kilogauss while the field at the inner winding is approximately 45 kilogauss. At the outer winding, the axial vector subtracts 5,400 gauss from the applied field to yield 26.6 kilogauss. Therefore, stability was fully achieved for this coil only when all windings were in a total field exceeding 26 kilogauss. Many short-sample tests on the type of ribbon used for the coil shown in Fig. 30 confirm that maximum instabilities exist over this same range.

A qualitative indication of the role of instabilities in solenoids is illustrated by the results of a stack of twelve 9/16-in. ID, 1-1/4-in. OD pies connected in series. Figure 34 shows the critical characteristics of this stack where, upon setting current initially and varying the background field, a more severe degradation occurs than when the current and field sequence are reversed. For this particular coil stack, sweeping the background field resulted in sudden changes in coil current which were assumed to be triggered by flux jumps. The magnitude of these changes peaked at a background field of between 5 and 10 kilogauss and tapered off at higher fields.

Increasing field sweeps with 10 and 20 amperes preset in the coil are shown in Fig. 35. With decreasing field sweeps a mirror image of the same pattern was obtained whereby amplitude of the current change increased. In these tests a reliable Hall probe was unavailable and only background field is indicated. From this test it is not known if field changes actually coincide with current changes. In these tests at LeRC a field sweep rate of approximately 1/2 kilogauss per second was estimated. While amplitude and frequency of current changes vary with field sweep rate, no further studies were made of this effect due the lack of a precision field rate control.

The real significance of these data is the decrease in amplitude of the disturbance at higher fields, and the occurrence of peak instability in the region near to or below 10 kilogauss. The severest degradation shown in Fig. 34 occurs very close to this region. There is little doubt that the mechanism causing coil-current fluctuations (presumed to be severe internal flux changes) is also the cause of coil performance degradation from expected short-sample critical current. Similar observations on Nb-Zr coils have been published (Boom, Roberts, Livingston, 1963). Overall degradation patterns in Nb-Zr coils similar to these shown in Figs. 30 and 7 have also been noted [(Rosner, Schadler, 1963) (Lubell, Chandrasekhar, Mallich, 1963)].

3. Layer-Wound Test Coils Description

The work on short samples and 9/16-in. ID, 1-1/4-in. OD pies clearly shows that Nb_3Sn material stability is equally as important as current-carrying capacity in determining coil-critical currents. Layer-wound coils more closely approximating conventional coil geometry were wound, using up to 100 meters of ribbon, as test vehicles to further study stability characteristics. Coil

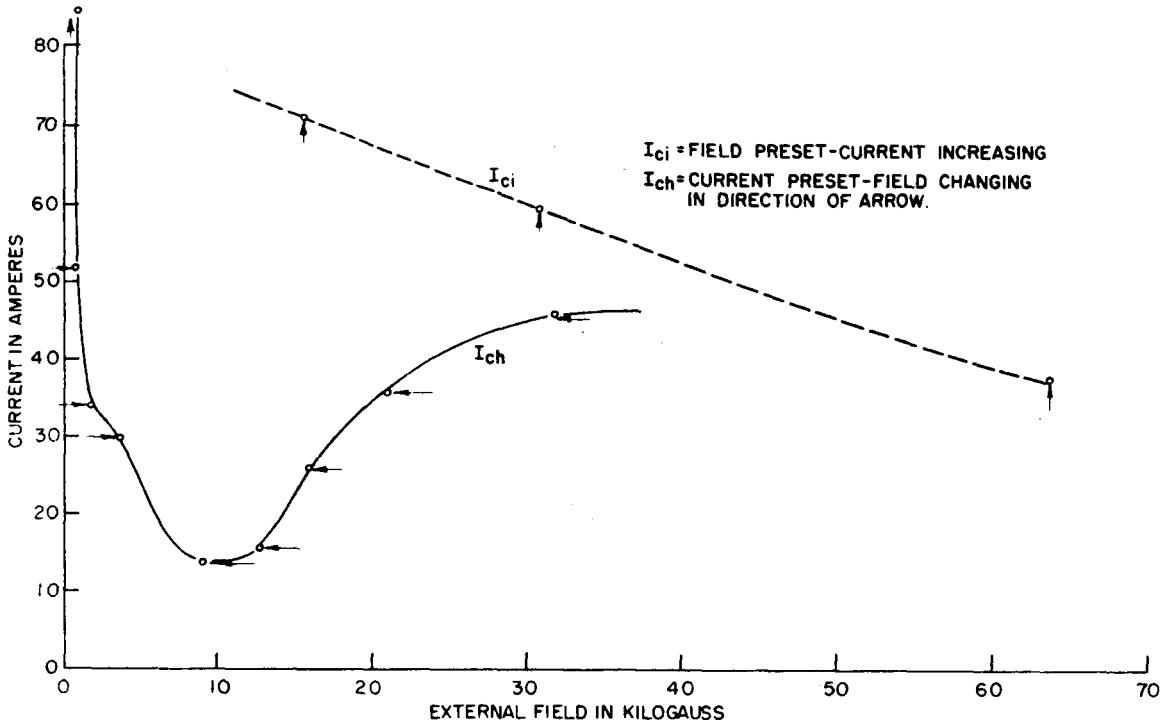

Fig. 34. H_c-I_c Characteristic of 12-Pie Stack in External Field.

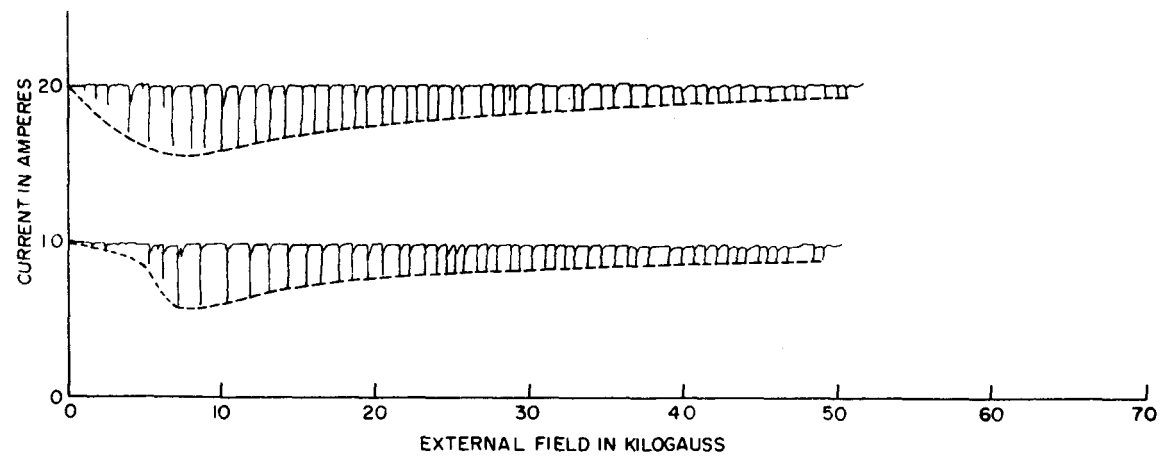

Fig. 35. Magnitude of Coil Current Changes in 12-Pie Stack.

form dimensions are 1-1/4-in. ID x 2-in. OD x 2 in. long, and the coil fits into the LeRC 2-3/8-in. ID dewar.

In winding and testing these coils, winding techniques and insulation were varied as well as types of Nb_3Sn ribbon. These are described below.

a. Winding Technique

When ribbon is layer-wound with approximately 400 grams of tension, and with no physical barrier between adjacent turns, the turns eventually shift

together and touch as higher field testing progresses. Shifting of turns can be reduced with higher winding tensions, and 2 kilograms of tension have been used with no adverse effects. In many of the coils described winding tension was maintained at 400 to 500 grams, and 0.003-in.-diam. Formvar-insulated copper wire was wound adjacent to each turn of ribbon, effectively filling the space between, and insulating the Nb_3Sn ribbon turns. To facilitate the winding, a common feedthrough device for Nb_3Sn ribbon and the copper wire was constructed so that both lay down simultaneously as the coil is wound.

b. Coil Protection

Test coils were generally not shunted so that the coil time constant remained low. This provided the most critical test conditions and also permitted relatively rapid changes in background field and in coil current with minimal lag in coil response. However, to protect coils against severe field collapse upon suddenly going normal, shorted 0.002-in.-thick OFHC copper sheet was interwound periodically with Mylar insulation.

For additional internal cooling, tests were run with corrugated copper sheet. The corrugations provide channels which permit easy access of liquid helium to the interior of the coil. Coils so wound recover their superconducting state only seconds after going normal.

The magnitude of secondary current induced into a shorted copper sheet when a superconductive coil goes normal has been estimated from voltage measurements to be of the order of hundreds of amperes. This can be appreciated by the physical distortion of an outer single-shorted sheet of 0.005 in. of copper due to external field forces on the induced current upon the coil going normal ($I_c \approx 80$ amperes) in fields near 100 kilogauss. This is shown by the deformation in the copper sheet in Fig. 36.

c. Insulation

The presence of high thermal and electrical conductivity material in close proximity to the superconductor is desirable in a superconductive coil. We have found that copperplating on the superconductive ribbon significantly improves the critical current of a coil by improving stability. From the work of Anderson (1962), flux changes result in power dissipation which must be kept small and quickly removed for successful superconductive coil operation. Improved coil performance through added stability was obtained by using sheets

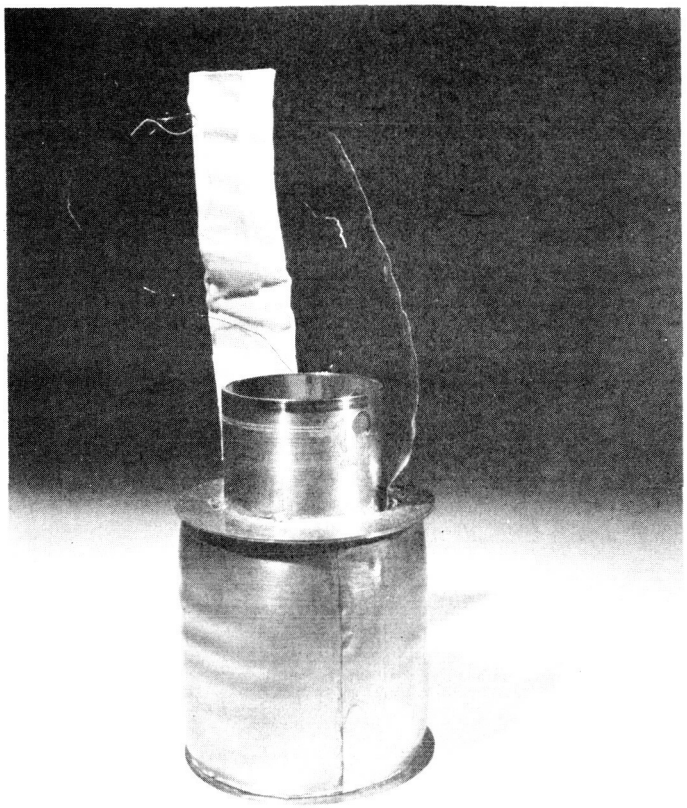

Fig. 36. The Deformation of the Copper Sheet Surrounding the Coil Windings.

of 0.0008-inch anodized aluminum for insulation in place of, or in addition to, Mylar. The aluminum provides the high thermal and electrical conductor while the anodized surface provides a reasonable electrical insulator of relatively good thermal conductivity. The less stable the Nb_3Sn ribbon, the greater will be the percentage improvement in critical current when anodized aluminum is used in place of Mylar, particularly in low magnetic fields, self-developed or externally applied. One possible disadvantage of the anodized surface as an insulator is low resistence to arcing caused by high-voltage gradients developed between turns when a coil goes normal. Several test coils have had reductions in critical current after continued testing. Upon unwinding one such coil, the arcing illustrated in Fig. 37 was noted. The aluminum foil was melted in each case.

4. Results of Testing Layer-Wound Test Coils

Actual outer winding diameters of these test coils vary slightly due to different ribbon lengths. A typical field plot for a coil wound with 100 meters

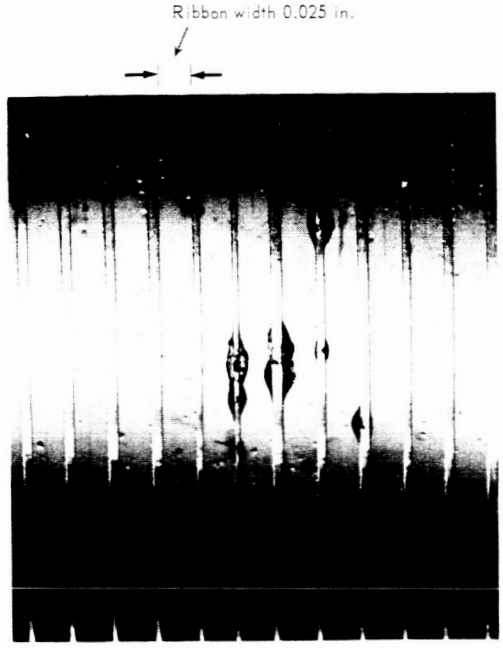

Fig. 37. Arcing Between Adjacent Turns of 0.025-in. Ribbon.

of wire is given in Figs. 38 and 39 for the axial and radial components, respectively. These values were calculated using the method of superposition of semi-infinite solid solenoids developed by LeRC (Brown, Flax, 1963). These plots will be referred to in the discussion on the results of testing layer-wound coils.

a. Achievement of Short-Sample Critical Currents

Figure 40 is a composite plot of the results of testing some of the coils listed in Table 17. Each coil represents a test of a variation of the Nb_3Sn vapor-deposition process or plating process as outlined in Table 17. Superimposed upon these results are the measured critical values for short samples of standard HDC type ribbon. In the coils discussed here, the necessary stability is achieved by the combination of copperplating on the Nb_3Sn deposit, the use of anodized aluminum foil between layers, and the presence of the high background magnetic field.

b. Variation in Plating

Experiments with silverplating of the Nb_3Sn ribbon were initiated on a parallel RCA project and were included on the high field testing because of the promising self-field critical currents of coils tested at RCA. For the coil shown in Fig. 40 an initial critical current of 206 amperes was achieved.

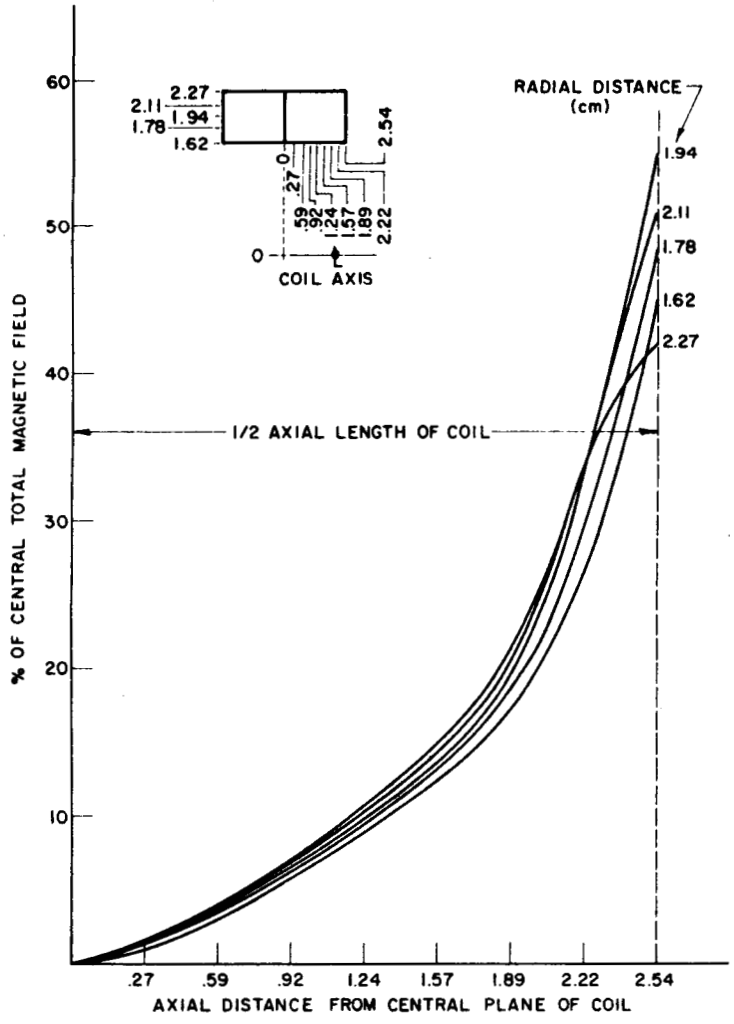

Fig. 38. Radial Magnetic Field Component of 1¼-in. ID, 2-in. OD, 2-in.-long Coil at Various Radial Distances.

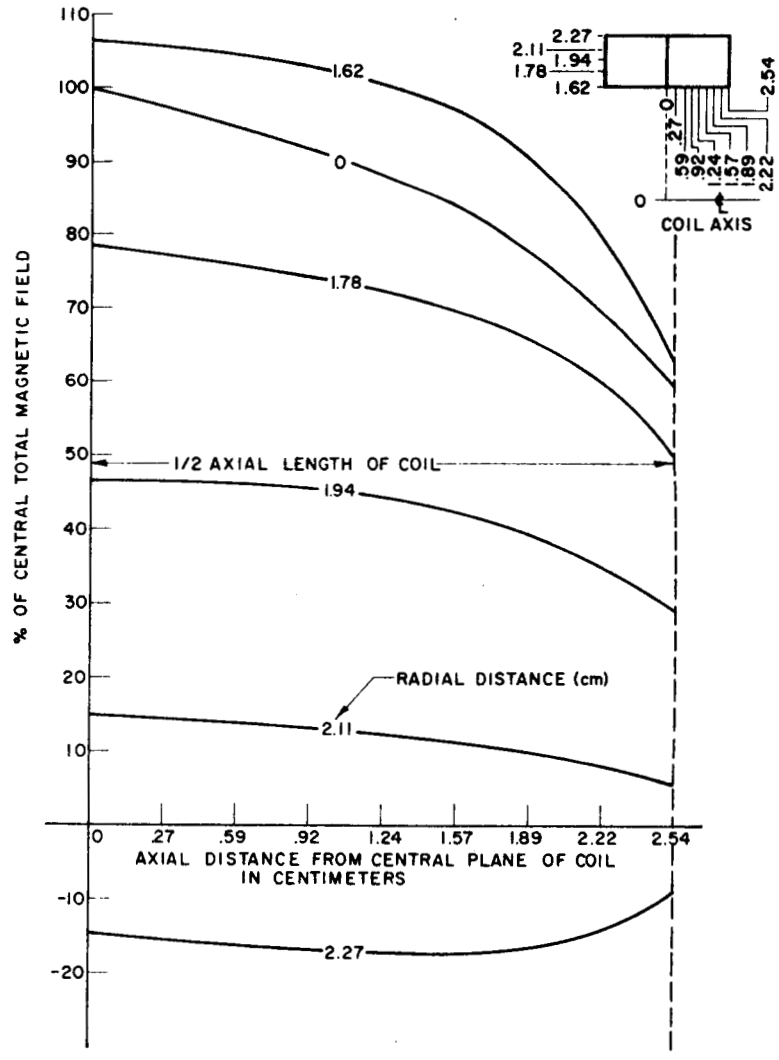

Fig. 39. Axial Magnetic Component of 1¼-in. ID, 2-in. OD, 2-in.-long Coil at Various Radial Distances.

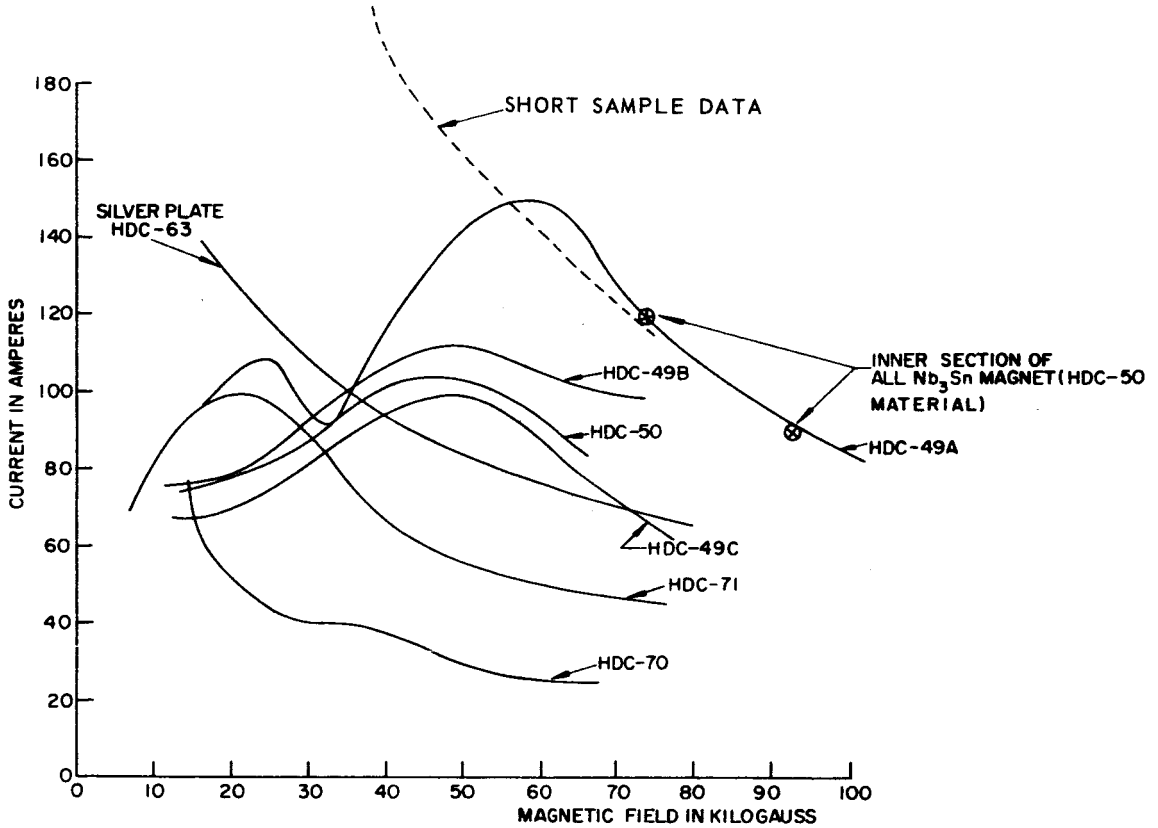

Fig. 40. Composite Plot of Test Coils in External Field of LeRC Solenoid. Current in Coils vs. Magnetic Field in Kilogauss.

Table 17

Test Coils Used in LeRC Solenoid

Material	Coil Parameters				No. of Turns	I_c (A)	H_c (kG)	Insulation	Plating	Ribbon Processing Speed (Meters/Hr.)	H/I
	a_1	a_2	2b	Meters of Ribbon		(Self field results)					
HDC-49A	1.625	2.27	5.08	120	1014	85	16	Anodized Aluminum	Cu	40	190
HDC-49B	1.625	2.27	5.08	120	1006	86	16	Anodized Aluminum	Cu	40	190
HDC-49C	1.025	2.27	5.08	120	1045	72	13	Anodized Aluminum	Cu	40	190
HDC-50	1.025	2.29	5.08	128	1034	78	15	Anodized Aluminum	Cu	40	190
HDC-63	1.625	1.80	5.08	60	650	206	24	Anodized Aluminum	Ag	10	116
HDC-70	1.625	2.27	5.08	120	1050	70	13	Anodized Aluminum	Ag	35	190
HDC-71	1.625	2.07	5.08	90	975	70	12	Anodized Aluminum	Ag	35	170

a_1 = inside radius of coil in cm

a_2 = outside radius of coil in cm

2b = length of coil in cm

Upon the quench from the superconducting-to-normal state damage to the Nb_3Sn or silver coating occurred and subsequent tests gave lower results as shown. However, it is significant that coil stability has improved in that no "dip" from the expected monotonically decreasing curve is seen. Further work on variations of silver-plating is scheduled.

c. Variation in Ribbon Geometry

Narrow ribbon (0.025 in. wide) had been used for Nb_3Sn vapor-deposition in early 1962. For improved process efficiency as well as better magnet design, a wider (0.087 in.) ribbon was subsequently used. However, at lower magnetic fields, current concentrates at the edges of the ribbon, and it was assumed that ribbon geometry might influence coil critical currents. The narrow ribbon (0.025 in.) coil, when originally tested at RCA, had a self-field critical current of 45 amperes. This value decreased to 20 amperes and less in tests at LeRC with accompanying violent fluctuations of coil current. Later, repeated tests in both locations showed that the power supply used at RCA presented an effectively lower shunt resistance to the coil, thereby increasing coil stability. When retested at NASA and with a coil shunt added, critical current increased to 40 amperes. Further tests did indicate some damage to the solenoid and by inspection of the windings the melting of aluminum due to arcing was detected. (Fig. 37).

Assuming the 45-ampere value as indicative of the best self-field current, the equivalent current of the wide ribbon would be of the order of 150 amperes. Under moderately stable conditions this is the order of current actually achieved with similar coils using the wide ribbon. It is reasonable to conclude that coils wound with narrow ribbon have the advantage of better critical current capacity in self-fields due to the necessary existence of low field regions with resulting superior current distribution across the ribbon width.

Figure 41 shows the results of a 9/16-in. ID, 1-1/4-in. OD coil wound with copperplated ribbon in which the Nb_3Sn was scribed down the center and a narrow band of Nb_3Sn ribbon was etched away. The narrow groove effectively provides two parallel superconductors approximately 0.040 in. in width.

The results of Figure 41 can be compared with those shown in Fig. 30 for a coil of comparable geometry. Since the scribed ribbon is connected in parallel, the total current shown in Fig. 41 is the total for two 0.040-in.-wide

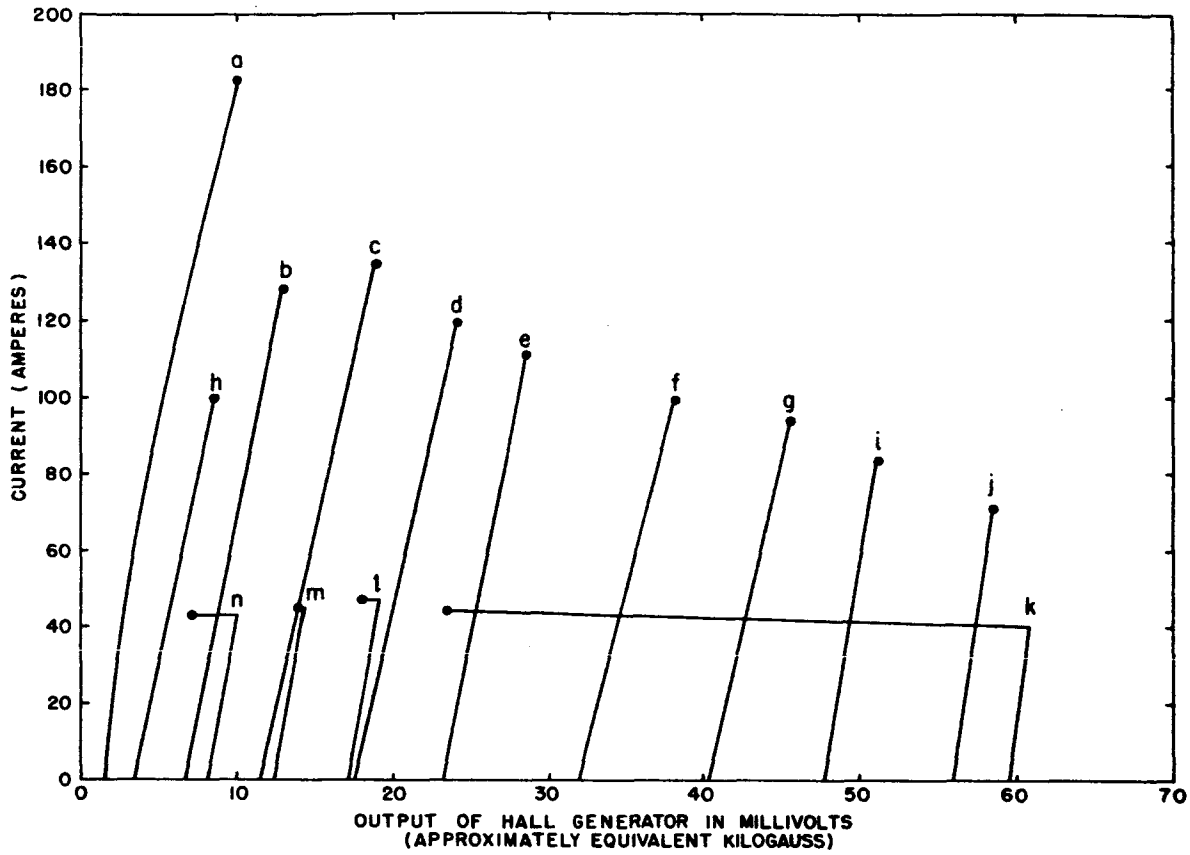

Fig. 41. Critical Current vs. Magnetic Field for 9/16-in. ID, 1½-in. OD Module Wound with Copperplated Scribed Ribbon and Tested in NASA 4-in. Magnet.

ribbons and can therefore be considered equivalent as far as the coordinates are concerned. At the higher magnetic fields, current levels are fairly similar. However, at lower magnetic field, current level of the scribed ribbon is higher, presumably due to higher stability corresponding to improved current distribution across the ribbon.

Coils tested in a background field are positioned with their axes corresponding to the axis of the LeRC magnet. Only the axial component of the field of the test coil is modified by the background field and this is the component aligned with the 0.088-in. dimension of the Nb_3Sn ribbon. The extreme asymmetry of the ribbon might possibly cause some modification of the effect of achieving coil stability in a background field other than axial.

To test asymmetry effects, a small coil wound with an earlier version of RCA ribbon by the Brookhaven National Laboratories was tested first with its axis aligned, then at right angles to the LeRC magnet. Results are given in Fig. 42. No significant difference in critical current results due to coil

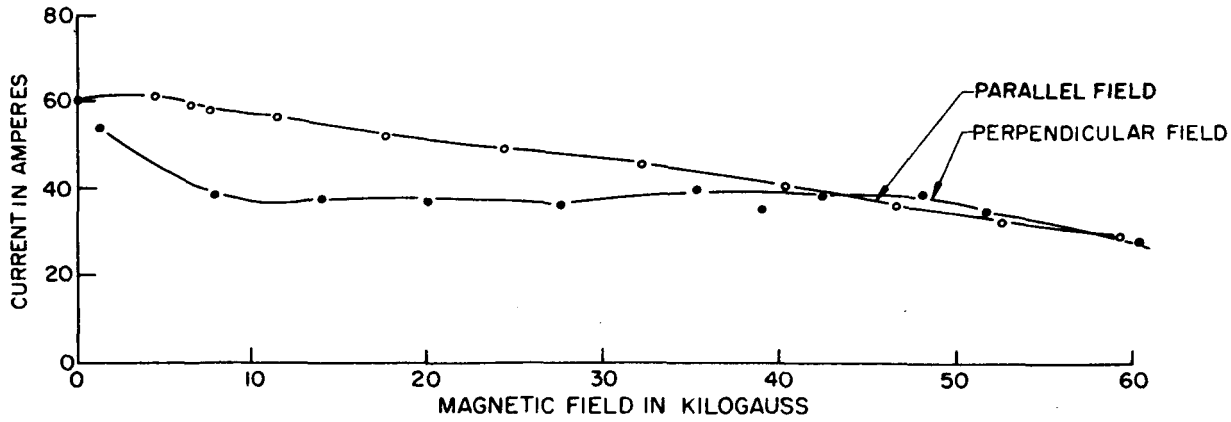

Fig. 42. Coil Wound at Brookhaven National Laboratory with Coil Axis Parallel and Perpendicular to External Field.

alignment at the higher fields. Below 40 kilogauss, the coil current remains at about 40 amperes throughout the complete low-field range for the perpendicular case as compared with currents approaching 60 amperes for the case of axial alignment of the LeRC magnet and test care. It cannot be ascertained from this test whether the lower critical current for the perpendicular case is due to ribbon movement or to the fact that the major portion of the ribbon is transverse to the applied background field. At higher fields, the critical currents are approximately equal. A similar effect, where coils of narrow (0.040 in.) or wide (0.088 in.) ribbon exhibit the same current density at higher fields (Figs. 30 and 41), indicates that the orientation or geometry of a ribbon immersed in high fields and surrounded by other ribbon lengths becomes unimportant. At the lower fields, the current and field distribution across the ribbon is determined, to some extent, by its own geometry. The results here indicate that the higher fields interact with the current in a hard superconductor on a geometric scale which is less than the gross ribbon dimensions.

An interesting result of the test with the coil axes at a right angle is shown in Fig. 43. The forces were sufficient to permanently distort the 1/8-in.-thick copper flanges of the coil form. No deterioration in Nb_3Sn ribbon performance was detected.

d. Normal Connections

The BNL coil discussed above had within the windings four normal connections made by overlapped soldered joints at the copperplated ribbon ends. The

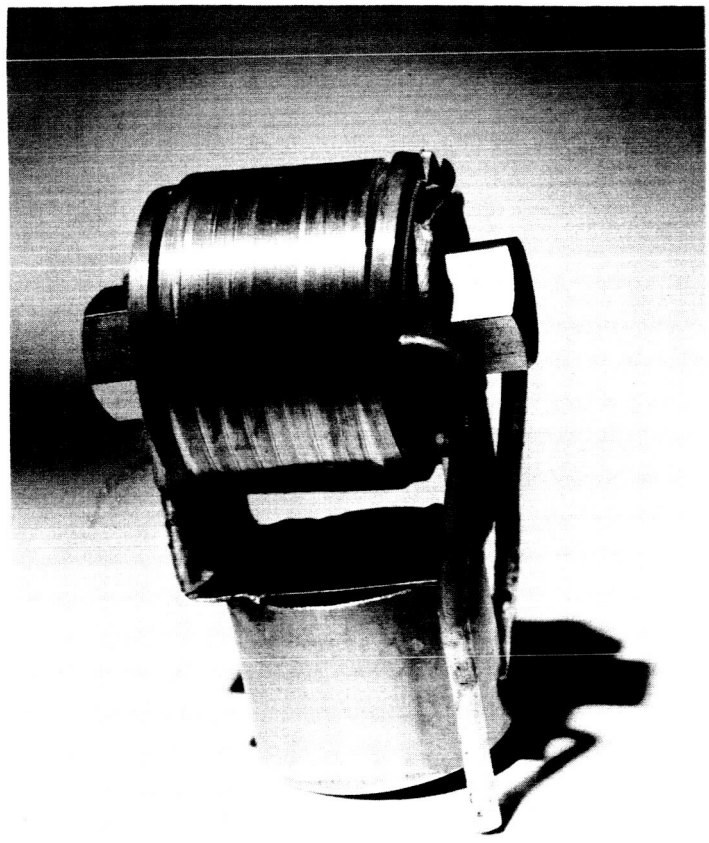

Fig. 43. Damage to Flanges of Coil After Perpendicular Field Test.

early work involving magnets made with stacked pies had two normal connections for each pie. Contact resistance measurements consistently confirm low power dissipation (Table 18).

Table 18

Contact Resistance Data

Material	Plating	Area of Contact in cm^2	Solder	Resistance
HDC-73-1	Copper	0.175	60/40	2.5×10^{-8} Ω
HDC-866	Silver	0.175	60/40	2.1×10^{-8} Ω

To directly test the practicality of soldered overlapped connections in a high field environment, the coil (1-1/4-in. ID, 2-in. OD) wound with a single 128-meter length of HDC 50 material was cut into six lengths and re-wound with 1/2-in. overlapped soft-soldered connections. The high field tests before and after are shown in Fig. 44 and no significant difference due to the normal joints is observed.

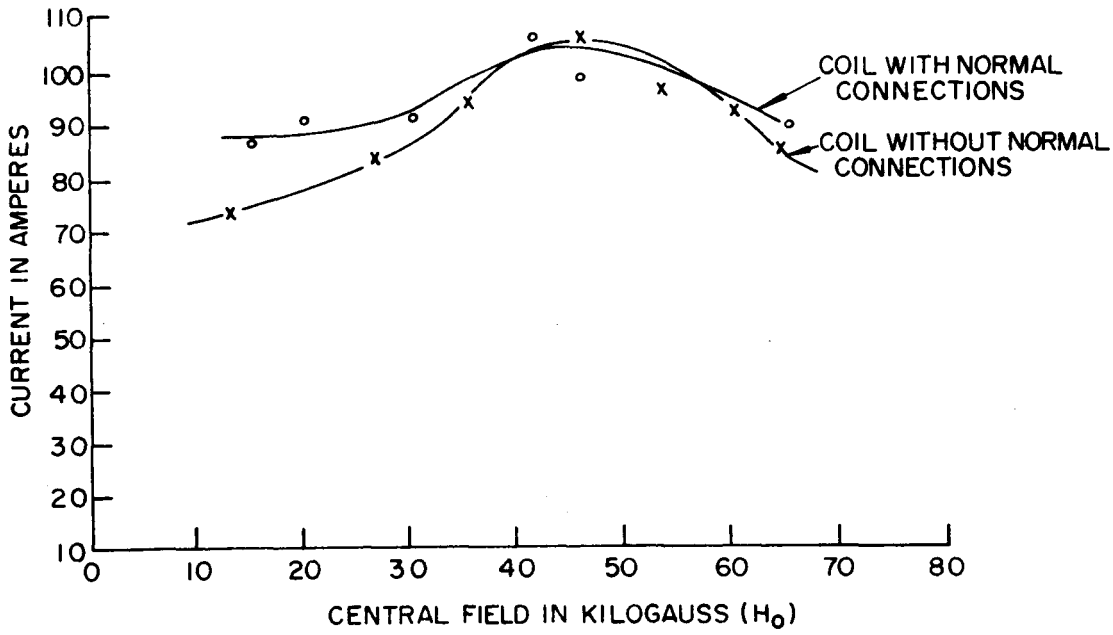

Fig. 44. Coil Performance with and without Normal Connections.

e. Variation in Coil Stability with Coil Geometry

The trace of instabilities in the 9/16-in. ID, 1-1/4-in. OD coils, as background magnetic field is changed, shows that instability decreases but does not vanish as magnetic fields become large. When instability is a problem at all, the extent of instability will depend upon coil geometry and testing procedures as well as on type of ribbon and coil construction. Exact dependence upon coil geometry is not quantitatively known since actual source and functional behavior of the instabilities in hard superconductors is still under speculation. The qualitative effects of a coil of given H/I and geometry interacting with a superconductor of given characteristics, i.e., degree of instability, have already been discussed elsewhere (Fakan, Schrader, 196). However, it would appear that the effective H_c-I_c characteristic of the coil to be used in this type of analysis is actually determined by the integrated effect of all sources of instabilities and that one effect is coil size. An experiment was performed using the coil discussed in the previous subsection (Normal Connections) to illustrate this point.

The coil was wound with 45 layers of HDC 50 ribbon, giving the critical characteristics curve previously shown in Fig. 44 and redrawn in Fig. 45. Figure 45 also shows the critical points after unwinding to 20 layers, then to 10. For 45 layers the unstable lower field portion is evident, giving the

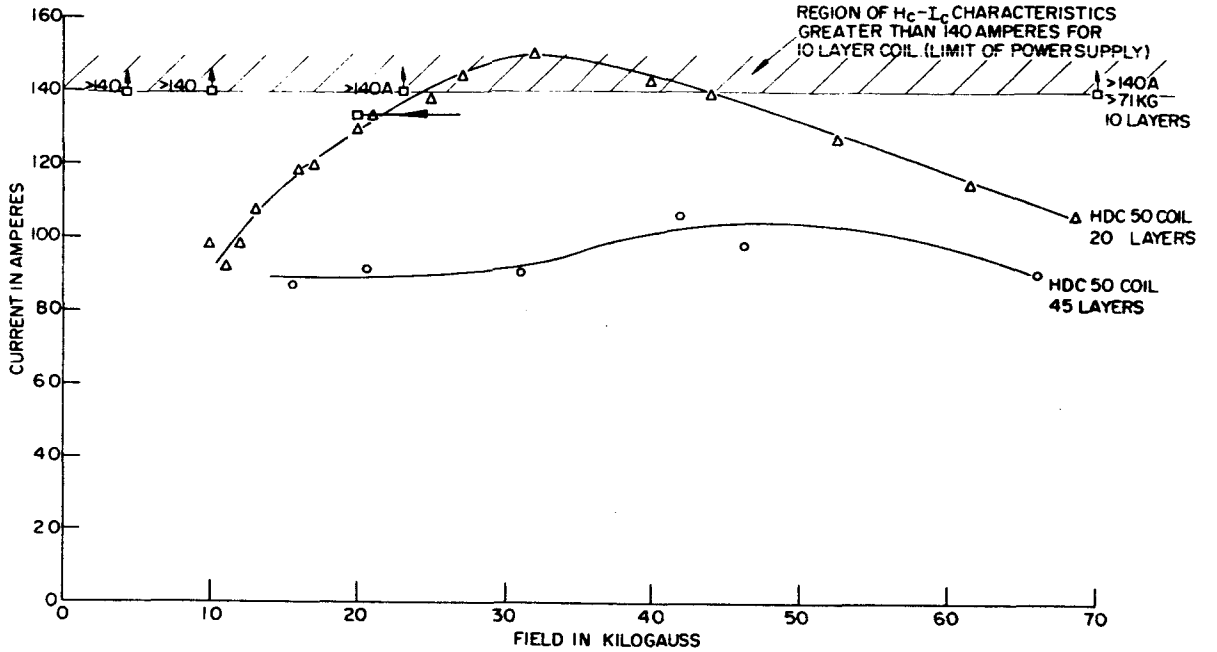

Fig. 45. Variation in Coil Stability with Coil Geometry.

impression of reaching the conventional H_c-I_c curve at the higher fields. However, the 20-layer coil of the same material shows higher critical currents even in the high field portion. The 10-layer coil went to the limit of the power supply (140 amperes) in most cases without going normal, giving an overall behavior found to be typical of short samples, i.e., generally very high currents with scattered instabilities having no definite pattern.

It is evident that the effects of the instabilities become more severe as coil size is increased unless other techniques, such as shunting, better cooling, or an increase in the amount of normal metal present are used.

5. Construction of an All-Nb_3Sn 92-Kilogauss Magnet

Concurrent with the series of tests at LeRC with the small test coils discussed above, a series of coils were constructed at RCA to apply the principle of stability control. A measured 92-kilogauss field in a 1/2-in. winding inner diameter was achieved (Schrader, Freedman, Fakan, March, 1964). The final magnet consisted of three physically independent, axially aligned coils, the outer section being composed of multiple ribbon lengths with current taps available at convenient points to allow for flexibility in power supply connection. The coil windings are two inches long with other characteristics as shown in Table 19.

Table 19

Parameters of the All-Nb_3Sn 92-Kilogauss Magnet

(All coils 2 in. long)

Magnet Sections	Winding (in.) ID	Winding (in.) OD	Bore (in.) ID	Ribbon Length (meters)	No. of Turns	L (henrys)	Calc. H/I	Current (Amperes) tested alone	Current (Amperes) max. achieved	Current (Amperes) for 92kG central field	Effective current density (A/cm^2) at 92kG test	Shunt
Inner Section	0.5	1.2	0.437	80	1320	0.010	300	80	120	90	2.63×10^4	0.5
Center Section	1.27	2	1.23	215	1644	0.051	325	70	120	90	3.11×10^4	0.5
Outer Section												
1st winding	2.2	2.75	2.15	255	1220	0.075	200	60	60	60	2.13×10^4	0.8
2nd winding	2.8	3.85	-	590	2238	0.335	285	63	63	61	1.92×10^4	0.5

The type of ribbon used for all the coils in this magnet has stability characteristics similar to those used in coil HDC 49A shown in Fig. 40. Each single coil section had a critical current in the range from 60 to 80 amperes when tested independently in self-field and is therefore "degraded" with some region of each coil in an unstable mode. As the inner and center sections are immersed in a background field of at least 10 kilogauss, critical currents become larger. The critical currents of the inner coils were not plotted as a continuous function of the background field of the outer coils, and it is not known what maximum critical currents could be attained. The maximum measured currents are indicated in Table 19. The value of 120 amperes for the inner section was achieved with a field of approximately 10 kilogauss supplied from the outer section. From the coil performance values plotted on Fig. 40 along with the value of 90 amperes obtained at 92 kilogauss, it is obvious that material performance is not degraded and meets short-sample performance characteristics.

Because of significant values of currents induced in adjacent coil sections as a coil section is being energized, experiments became time-consuming and an optimum combination of geometry and critical currents is still being investigated. Values of central field in excess of 85 kilogauss at $4.2^{\circ}K$ were reached repeatedly with various coil combinations; the highest value was 92 kilogauss.

The fields were measured with a Hall probe calibrated at LeRC and spot-checked with a search coil. The difference between the calculated 86 kilogauss and the measured maximum of 92 kilogauss is believed to be partially due to mechanical shifting of the windings toward the coil center as tests

proceeded, thereby concentrating the field. It is noted that a precise relationship between true flux distribution for superconducting coils as compared with the calculated value based on conventional copper solenoids is not yet proven.

V. SUMMARY DISCUSSION

The work described in this report definitely establishes the feasibility of constructing large-bore, high-field solenoids with RCA vapor-deposited Nb_3Sn ribbon. This feasibility stems from the advances in the technology of the use of hard superconductors as described in this report. The work covers many aspects of materials and magnet behavior and has been directed toward the single aim of large magnet feasibility, not necessarily toward the complete understanding of each facet of the technology. Because of the extent and diversified nature of this work, the following text will serve as a technical summary as well as a set of conclusions concerning this work. The text is divided into three sections. The first treats the effects of the Nb_3Sn vapor-deposition process variables; the second, the conclusions concerning the basic effects due to the winding of solenoids; and the third, the practical aspects of the present technology and the meaning of the future.

A. EFFECTS OF PROCESS VARIABLES ON SUPERCONDUCTIVE PROPERTIES

Niobium-stannide is deposited on a resistance-heated substrate by a gaseous-phase hydrogen reduction of niobium and tin chlorides as indicated by the following reaction.

$$3NbCl_4 + SnCl_2 + 7H2 \longrightarrow Nb_3Sn + 14HCl \qquad (4)$$

The superconductive ribbon is currently produced in lengths up to 1,000 meters, and the composition and electromagnetic performance is uniform from beginning to end. No basic process limitations prevent attaining longer lengths. The substrate strongly influences the initial crystal deposit. The earliest niobium-stannide was grown on a platinum substrate. However, due to a combination of high cost and low tensile strength in conjunction with high ductility, the platinum substrate was quickly abandoned in favor of an inexpensive high tensile strength Hastelloy substrate. The Hastelloy substrate is platinum-plated to create the same deposition surface as the platinum ribbon. The niobium-stannide deposited on this new substrate exhibits the same high current densities as obtained previously with the platinum substrate.

The Nb_3Sn layer composition is a function of the deposition conditions.

Experimentally it has been observed that:

1. As the $SnCl_2/NbCl_4$ ratio is increased, the atomic percent of niobium in the Nb_3Sn layer decreases.
2. As the quantity of HCl gas inserted into the deposition zone is increased, the atomic percent of niobium in the Nb_3Sn layer increases.
3. As the temperature on the ribbon is increased, the atomic percent of niobium in the Nb_3Sn layer increases.
4. As the ribbon speed is increased, the atomic percent of niobium in the Nb_3Sn layer decreases.

Electromagnetic evaluation of some short samples reveals that critical currents at constant transverse magnetic fields or critical fields at constant current and swept fields are repeatable over the entire magnetic field region. At another extreme, other samples are completely nonrepeatable over the entire region, and still others are nonrepeatable in the low-field region and repeatable in the high-field region. This variation of repeatability of critical currents and fields has been termed stability. In general, the most unstable niobium-stannide deposits have yielded the highest current densities, while very stable deposits have yielded lower current densities. The stability of the niobium-tin layer can be controlled, and is a function of the Nb_3Sn deposition conditions. No correlation has been established to date between stability and (1) composition, (2) critical current, (3) lattice constant, and (4) impurity in deposits.

The stability of the Nb_3Sn layer can be improved by depositing a copper or silver conductive layer over the Nb_3Sn. The conductive layer acts as a sink for eddy currents and decreases the superconducting-to-normal transition velocity. With copperplating, an unstable Nb_3Sn layer becomes partially-to-completely stable, a partially stable Nb_3Sn becomes stable, while no effect is observed with an Nb_3Sn layer that is initially stable. High purity silver-plating can be substituted for copperplating. Silver-plating additionally aids in stabilizing the Nb_3Sn layer.

The stabilized current level of the plated unstable ribbon can be described by the expression of Kim, Hempstead, and Strnad (1962):

$$J_c = \frac{\alpha}{B_o + H} \qquad (8)$$

where $\alpha = 30 \times 10^6$ kilogauss-amperes per square centimeter, B_o is 7 kilogauss, J_c is current density, and H is the applied field. An α of 30 is the highest current density of niobium-stannide reported to date. These high-current densities are attained as a result of the unique vapor-deposition process developed by RCA.

According to recent theories on Type II superconductors, α is a material constant proportional to densities of pinning centers (lattice imperfections and impurities). The RCA Nb_3Sn vapor-deposition process permits controlling the amount of type of lattice imperfections and impurities. The ultimate current density of Nb_3Sn may not have yet been attained since optimization of pinning centers within the lattice structure has not been attempted. At this time, it appears that very high current densities can only be attained with a process, such as that developed at RCA, where the composition and structure can be precisely controlled.

B. EFFECTS OF COIL WINDING ON THE SUPERCONDUCTING PROPERTIES OF Nb_3Sn VAPOR-DEPOSITED RIBBON

Prior to the start of this contract, Montgomery (July, 1962) had published a proposed quantitative analysis for the degradation of superconducting coils (lower critical currents in coils as compared with the critical currents of short samples). He assumed the existence of diamagnetic or "shielding" currents which were a function of coil geometry and the central field developed by a solenoid. These diamagnetic currents were considered as subtracting from the true critical current of the superconductor to yield a reduced value of current through the coil. While application of this model to Nb_3Sn coil results does not show quantitative agreement, the general concept of shielding currents being a part of the mechanism of degradation is considered likely as a result of the work reported here.

More detailed reasons for coil degradation began to be evident in March of 1963 as a result of extensive short-sample testing both at RCA and in the high-field magnet at the Lewis Research Center. A pattern of behavior was seen which qualitatively established the presence of instabilities in short samples. This showed up by a scattered distribution of critical currents at various fields which were lower than the true thermodynamic superconducting-to-normal transition. This reduction in critical current was usually more

severe at lower fields (0 to 10 kG), with higher rates of field and current change, and worse for field changes than for changes in current through the sample. Rate dependence of short samples had been previously noted by others on niobium-zirconium.

The concept of instabilities invalidated any simple comparison between coil data and short-sample data since the effect of "degradation" also applied to the short samples. The scattered values of critical current with unstable samples make it difficult to uniquely specify the critical characteristics of such superconductive material. However, the concept that instabilities were causing the observed low coil currents became clear. As mentioned in Part A of this Summary Discussion, the vapor-deposited ribbon (unplated) can be made with a spectrum of critical characteristics exhibiting various degrees of stability such that the more stable material would generally have a lower thermodynamic critical transition to the normal state than would a less stable material. Each subsequent step in the treatment of any version of this bare Nb_3Sn or its use in coils modifies this stability. When plated with a high electrical conductive material such as copper or silver, stability is increased and critical currents closer to the maximum achievable by the material are seen in tests. On the other hand, when wound into coils, stability is effectively decreased, presumably due to flux movement as discussed below. Stabilizing the material in the coil form is partially achieved by secondary means, such as the introduction of layers of high electrical conductivity metal and by the use of shunts. The noise characteristics of the power supply used to activate the coil were found to be important. A significant conclusion that can be drawn from observations of the many tests performed is that there is seldom a unique degradation factor for a coil. When coils are wound with the less stable Nb_3Sn, the observed critical current of the coil usually falls in a range depending upon experimental conditions.

To wind high-current, high-field coils, two things are needed: superconductive material capable of yielding high currents at high fields and the ability to control the inherent instabilities such that the true critical current can be achieved. The first requirement of high current capability has been achieved by the RCA vapor-deposited material. The second requirement of controlling stability has been attained to a high degree by experience and it is in this area where future effort will be directed. The control of stability

is achieved locally at the ribbon by coating the Nb_3Sn with high electrically conductive metals. At the coil, it is achieved by interleaving with additional conducting metals (i.e., aluminum foil) and circuit control. The plating on the ribbon serves to reduce the probability of the propagation of the normal phase, and the metals dispersed throughout the coil serve as magnetic shields such that flux movement throughout the coil volume is damped. Since numerous tests of short samples and small coils in varying background fields show the low field portion to yield the most unstable critical currents, it is probable that flux movement and the resulting reaction with the ribbon in the low-field region of a coil is the cause of low critical currents in coils.

While the theory of the propagation of a normal mode [(Cherry, Gittleman, 1960), (Stekly, 1963)] and the analysis of flux flow (Strnad, Hempstead, Kim, April, 1964) have been treated, no comprehensive mathematical treatment of the complete problem is available at this time. However, the significant observation that can be made here is that it is certain that stability of coils can be controlled for solenoids developed on the order of 100 kilogauss in small (approximately 1 inch) bores. This fact, due to the work done during this contract, results from the recognition of the importance of the added stability which can be given to superconductors by immersing them in a background magnetic field. This is thought to be due to the reduction of the magnetization currents at higher fields (Montgomery, 1964).

Chandrasekhar and Hulm (January, 1963) developed a model based upon the magnetization currents as being responsible for degradation. However, this predicts a similar degradation pattern for all coils wound with the same wire. It is known from the work reported herein that, although the magnetization currents are certainly an important factor, there is no unique degradation for all coils wound with any one material. Any model which would explain the relationship between short-sample data and coil data must take into account the family of critical characteristics for a hard superconductor which consists of the true thermodynamic transition from the superconducting-to-the-normal mode under ideal conditions, and lower critical characteristics caused by the input of external energy. The role of the sample length (i.e., whether a short sample or a coil), the treatment of the ribbon and a coil (i.e., plating, interleaved foil), and the experimental conditions (i.e., H, $\frac{dH}{dt}$) all serve to modify the extraneous dissipated energy at the superconductor. For any situation, some particular reduced critical characteristics in Nb_3Sn apply.

C. TECHNOLOGY OF SUPERCONDUCTIVE SOLENOIDS

The discussion in Parts A and B gives some of the important characteristics of the vapor-deposited Nb_3Sn ribbon and some observations of its behavior when it is wound into coils. This establishes a series of guide lines for the future development of the technology of superconductive magnets of larger size and higher fields than are currently available. Most of the conclusions made are a result of empirical developments including actual successful construction of a 92-kilogauss, 1/2-inch bore solenoid which confirmed the qualitative aspects of the ideas developed to that date.

The RCA vapor-deposited superconductive ribbon requires very little special care in terms of winding and handling. The ribbon can be layer-wound over coil forms as small as 1/2-inch diameter. Winding tensions up to two pounds were commonly used. Brookhaven National Laboratories reported transient winding tensions up to eight pounds with this material with no ill effects. Layer winding is generally done with a pitch of approximately 0.100 inch to provide adequate spacing between adjacent windings. On smaller coils, ribbon shifting was minimized by bi-filar windings of an insulated thread, (.003-inch diameter Formvar-coated copper wire).

The coil form material most often used was 304 stainless steel. However, other materials were used successfully for coil forms; a convenient one was anodized aluminum which eliminates the need for electrical insulation of the coil form. In the case of the stainless steel or any other conducting type coil form, Teflon insulation was found to be satisfactory. The width of the 0.090-inch ribbon also makes it possible to wind coils one-ribbon-width wide in the form of a spiral. With the inner and outer ends of the spiral connected to inner and outer copper rings to form a "pie", these modules can be series-stacked to form a larger magnet.

Of major importance is the insulation used between layers. It was found during the work done on this contract that the copper- or silver-plating on the ribbon did not fully stabilize a coil and that further damping of the flux transients was necessary. To do this, anodized aluminum foil is interleaved between ribbon layers. The foil before anodizing is either 0.8 or 1.2 mils thick. The stability offered by the introduction of the layers of normal metal generally increases coil output by at least 20 percent when using unstable Nb_3Sn ribbon. The effect of the aluminum foil is greatest on coils which have low-field

portions within their windings. For coils which are immersed in the background field of outer coils, the effect is less.

For coils wound with the more stable Nb_3Sn ribbon, it is possible to use Mylar insulation with less severe degradation than when using Mylar with unstable ribbon. Shunts were unnecessary for coil protection against physical damage in going normal in the coils wound with 0.090-inch wide Nb_3Sn RCA ribbon. When used, shunts aided in achieving higher critical currents by relieving the effects of the instabilities. It is anticipated that coils of several henrys and more using RCA ribbon will require energy dissipation mechanisms in the form of shorted secondary turns and windings in addition to shunts. The largest coil (92-kilogauss, 1/2-inch bore) made at the end of this contract safely dissipated the contained energy within the helium bath and the coil form with no damage to the ribbon.

Early in the contract, in a continuation of an initial RCA program, experiments were completed on coil encapsulation. The most successful, in terms of handling and results, was urethane which retains its elastomeric properties down to very low temperatures. Encapsulants which are fluid at room temperature, such as mineral oil, were also tried. In all cases, there was some degraded effect such that the critical coil in its self-field was lowered.

At no time in any of the coils wound with RCA Nb_3Sn ribbon has there been anything which resembled the training reported for niobium-zirconium coils. Unstable Nb_3Sn ribbon coils when tested in self-field, exhibit variations in critical current, but these are generally random in nature. Test coils which were immersed in the Lewis Research Center's magnet, and therefore subject to high-field forces, did sometimes exhibit a trend in testing. This showed up, however, as scattered critical-current, critical-field points through the initial quenchings, with a later smoothing of the data. This initial scatter was found due to shifting of the windings under high magnetic fields. When the windings attained an equilibrium position, a stabilized critical curve was attained. It is expected that training effects will not be of consequence in coils wound with vapor-deposited Nb_3Sn ribbon.

Of prime interest at the conclusion of work on this contract is the ability to determine the feasibility of designing a superconductive magnet of at least 1-foot bore that will develop fields of 150 kilogauss. At the time this section was being written (May 1964), RCA had just announced a three-

section, 1-inch-bore solenoid which developed 107 kilogauss. This is the highest field superconducting magnet of its size known to exist. This was made possible by the understanding and the application of the principles described in this report. In the large compound coils which developed these high fields, two of the three sections operated with zero degradation. The reasons for the degradation of the outer coil of this compound magnet have been discussed and are adequately understood. It is now known that "degradation", when it does exist, is only a matter of the control of the stability of the superconductor.

The work under this contract has removed the concept of degradation from that of a limiting basic problem to one which is amenable to solution by engineering technology. At this time, there is no apparent technical reason why superconductive magnets of the objective size and performance cannot be made.

A problem which has not been treated in this report is that of the containment of the windings subject to high-field forces. It has been shown that encapsulation is feasible. This is perhaps the extreme step to be taken if required. However, the high strength of the RCA vapor-deposited ribbon, the ability to wind under high tension, and the availability of methods of interlocked windings and partial encapsulation offer other possibilities for meeting this problem. In addition, modular construction of larger magnets with an effective cellular structure can be effectively used to relieve local magnetic stresses and to act as a secondary supporting structure to the windings.

The necessity of perfecting the technology of actual large magnet construction requires further work in cryogenic and structural technology. At the time this report is being issued, RCA is engaged in a follow-on contract (NAS 3-5240) in which large superconductive modules (8-1/2 in. OD) will be constructed and tested. The successful completion of this phase of the work will establish a firm foundation for large high-field practical solenoids.

REFERENCES

Anderson, P.W. (1962), "Theory of Flux Creep in Hard Superconductors," Phys. Rev. Letters 9, No. 7.

Boom, R.W., Roberts, L.D., and Livingston, R.S. (1963), "Developments in Superconducting Solenoids," Nucl. Inst. Methods 20, 495.

Brown, G.V. and Flax, L., "Superposition of Semi-Infinite Solenoids for Calculating Magnetic Fields of Thick Solenoids," Internal NASA Report.

Cherry, W.H. and Gittleman, J.I. (1960), "Thermal and Electrodynamic Aspects of the Superconductive Transition Process," Solid State Electronics (Pergamon Press) Vol. 1, p. 287-305.

Cullen, G.W., Cody, G.D., and McEvoy, J.P., Jr. (1963), "Field and Angular Dependence of Critical Currents in Nb_3Sn," Phys. Rev. 132, No. 2.

Enstrom, R.E. (1963), ScD Thesis, MIT (unpublished).

Fakan, J. and Schrader, E.R. (June 1964), "Experimental Evidence of Degradation Effects in Short Samples of Hard Superconductors," NASA TN D-2345.

Hanak, J.J., Cody, G.D., Aron, P.R., and Hitchcock, H.C. (1961), "Some Physical Properties of Deposited Nb_3Sn," Proceedings of the International Conference on High Magnetic Fields, MIT, (John Wiley and Sons, Inc., New York) p. 592.

Hanak, J.J. (1963), Metallurgy of Advanced Electronic Materials, G.E. Brock, Editor, (Interscience Publishers, New York) p. 161.

Kim, Y.B., Hempstead, C.F., and Strnad, A.R. (1962), "Critical Persistent Currents in Hard Superconductors," Phys. Rev. Letters 9, No. 7.

Lubell, M.S., Chandrasekhar, B.S., and Mallick, B.S. (1963), Appl. Phys. Letters 3, 79.

Marcus, P.M. (Sept. 1960), "Currents and Fields in a Superconducting Film Carrying a Steady Current," Proc. of the VIIth International Conference on Low Temp. Physics, Toronto, Canada.

Meyers, N.H. (1960), "An Analog Solution for the Static London Equations of Superconductivity," Proc. IRE 48, 1603.

Montgomery, D.B. (July 1962), "Current-Carrying Capacity of Superconducting Nb-Zr Solenoids," AD 282158.

Montgomery, D.B. (1964), "Superconducting Magnets," IRE Spectrum 1, 103.

Rosner, C.H. and Schadler, H.W. (1963), J. Appl. Phys. 34, 2107.

Schrader, E.R., Freedman, N.S., and Fakan, J.C. (March 15, 1964), "High Field Nb_3Sn Superconducting Magnets by Magnetic Field Stabilization," Appl. Phys. Letters 4, No. 6.

Stekly, Z.J.J. (1963), "Theoretical and Experimental Study of an Unprotected Superconducting Coil Going Normal," Advances in Cryogenic Engineering, K.D. Timmerhous, Editor, (Plenum Press) Vol. 8, p. 585.

REFERENCES (Continued)

Strnad, A.R., Hempstead, C.F., and Kim, Y.B. (April 1964), "Flux Flow in Type II Superconductors," A.P.S. Meeting, Washington, D.C.

Wischmeyer, C.R. and Kim, Y.B. (April 1964), "Flux Migration and Instabilities in Hard Superconductors," A.P.S. Meeting, Washington, D.C.

APPENDIX

PROCESS CONDITIONS

(Unless otherwise specified, substrate used is Hastelloy.)

Run No.[1]	Furnace Temp. °C	Substrate Speed meter/hr	Ratio of Sn/Nb in Chloride Feed	Total Hydrogen Flow ml/min	Total Helium Flow ml/min	Wattage on Ribbon	Nb_3Sn Layer Composition[2] Atom. % Nb	Plating[3,4]
PNDC 3	730	10	3/1	250	135	50	78.6	—
PNDC 70	730	10	3/1	250	135	50	75.7	—
PNDC 71	730	10	3/1	250	135	50	76.0	—
PNDC 72	730	10	3/1	250	135	50	76.4	—
PNDC 73	730	10	3/1	250	135	50	76.7	—
PNDC 74	730	10	3/1	250	135	50	75.9	—
PNDC 75	730	10	3/1	250	135	75	76.1	—
PNDC 77	730	10	3/1	250	135	30	75.9	—
PNDC 78	730	10	3/1	250	135	20	75.1	—
PNDC 81	730	10	6/1	250	135	50	68.4	—
PNDC 82	730	10	5/1	250	135	50	73.9	—
PNDC 83	730	10	4/1	250	135	50	75.0	—
PNDC 86	730	10	3/1	250	135	50	76.1	—
PNDC 87	730	10	2/1	250	135	50	76.9	—
PNDC 88	730	10	1/1	250	135	50	77.9	—
PNDC 96R	730	10	3/1	250	135	50	76.2	—
PNDC 97R	730	15	3/1	250	135	50	75.7	—
PNDC 98R	730	17.5	3/1	250	135	50	75.7	—
PNDC 99R	730	20	3/1	250	135	50	75.4	—
PNDC 100R	730	22.5	3/1	250	135	50	75.3	—
PNDC 101	730	10	4.5/1	250	135	50	74.5	—
PNDC 102	730	10	4.5/1	250	135	50	74.7	—
PNDC 103	730	10	4.5/1	250	135	50	75.5	—
PNDC 104	730	10	4.5/1	250	135	50	75.9	—
PNDC 114	730	10	4/1	250	135	50	77.0	—
PNDC 115	730	15	4/1	250	135	50	76.9	—
PNDC 116	730	17.5	4/1	250	135	50	76.4	—
PNDC 117	730	20	4/1	250	135	50	76.1	—
PNDC 118	730	22.5	4/1	250	135	50	75.9	—
PNDC B	730	10	6.3/1	250	135	50	71.1	—
PNDC C	730	10	4/1	250	135	50	75.1	—
PNDC D	730	10	2/1	250	135	50	76.2	—
PNDC E	730	10	1/1	250	135	50	77.7	—
PNDC F	730	10	1/2	250	135	50	77.8	—
PNDC G	730	10	1/3	250	135	50	78.3	—
PNDC H	730	10	1/4.5	250	135	50	78.6	—
PNDC I	730	10	1/6.4	250	135	50	79.1	—
PNDCR 3	730	10	4/1	470	135	50	72.2	—
PNDCR 12	730	10	4/1	470	135	50	75.5	—
PNDCR 14	730	10	4/1	470	135	50	75.1	—
PF 28	450	20	1/1	735	340	110	76.0	—
PF 8C	450	20	1/1	735	340	110	76.0	—
PF 10-5	450	20	1/1	735	340	110	72.7	—
HDC 6	730	10	3/1	250	195	50	75.7	Copper
HDC 6-1,1	730	10	3/1	250	195	50	75.7	Copper
HDC 6-1,1	730	10	3/1	250	195	50	75.7	Copper
HDC 6-2,1	730	10	3/1	250	195	50	75.7	Copper
HDC 6-3,1	730	10	3/1	250	195	50	75.7	Copper
HDC 8	730	10	3/1	250	195	50	—	Copper
HDC 34	730	10	3/1	250	195	50	75.0	Copper
HDC 41	730	10	3/1	250	195	50	—	Copper
HDC 46 Beg	730	10	3/1	250	195	50	74.9	—
HDC 46 End[5]	730	10	3/1	250	195	50	75.8	—
HDC 49A	730	10	3/1	250	195	50	76.5	Copper
HDC 49B	730	10	3/1	250	195	50	76.5	Copper
HDC 49C	730	10	3/1	250	195	50	76.5	Copper
HDC 50	730	10	3/1	250	195	50	76.0	Copper
HDC 56	730	10	3/1	250	195	50	—	Copper
HDC 58	730	10	3/1	250	195	50	—	Silver
HDC 63	730	10	3/1	250	195	50	—	Silver
HDC 70	730	35	3/1	470	195	70	76.0	Silver
HDC 71	730	10	3/1	470	195	70	76.7	Silver
HDC 73-1	730	10	3/1	250	195	50	—	Copper
HDC 86	730	10	3/1	250	195	50	—	Silver

1. The prefixes of the run numbers denote the following:
   a. PNDC and PNDCR - Ribbon processed at RCA Laboratories, Princeton, New Jersey.
   b. HDC - Ribbon processed at RCA, Harrison, New Jersey, pilot line.
   c. PF - Ribbon processed at RCA Laboratories, Princeton, New Jersey. The metal chlorides were premixed to the desired ratio and injected into the deposition zone as a solid.
2. The thickness of the Nb_3Sn layer in the above runs ranged from 0.2 to 0.3 mil per side of ribbon.
3. A nickel flash coating was deposited on runs HDC-6 to HDC-86 prior to copper- or silver-plating.
4. The nominal copper- or silver-plating thickness is 0.25 mil.
5. Platinum substrate.